Calcareous Nannoplankton Biocoenosis:

Sediment Trap Studies in the Equatorial Atlantic, Central Pacific, and Panama Basin

John C. Steinmetz

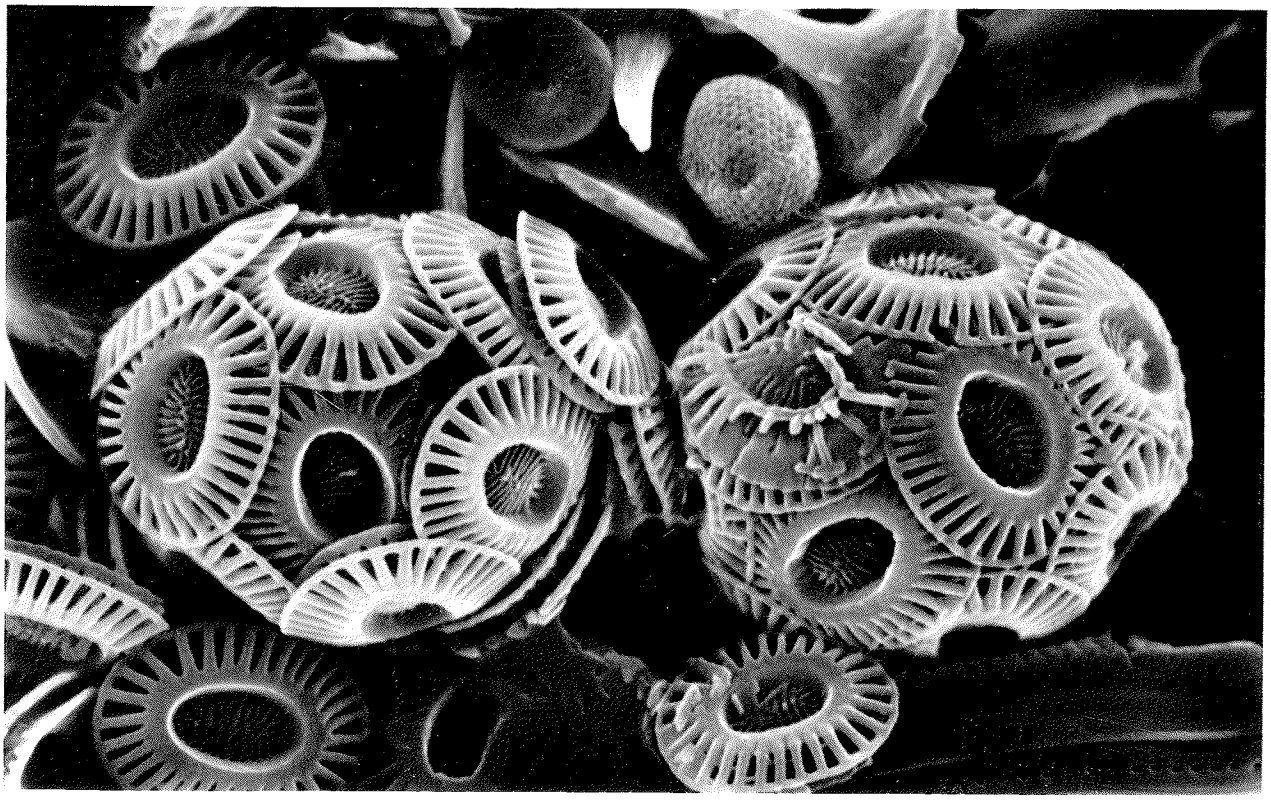

Edited by

Susumu Honjo

Woods Hole Oceanographic Institution
Woods Hole Massachusetts 02543
U.S.A

Ocean Biocoenosis Series No. 1

Calcareous Nannoplankton Biocoenosis:

Sediment Trap Studies in the Equatorial Atlantic, Central Pacific, and Panama Basin

John C. Steinmetz
Marathon Oil Company
Petroleum Technology Center
Littleton, CO 80160-0269

Edited by

Susumu Honjo

Woods Hole Oceanographic Institution
Woods Hole Massachusetts 02543
U.S.A

Ocean Biocoenosis Series No. 1

Ocean Biocoenosis Series No. 1
Woods Hole Oceanographic Institution, Woods Hole, MA 02543

Published 1991
Printed in the United States of America

Availability: Office of the Research Librarian
Woods Hole Oceanographic Institution
Woods Hole, Massachusetts 02543
U.S.A.

$10.00 U.S.

Explanation of Cover Photo: Two coccospheres of *Emiliania huxleyi* (Lohmann) from PARFLUX Station E in the western Tropical Atlantic Ocean collected at a trap depth of 389 m. *E. huxleyi* is the dominant species of coccolithophore in the world's oceans. Each coccosphere pictured here is 6 μm in diameter.

Contents

List of Tables

List of Figures

Calcareous Nannoplankton Biocoenosis: Sediment Trap Studies in the Equatorial Atlantic, Central Pacific, and Panama Basin

John C. Steinmetz

Abstract

Sediment traps deployed on three moored vertical arrays collected particles at various depths in the equatorial Atlantic (Station E), central Pacific (Station P_1), and in the Panama Basin (Station PB_1). The calcareous nannoplankton from the <63 μm size fraction were studied in order to characterize the flux of coccospheres and coccoliths, the taxa present, and their condition of preservation throughout the water column.

The average calculated flux of coccospheres ranged from a low value of 24 coccospheres/m^2 /day in the central Pacific, to an intermediate value of 4725 in the equatorial Atlantic, to a high of 8030 in the Panama Basin. In general, the coccosphere flux decreased with depth at all three sites.

Coccolith fluxes and flux profiles were significantly different at each of the three sites. At Station E, the flux decreased regularly with depth but increased sharply at the lowermost trap (724 m above the bottom). The average flux for the entire column was 316 × 10^6 coccoliths/m^2/day. At Station P_1, the flux was low in the shallowest two traps and increased markedly in the three deepest traps. This increase is due mainly to a suspected Umbilicosphaera sibogae *bloom which occurred shortly before the traps were deployed in September 1978. The highest coccolith flux was recorded in the Station PB_1 traps averaging 910 × 10^6 coccoliths/m^2/day. The flux profile at this station was essentially constant in the shallowest four traps and decreased almost 59% in the lowermost two traps. The average coccolith carbonate fluxes for the entire columns for the Stations E, P_1, and PB_1 are, respectively, 2.53, 2.68, and 7.28 mg/m^2/day. These fluxes represent minimum values, since coccospheres and coccoliths were also contained in fecal pellets and other particles larger than the size fraction studied (<63 μm).*

Scanning electron microscopic examination of the trap samples revealed 56 species belonging to 33 genera of calcareous nannoplankton. Three new species are described and illustrated: Alisphaera spatula *n. sp.,* Umbilicosphaera calvata *n. sp., and* Umbilicosphaera scituloma *n. sp.*

A census of taxa present, including their relative frequency and state of preservation, is presented together with a photographic atlas of the taxa. Station E is the most diverse with 50 species, and is the best preserved of the three sites. Station PB_1 the least diverse with 26 more poorly preserved species. In general, the best preserved specimens were observed in the shallowest sample at each of the three sites; diversity and state of preservation diminished with increasing depth.

Introduction

Calcareous nannoplankton, or coccolithophores, are pelagic, single-celled, golden-brown algae that secrete calcite plates or shields. Nannoplankton are one of the major constituents of marine phytoplankton and are, therefore, important primary producers in the food chain (e.g. Haq, 1978). Together with planktonic foraminifera and pteropods, they constitute the major contributors of calcium carbonate to the water-column and the sea-floor.

Calcareous nannoplankton characteristically form spherical cells known as coccospheres. Each coccosphere is covered with a layer or several layers of calcite shields called coccoliths. Coccoliths are secreted internally and then extruded to the surface of the coccosphere where they form a coating or armor around the cell. Coccoliths range in size between 1 and 10 μm in diameter, and the average coccosphere is between 5 and 20 μm in diameter. Occasionally coccoliths are sloughed off or lost, or they may be freed when a coccosphere disaggregates.

Much of our knowledge regarding the geographic distribution and preservation of calcareous nannoplankton is derived from plankton-tow, water-casting and surface-sediment studies. Plankton-tow or water-casting studies have provided us with qualitative and quantitative information regarding the vertical distribution and seasonal variation in abundance and composition, and with standing stock estimates of nannoplankton. Such measurements, however, do not translate directly into sedimentation rate, accumulation rate, or even preservational state of nannoplankton on the sea-floor. Surface-sediment studies may yield information concerning the spatial distribution of calcareous nannoplankton in the overlying waters; however, they provide little to the understanding of rates of coccolith production and vertical transport. Until recently, oceanographers have not had a means to investigate the processes by which these minute particles settle to the sea-floor.

Simple, yet elegant, calculations by Honjo (1976), using the Stokes' relationship for the settling of particles in a fluid, have shown that an individual coccolith from a coccosphere would take several tens of years to settle unassisted in the open ocean. Certainly, within a fraction of that time, a calcite particle would likely drift far beyond its original latitudinal zone distribution and would undergo marked, if not complete, dissolution. Yet, well-preserved coccolith ooze is present on the deep-sea floor beneath an overlying euphotic community that is identical to it in assemblage composition.

Nannoplankton populations in the open ocean are under high grazing pressure from zooplankton and are therefore likely to be consumed before completing their life cycle (Honjo, 1975). Nannoplankton are among the flora consumed by grazing zooplankton and commonly pass through the gut of these tiny organisms with no mechanical or chemical effect on the calcite coccoliths. Fecal pellets of zooplankton occasionally consist almost exclusively of coccoliths. Often delicately preserved, intact coccospheres are found within pellets (Honjo, 1975, 1976; Honjo and Roman, 1978). Fecal pellets and other oceanic macroaggregates are believed to be responsible for the rapid vertical transport of the majority of coccospheres and coccoliths through undersaturated waters to the sea-floor (Honjo, 1975, 1976; Honjo and Roman, 1978). Such a transport mechanism also explains why coccoliths occur below the calcite saturation depth and may exhibit little or no effect of progressive dissolution.

Individual coccoliths found at depth in the water column have either descended very slowly to that point (very unlikely) or have been released from a fecal pellet that transported

them to that depth (Honjo, 1976). In this paper, the term "free-coccolith" is used, and is here defined as a coccolith found separate or free in the water column or retained in a sediment trap. Free-coccoliths are likely to have been liberated (released) from fecal pellets (or similar aggregate particles) which have broken or biodegraded and spilled their contents. Fresh coccoliths or coccospheres are thus replenished at all depths by descending fecal pellets (Honjo, 1976). If coccoliths are released from the host fecal pellets, their rate of descent decreases a thousand-fold, and they are fully exposed to undersaturated deep water (Honjo, 1975). Upon their release from a fecal pellet, their residence time at depth in the water column is relatively short and they are quickly remineralized. Thus, free-coccoliths dissolve before they arrive at the sea-floor and do not disturb the bio-thanatocoenosis correspondence between the surface water community and the surface sediment assemblage (Honjo, 1976).

With the advent of sediment-trap technology, scientists are now able to deploy anchored or floating collecting devices for days to months in the open ocean. Once retrieved, the quantities and identities of these particles can be ascertained, and particle fluxes directly calculated (Wiebe et al., 1976; Honjo, 1978, 1980; Spencer et al., 1978; Soutar et al., 1977; Knauer et al., 1979; Rowe and Gardner, 1979; Thunell and Honjo, 1981). By measuring the flux of calcareous nannoplankton to the sea-floor we can determine how the biocoenosis (living assemblage) is transformed into the thanatocoenosis (death, or sedimentary, assemblage). We can then better estimate the importance of calcareous nannoplankton to the calcium carbonate cycle in the oceans.

To date, little assessment of the assemblage composition, amount, and preservational condition of calcareous nannoplankton from sediment trap experiments has been attempted. Honjo (1976) reported on a study of the contents of zooplankton fecal pellets collected in a sediment trap (Wiebe et al., 1976). The trap was deployed at 2,200 m for two months in the Tongue of the Ocean, Bahamas. He found that about 80% of the pellets contained hard skeletons of phytoplankton (coccoliths and diatoms) and clay mineral-like particles. The preservation of the coccoliths was excellent. Honjo (1976) determined that the average fecal pellet collected contained 0.8 μg of $CaC0_3$, which he estimated to be equivalent to approximately 1×10^5 coccoliths or 5,000 average-size coccospheres. He also calculated the horizontal drift of an average fecal pellet descending through a 5,000 m water column and estimated the resolution of replication of the bio- and thanatocoenosis to be better than 200 km.

Sediment trap experiments are particularly important in obtaining information about the transport of material through the water column. The Particulate Flux Experiment (PARFLUX) was designed to measure total particulate flux to the sea-floor (Honjo, 1980). A part of the program involved deploying a series of sediment trap arrays in different oceanographic conditions. Material collected provides an unusual opportunity to measure and compare total coccosphere and coccolith fluxes in regions of vastly different surface productivity, as well as to document the biocoenosis of calcareous nannoplankton at these locations.

Time-series PARFLUX sediment traps were utilized by Samtleben and Bickert (1990) to collect coccoliths at monthly increments for a year at three locations in the Norwegian Sea. Results of the analyses are an important contribution to our understanding of coccolith seasonality, species composition, and selective preservational processes in high-latitude waters.

The purpose of this article is to document the character, quantity, and preservation of coccospheres and coccoliths recovered from three vertical sediment-trap arrays deployed in different water masses. Presented for the first time are measured flux values for coccospheres and coccoliths in tropical areas. These values are presented in both flux of particles, as well as in flux of equivalent calcium carbonate to their respective locations in the water column. An atlas of calcareous nannoplankton illustrates the taxa recovered at the three trap sites.

Oceanographic Setting of the Sediment-Trap Stations

The PARFLUX experiment was designed to measure, characterize, and compare the flux of particulate matter in different oceanographic regions having significantly different levels of productivity. Of the three locations discussed here, the Panama Basin has the highest level of primary productivity. The levels of biological productivity in this region of upwelling exceed an annual average of 1,000 mg $C/m^2/day$ in the euphotic zone (Forsbergh, 1969; Love, 1970, 1971; Moore et al., 1973). Station P_1 in the central Pacific lies within the area of lowest level of biological productivity of the three regions considered. The station is north of the eastern equatorial Pacific high productivity region and exhibits a productivity of less than 100 mg $C/m^2/day$ (Koblentz-Mishke et al., 1970; van Andel et al., 1975). Station E in the western tropical Atlantic displays a level of primary productivity that is somewhat intermediate between those of the Panama Basin and central Pacific stations.

Station PB_1 is located in the northeast quadrant of the Panama Basin. The Panama Basin lies in the eastern equatorial Pacific Ocean and is bounded on the east by the Isthmus of Panama between Central America and South America, on the northwest by the Cocos Ridge, and on the south by the Carnegie Ridge. The hydrography of the east tropical Pacific region adjoining the Panama Basin is dominated by the Equatorial Current system. Here lies the eastern terminus of the Equatorial Counter Current and the place of origin of the westward flowing North and South Equatorial Currents (Smayda, 1966). Surface circulation in the Panama Basin is characterized by a counterclockwise eddy, except during February and March. During these months of the upwelling season, the southernmost loop of the eddy continues directly into the South Equatorial Current (Cromwell and Bennett, 1959; Smayda, 1966), instead of flowing eastward toward the coast of South America and then northward into the Gulf of Panama as the Columbia Current (Wooster, 1959).

Annually, the region is successively influenced by the movement of the Trade Winds-Calm Belt (Doldrums) climatic system. From January through April, the dry, northerly, offshore winds of the northeast Trade Winds prevail over the area and induce upwelling. During upwelling, the surface waters are displaced offshore and replaced by colder, more saline and nutrient-rich water. In late April or May, the northeast Trade Winds usually weaken and dissipate, move northward, and are progressively replaced by the Doldrums and the southeast Trade Winds. The rain-bearing southeast Trade Winds are southwest, relatively light and shallow onshore winds that usually persist until mid-December. For 8 months, heavy rains diminish ocean mixing. The surface waters become warm, diluted, and nutrient-impoverished. A slight resurgence of northerly winds during July and/or August may induce mixing or even cause a slight upwelling. During the rainy season, a progressive southerly migration of the Trade Winds-Calm Belt (Doldrums) system re-establishes the northeast Trade Winds in the region by December (Wooster, 1959; Smayda, 1966).

Details of the oceanography of the Panama Basin have been described in reports by Wooster and Cromwell (1959), Wyrtki (1967), Forsbergh (1969), and Stevenson (1970). Upwelling in the Panama Basin is largely responsible for the high productivity of the waters. Productivity is highest near the coastal margins and over the Carnegie Ridge (Moore et al., 1973). The sediments in the Basin are dominated by biogenous components, except near the coast where terrigenous input is high. The character and distribution of the sediments are discussed by Kowsmann (1973), Moore et al. (1973), van Andel (1973), Heath et al. (1974), and Yamashiro (1975).

Station P_1 is located between the Molokai and Clarion Fracture Zones in the east Hawaii Abyssal Plain, one of the largest basins in the North Pacific Ocean. The area exhibits unusually monotonous flat topography, and no significant submarine features (ridges, seamounts, or volcanoes) occur within 450 km of the station (Honjo, 1980). The nearest continental landmass is 3,350 km away (Monterey, California). Station P_1 lies within the main axis of the westward-flowing North Equatorial Current (Tchernia, 1980). Bottom sediments in the area consist of consolidated clay with alternating thin ferro-manganese laminations (R/V KANA KEOKI Cruise Report, September 1978, Hawaii Institute of Geophysics). Calcium carbonate comprises less than 10% of the sediment (Berger et al., 1976).

Station E is located in the western tropical Atlantic at least 750 km from the nearest landmass (Guyana coast). The station is situated within the north westward-flowing North Equatorial Current (Tchernia, 1980). The underlying Demerara Abyssal Plain has a gentle topography, is relatively flat, and gradually deepens northward toward the eastern end of the Puerto Rico Trench.

Logistics

The samples used in this study were collected from sediment trap arrays located in the western equatorial Atlantic (Station E), the central North Pacific (Station P_1) and the Panama Basin (Station PB_1) (Figure 1 and Table 1). At Station E (13°31′N, 54°00′W) four sediment traps were deployed at various depths between 389 and 5,068 m in 5,288 m of water for a period of 98 days from November 1977 to February 1978. At Station P_1 (15°21′N, 151°28′W) five sediment traps were deployed between 378 and 5,582 m in 5,792 m of water for a period of 61 days from September to November 1978. The third array, at Station PB_1 (5°21′N, 81°53′W), consisted of six traps placed at depths between 667 and 3,791 m in 3,856 m of water for 112 days from July to November 1979.

The PARFLUX Mark II sediment trap was used at all three locations. The details of the design and engineering were presented in Honjo (1980) and Honjo et al. (1980). The trap opening is 1.5 m^2 and contains hexagonal baffle cells to minimize water turbulence in the trap. The sediment receiving cup is located at the bottom of the trap. Sodium azide (NaN_3) bacteriocides diffuse through a series of porous membranes to prevent degradation of organic matter in the cup. Each receiving cup was automatically sealed 3 days prior to recovery.

Table 1: Sediment Trap Logistics.

	PARFLUX E	PARFLUX P_1	PARFLUX PB_1
Location	13°30'N, 54°00'W	15°21'N, 151°28'W	5°21'N, 81°53'W
Ocean/Basin	Equatorial Atlantic/ Demerara Abyssal Plain	Central Pacific/ E. Hawaii Abyssal Plain	Eastern Pacific/ Panama Basin
Term	11/77–2/78	9/78–11/78	7/79–11/79
Duration	98 days	61 days	112 days
Trap Depths	389 m 988 m 3,755 m 5,068 m	378 m 978 m 2,778 m 4,280 m 5,582 m	667 m 1,268 m 2,265 m 2,869 m 3,769 m 3,791 m
Ocean Depth	5,288 m	5,792 m	3,856 m

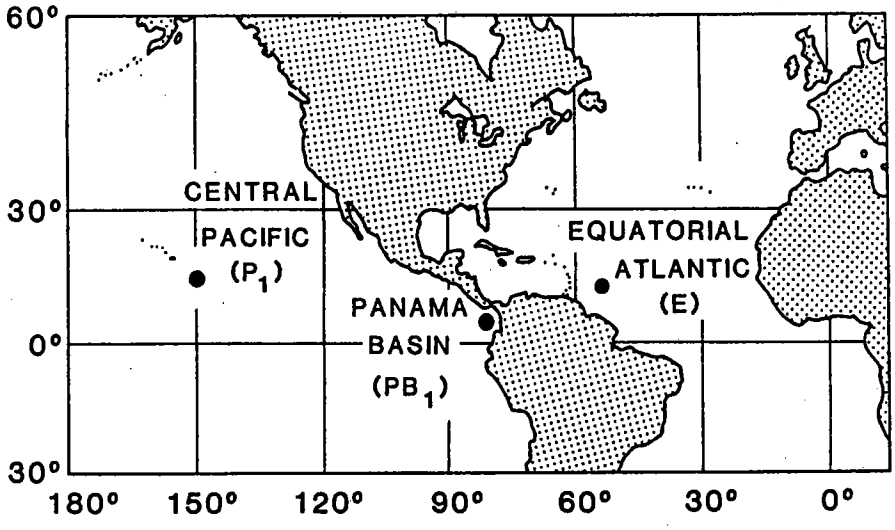

Figure 1: Geographical locations of the three sediment-trap sites.

Laboratory Procedures

Sample Preparation

The sediment trap samples were processed, split, and stored according to the methods discussed in Honjo (1980). The <63 μm size-fraction from each sediment trap sample was wet split into aliquots using a precision rotary splitter (Honjo/Erez splitter, Honjo, 1978). The laboratory procedures were performed on the following fractional aliquots: Station P_1 samples: 1/256 aliquot; Station E samples: 1/256 aliquot; and Station PB_1 samples: 1/1024 aliquot. Using pipettes, subsamples in the fractional aliquots were taken for the three assessments to be described (i.e., coccosphere studies, coccolith studies, and SEM studies). The coccospheres and coccoliths were enumerated using separate procedures. This is because of the size differences between coccospheres and coccoliths, but particularly due to the frequency of coccoliths that was several orders of magnitude greater than that of coccospheres.

The total liquid volume of each sample was between 60 and 160 ml. Each sample was stored in a 1-liter bottle. The size of the bottle and amount of liquid in each were such that the sample could be gently swirled and thoroughly agitated to disperse and randomize the solid particles within the liquid without losing sample. A few crystals of mercuric chloride ($HgCl_2$) were added to each bottle to inhibit bacterial growth.

Coccosphere Studies

The Utermöhl or Inverted Microscope Method (Utermöhl, 1958; Lund, Kipling and LeCren, 1958) was used to count coccospheres. In order to concentrate the particulate material, a 5-ml aliquot of liquid was withdrawn from an agitated sample container and deposited in a 10-ml-capacity glass settling chamber. The particles were allowed to settle to the bottom of the settling chamber for two hours and were then identified and counted from beneath, using an inverted microscope.

Samples observed to be too dense were diluted with buffered, filtered sea-water to either 1/10 or 1/20 their original volume. Five diameter-transects of the settling chamber were counted, and based on the average number of coccospheres per transect, the total number of coccospheres in the entire chamber was estimated. The following rationale was used in making this calculation: The ratio of the whole settling chamber bottom area to the area of a one-diameter transect is:

$$\frac{\pi r^2 2}{2rw} = \frac{\pi r}{2w}$$

where **r** is the radius of the chamber and **w** is the width of the diameter transect. The total number of coccospheres in the entire chamber equals:

$$\frac{\pi r}{2w} \times N$$

where **N** is the average number of coccospheres in a one-diameter transect.

In this study, for example, the 10-ml-capacity settling chamber had a diameter of 25 mm, and the width of the transect (defined using a ×40 objective lens) was 0.54 mm. Therefore, the ratio of the whole bottom area to the area of one diameter transect was 36.36.

Only complete coccospheres or obviously ruptured spheres were counted; aggregates or clumps of coccoliths were not. The estimates of the numbers of coccospheres per milliliter represent a minimum; coccospheres less than about 10 μm were not recognizable using a $\times$40 objective lens ($\times$400 total magnification). Therefore, all small coccospheres, especially *Emiliania huxleyi*, were not accounted for in the estimates. Thoracospheres and individual scyphospheres also were not counted.

The total number of coccospheres in the original sediment trap sample was calculated by taking the product of the number of coccospheres per milliliter, the original volume of liquid sample in the fraction aliquot, and the inverse of the fractional aliquot. The coccosphere flux was calculated by dividing the total number of coccospheres by the area of the sediment trap opening (1.5 m^2), and by the number of days the trap was deployed (see Table 1).

Coccolith Studies

Experiments were performed using various cell-counting chambers in order to find the most appropriate for counting coccoliths at the magnification required for their identification. The Sedgwick-Rafter and Palmer-Maloney types provide for small volumes of liquid (1.0 ml and 0.1 ml, respectively), but the densities of coccoliths present were too great to count practically. The hemocytometer with improved Neubauer ruling was found effective for counting coccoliths, considering the magnification required and the density of individuals per sample volume. The hemocytometer has two counting chambers consisting of nine ruled squares, each 1.0 mm on a side. Each 1 mm^2 area is further equally subdivided into twenty-five squares. With the coverslip in place, the chamber is 0.1 mm deep and the volume of a 1 mm^2 area is 1 mm^3. Since 1 ml = 10^3 mm^3, the volume of one 1 mm^3 area is 0.0001 ml. Similarly, the volume of a 1/25 mm^2 area is 0.000004 ml (= 4×10^{-6} ml). The conversion factor used to obtain the number of coccoliths per milliliter, from the average number of coccoliths in a 1/25 mm^2 area is 4×10^6.

Sample preparation for the hemocytometer consisted of withdrawing a 2-ml aliquot of liquid from the agitated sample container and depositing it in a test tube. The tube was agitated for thirty seconds on a vortex mixer at its highest speed setting to disarticulate coccospheres and aggregates. A drop of liquid containing the sample was then introduced into each of the two chambers of the hemocytometer. Rapid, continuous diffusion beneath the coverslip ensured that the distribution over the counting grid was even. The coccoliths in the liquid were allowed to settle 2–4 minutes before enumeration.

A 1/25 mm^2 area of the hemocytometer fills the field of view of a compound microscope set for a magnification of $\times$250 with a $\times$20 objective. Coccoliths are readily visible at this magnification. The coccoliths in twenty to forty 1/25 mm^2-areas in each of the two chambers were counted, with the aid of a hand tally, and an average number of coccoliths for each area calculated.

Immediately following a counting procedure, the chambers were rinsed with fresh water, followed by ethyl alcohol, and wiped dry with lens paper. This ensured rapid and smooth distribution of the next sample.

The total number of coccoliths in the original sediment trap sample and the coccolith flux were respectively calculated in the same manner as those for coccospheres. The coccolith carbonate flux was calculated by assuming coccoliths to be pure calcium carbonate with an

average mass of 8×10^{-12} gm per individual coccolith (Honjo, 1976). The product of the flux and the average mass yields the carbonate flux in $mg/m^2/day$.

SEM Studies

The scanning electron microscope (SEM) was used to assess the taxa of coccolithophores present in each trap sample, as well as their relative abundance and condition of preservation. The procedure for the preparation of samples was as follows: the sample was gently agitated, and a small volume (1–2 ml) withdrawn into a pipette. The suspended sample was released into a funnel of a vacuum filtering apparatus and deposited onto a Nuclepore© polycarbonate filter membrane 47 mm diameter, 0.4 μm nominal pore size. It was not necessary to treat any of the samples with an oxidant to remove organic matter before filtering. A gentle vacuum (30 cm Hg), supplied by hand vacuum pump, ensured the preservation of fragile coccospheres. Several washes of 10 ml buffered (with ammonium hydroxide) distilled water removed any salts. The filter was vacuum-filtered until dry. The filter was removed, placed in a petri dish on absorbent paper, and stored or air-dried overnight.

Small sections of the dried filter were carefully cut and shaped with a dissecting scissors to fit an SEM stub. The periphery of the filter was fixed to the stub using conductive silver paste, applied with a wooden toothpick. After the paste was dry, the sample was coated with about 150 Angstroms gold-palladium (Au/Pd:60/40) alloy in a Technics Hummer Jr.© diode sputter coater apparatus applying 40-80 millitorr argon gas as an ionizer at 10 milliamperes for 2 minutes. The sample was examined on the high resolution, top stage of an International Scientific Instruments© DS-130 scanning electron microscope. Images were recorded on Kodak© 35 mm Pan-X (ASA 32) film.

Each sample was studied several times; first to document (list and photograph) all of the species present, later to estimate the relative frequency and state of preservation of each species in the assemblage. The presence of whole coccospheres was also noted. Groups of closely distributed coccoliths of the same species were assumed to have been derived from a coccosphere which collapsed during the preparation procedure.

Frequency estimations of each species in the trap assemblage were semiquantitative. That is, those taxa observed only once were designated as rare in occurrence; 2–10 times: frequent; 10–100 times: common; and 100 or more times: abundant. Any one taxon overwhelmingly abundant in the assemblage was designated: dominant. Several thousand individuals were observed in each sample. Only after traversing the sample several minutes (i.e., encountering several hundred individuals) without observing an as-yet-unseen taxon, was the search terminated. This procedure proved to be rapid, efficient, and reliable (i.e., reproducible). Using the same frequency estimation technique for smear-slide examination of coccolith assemblages in the optical microscope (Gartner, 1972; Steinmetz, 1979), the observer encounters and records the most abundant taxa first. These can then be ignored, while attention is paid to the increasingly more infrequent taxa.

Results

Coccosphere Studies

A typical sediment trap sample in the <63 μm particle size range contained few complete coccospheres, but many individual coccoliths. Settled samples, deposited on the bottom of the counting chamber, consisted of what was essentially a monolayer of particulate material evenly dispersed and exhibiting no aggregates. The average size of the coccospheres observed was 18.7 μm (n = 17, range: 12–24 μm). Other particles in this size range included diatoms, silicoflagellates, radiolaria, small planktonic foraminifera, fragments of larger representatives of the same, and assorted amorphous biogenic and unidentifiable mineral particles.

The total number of coccospheres, and the calculated fluxes of coccospheres, for each sample are presented in Table 2 and shown graphically in Figure 2. The total number of spheres represents an estimate of the minimum number, since the frequency of coccospheres observed is limited by the methods applied in their enumeration. The range of total coccospheres results from replicate, separate counting procedures performed on various subsamples.

In general, the coccosphere flux decreases with depth at all three sites. The flux is lowest, among the three sites, at Station P_1 where the average flux is greatest in the shallowest trap (378 m), i.e., 122 coccospheres/m^2/day, and is zero at all other depths. At Station E, the flux increases slightly from the shallowest trap (389 m) to the next deeper (988 m), and then decreases to the lowest trap. This increase may, in fact, be an artifact of the laboratory method, considering the range of fluxes calculated (Table 2). The average flux for the entire water column is 4725 coccospheres/m^2/day.

The highest fluxes were calculated at Station PB_1. The average coccosphere fluxes for the shallowest trap (667 m) and for the entire water column were, respectively, 23,413 and 8,030 coccospheres/m^2/day.

Coccolith Studies

Typically, a sample in the hemocytometer exhibited an even distribution of coccoliths, with no aggregates of coccoliths, and no coccospheres. The usual number of coccoliths per 1/25 mm^2 area ranged from 0 to 5.

The term "coccolith" includes all calcareous nannoplankton with round or oval outlines (placoliths), as well as discospheres, ceratoliths, rhabdoliths, helicospheres, and scyphospheres. Additionally, the samples contained whole or fragmented diatoms, radiolaria, silicoflagellates, planktonic foraminifera, and unidentifiable debris.

The total number of coccoliths, calculated flux of coccoliths, and total coccolith carbonate flux, for each sample in the <63 μm particle size range are presented in Table 3 and shown graphically in Figure 3. The range of total coccoliths results from replicate counting procedures performed on various subsamples.

Table 2: Comparison of coccosphere fluxes in <63 μm size fraction. (The range results from several separate counting experiments.)

Station: Depth (m)	Average Total Coccospheres	Range of Total	Average Coccosphere Flux # spheres/m²/day)	Range of Coccosphere Flux # spheres/m²/day)
E: 389	860,092	660,480 – 1,215,283	5,851	4,493 – 8,267
988	1,150,886	60,877 – 2,439,270	7,829	414 – 16,594
3,755	536,832	336,384 – 737,280	3,652	2,288 – 5,016
5,068	231,941	198,676 – 265,206	1,578	1,352 – 1,804
P_1: 378	11,136	0 – 22,272	122	0 – 243
978	0	—	0	—
2,778	0	—	0	—
4,280	0	—	0	—
5,582	0	—	0	—
PB_1: 667	3,933,389	—	23,413	—
1,268	2,085,888	—	12,416	—
2,265	471,020	0 – 942,039	2,804	0 – 5,607
2,869	489,984	0 – 982,941	2,916	0 – 5,851
3,769	145,101	0 – 290,202	864	0 – 1,727
3,791	968,448	0 – 1,936,896	5,764	0 – 11,529

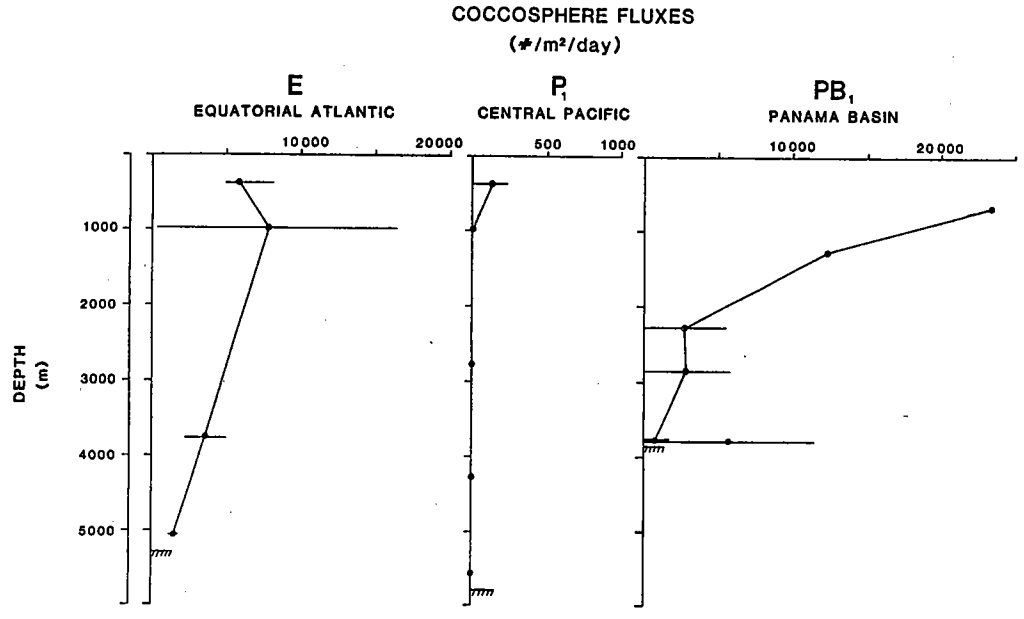

Figure 2: Variation in coccosphere flux with depth at Stations E, P_1, and PB_1. The flux is reported in number of coccospheres/m²/day. Horizontal bars represent range of variation among several counting experiments.

Table 3: Comparison of coccolith fluxes and coccolith-carbonate fluxes in <63 μm size fraction. (The range results from several separate counting experiments.)

Station: and Depth (m)	Average of Total Coccoliths ($\times 10^9$)	Range of Total Coccoliths ($\times 10^9$)	Average Flux of Coccoliths ($\times 10^6$)/m^2/day	Range of Flux of Coccoliths ($\times 10^6$)/m^2/day	Average Coccolith Carbonate Flux mg/m^2/day	Range of Coccolith Carbonate Flux mg/m^2/day
E: 389	51.08	39.6 - 68.3	347.46	269.6 - 464.9	2.78	2.16 - 3.72
988	38.29	12.6 - 75.4	260.47	85.7 - 512.7	2.08	0.68 - 4.10
3,755	18.43	9.2 - 27.6	125.39	62.7 - 188.0	1.00	0.50 - 1.50
5,068	78.20	63.8 - 113.9	531.94	434.0 - 775.0	4.26	3.47 - 6.20
P_1: 378	0.003	—	0.03	—	Tr	—
978	3.07	—	33.57	—	0.27	—
2,778	48.42	30.0 - 70.6	529.13	327.7 - 772.2	4.23	2.62 - 6.18
4,280	69.49	67.6 - 71.4	759.44	738.6 - 780.2	6.08	5.91 - 6.24
5,582	32.26	13.8 - 68.3	352.52	151.1 - 746.7	2.82	1.21 - 5.97
PB_1: 667	198.16	101.4 - 283.8	1,179.50	603.4 - 1,689.6	9.44	4.83 - 13.52
1,268	195.83	150.5 - 272.4	1,165.66	896.0 - 1,621.3	9.32	7.17 - 12.97
2,265	178.25	43.2 - 345.7	1,061.03	257.2 - 2,057.8	8.49	2.06 - 16.46
2,869	187.07	141.9 - 256.8	1,113.52	844.8 - 1,528.7	8.91	6.76 - 12.23
3,769	86.53	59.9 - 106.5	515.05	356.6 - 633.9	4.12	2.85 - 5.07
3,791	71.09	53.2 - 106.5	423.13	317.0 - 633.9	3.38	2.54 - 5.07

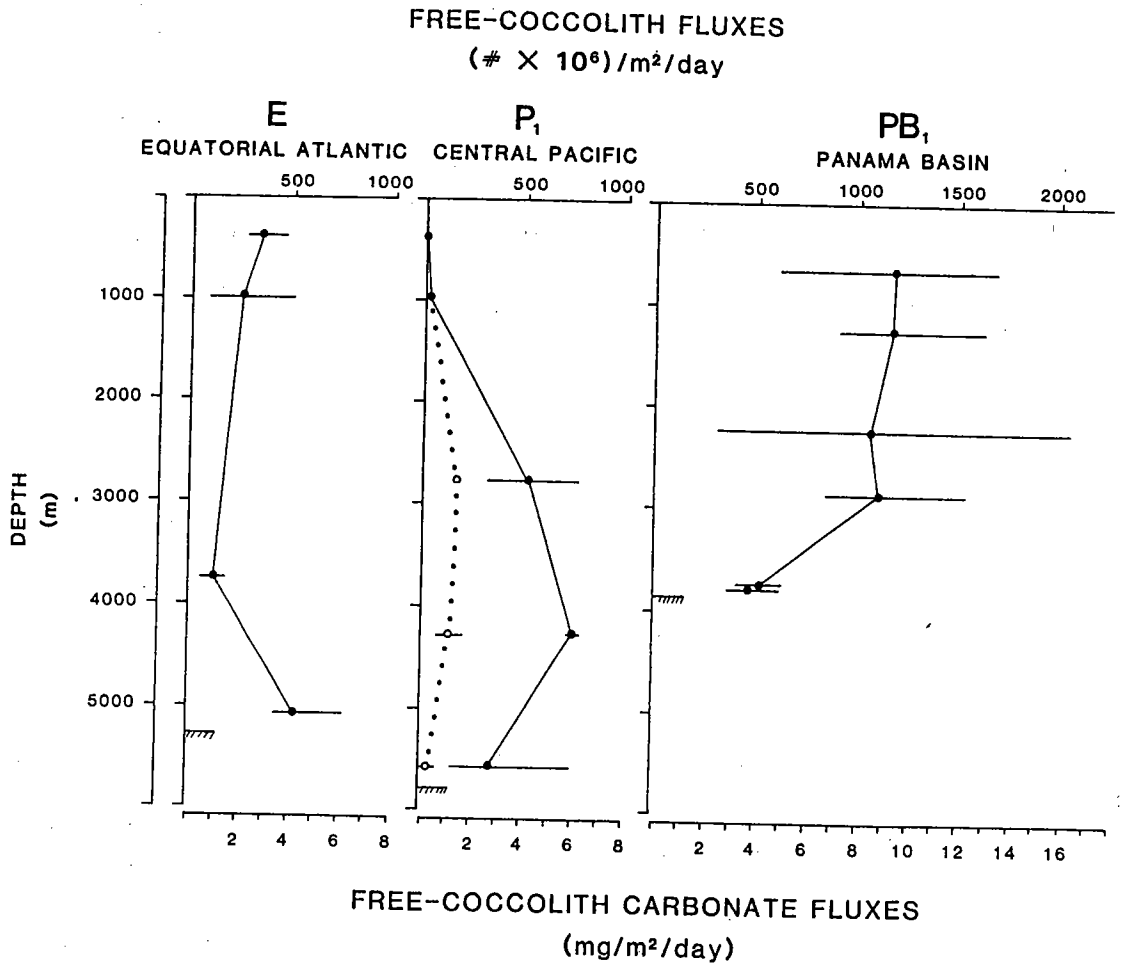

Figure 3: Variation in free-coccolith flux with depth at Stations E, P_1, and PB_1. The flux is reported in coccoliths $(\times 10^6)/m^2/day$ along the upper horizontal axis, and in $mg/m^2/day$ along the lower horizontal axis. Horizontal bars represent range of variations in the calculations resulting from several counting experiments. The dotted line in the P_1 profile represents a "fractional" estimate of the flux (see text for an explanation).

Coccolith fluxes and flux profiles are very different at each of the three sites. At Station E, flux decreases regularly with depth, but increases sharply at the lowermost trap (5,068 m) to its highest value in the profile. The average flux for the entire column is 316×10^6 coccoliths/m^2/day. Station P_1 has a slightly higher average for the entire column, 335×10^6 coccoliths/m^2/day, but the profile is not the same. Instead of decreasing with depth, there is a marked increase in flux below the shallower two traps. The fluxes for these two shallow traps (378 m and 978 m) are the lowest among all traps under consideration, 0.03 and 33.57×10^6 coccoliths/m^2/day, respectively. The average coccolith flux in the Station PB_1 traps is almost three times greater than the average flux in either Station E or P_1 (910×10^6) coccoliths/m^2/day. The uppermost four traps show a steady, similar flux averaging $9.04 \pm .55 \times 10^6$ coccospheres/m^2/day. There is a marked drop in flux in the two lowest traps (3,769 m and 3,791 m) to an average of $3.70 \pm .42 \times 10^6$ coccospheres/m^2/day.

If we assume the average coccolith has a mass of 8×10^{-12} gm (Honjo, 1976), it is possible to express the coccolith fluxes in terms of carbonate fluxes (Table 4 and Figure 4). The average coccolith carbonate fluxes for the entire columns for Station E, P_1, and PB_1, are, respectively, 2.53, 2.68, and 7.28 mg/m^2/day.

Based on biogenic carbonate flux data for each sample (Honjo et al, 1982a), it was possible to calculate the contribution of free-coccolith carbonate in <63 μm size-fraction to the biogenic carbonate flux (Table 4 and Figure 4). This contribution ranges from 0% (Station P_1: 378 m) to 50.67% (Station P_1: 4,280 m). The relative contribution of free-coccolith carbonate to the biogenic carbonate flux is lowest at Station E (averaging 9.1% for the entire column), moderate at Station PB_1 (16.4%), and highest at Station P_1 (26.6%).

SEM Studies

The calcareous nannoplankton recovered in the sediment traps are presented in Table 5 according to the hierarchial classification suggested by Tappan (1980). Fifty-six species, belonging to thirty-three genera and representing fifteen families, are recorded. A census of the taxa present in each trap, including relative frequency and preservational data, is found in Table 6. The most diverse assemblage was found at Station E with 50 species. The least diverse assemblage was found at Station PB_1 with 26 species. Station P_1 had 35 species of coccolithophores.

Preservation of the taxa ranged from good (pristine) to poor in most of the samples. Only at the shallowest trap at each site were all specimens preserved in good condition. In general, well-, moderate-, and poorly-preserved specimens of the same species were all found in the same trap sample. This substantiates two previous assumptions: 1) well-preserved specimens in traps at great depth were rapidly transported there, even through undersaturated waters; and 2) the breakdown of fecal pellets or oceanic aggregates proceeds within (or just above) the traps, allowing coccoliths to be partially, if not wholly, dissolved.

Table 4: Flux of free-coccolith carbonate.

Station	Depth m	Biogenic Carbonate Flux[a] (mg/m²/day)	Free-Coccolith Carbonate Flux (mg/m²/day)	% Free-Coccolith in Biogenic Carbonate Flux
E:	389	43.5	2.78	6.39
	988	27.1	2.08	7.68
	3,755	26.1	1.00	3.83
	5,068	23.0	4.26	18.52
P_1:	378	4.0	Tr	Tr
	978	5.4	.27	5.00
	2,778	11.7	4.23	36.15
	4,280	12.0	6.08	50.67
	5,582	6.8	2.82	41.47
PB_1:	667	41.2	9.44	22.41
	1,268	41.0	9.32	22.73
	2,265	44.9	8.49	18.91
	2,869	50.9	8.91	17.50
	3,769	45.2	4.12	9.12
	3,791	46.9	3.38	7.21

[a]Data from Honjo et al., 1982.

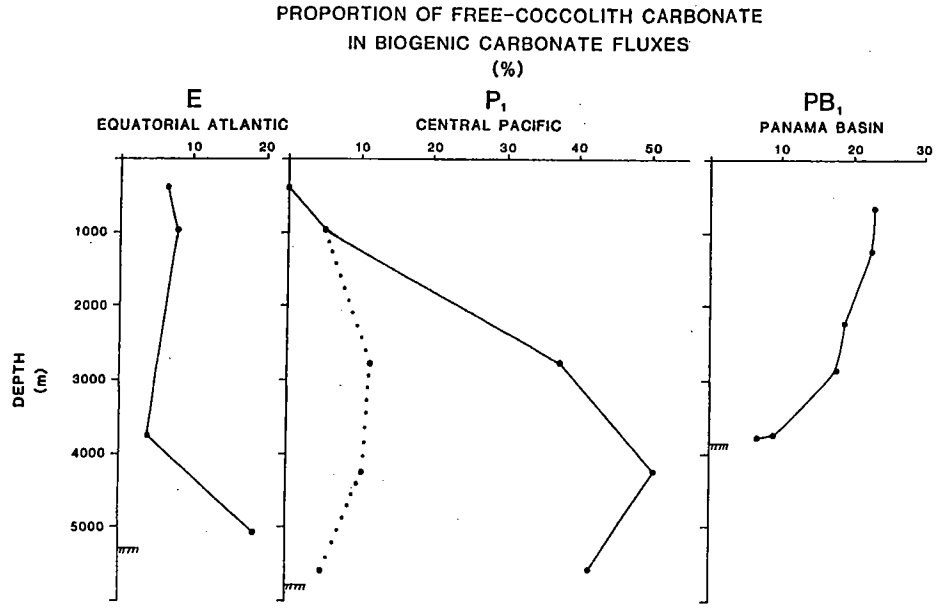

Figure 4: Variation in proportion of free-coccolith carbonate in biogenic carbonate flux with depth at Stations E, P_1, and PB_1. The dotted line in the P_1 profile represents a "fractional" estimate of the flux (see text for an explanation).

Table 5: Taxonomic list of calcareous nannoplankton from sediment traps.

Kingdom PLANTAE

Division HAPTOPHYTA

Class COCCOLITHOPHYCEAE ROTHMALER, 1951

Order ISOCHRYSIDALES PASCHER, 1910

Family GEPHYROCAPSACEAE HAY, 1977

Genus *Crenalithus* ROTH, 1973

C. sessilis (Lohmann) OKADA AND MCINTYRE, 1977

Genus *Emiliania* HAY AND MOHLER, 1967

E. huxleyi (Lohmann) HAY AND MOHLER, 1967

Genus *Gephyrocapsa* KAMPTNER, 1943

G. oceanica KAMPTNER, 1943

Family THORACOSPHAERACEAE SCHILLER, 1930

Genus *Thoracosphaera* KAMPTNER, 1927

T. heimii (Lohmann) KAMPTNER, 1941

T. tuberosa KAMPTNER, 1963

Order ZYGOSPHAERALES HAY, 1977

Family CALYPTROSPHAERACEAE BOUDREAUX AND HAY, 1969

Genus *Calyptrosphaera* LOHMANN, 1902

C. catillifera (Kamptner) GAARDER, 1962

C. oblonga LOHMANN, 1902

C. pirus KAMPTNER, 1937

Genus *Corisphaera* KAMPTNER, 1936

C. gracilis KAMPTNER, 1937

Genus *Helladosphaera* KAMPTNER, 1936

H. aurisinae KAMPTNER, 1941

H. cornifera (Schiller) KAMPTNER, 1937

H. dalmatica (Kamptner) OKADA AND MCINTYRE, 1977

H. fastigata OKADA AND MCINTYRE, 1977

Genus *Homozygosphaera* DEFLANDRE in GRASSÉ, 1952

H. ponticulifera (Kamptner) KAMPTNER, 1954

H. quadriperforata (Kamptner) GAARDER, 1962

H. schilleri (Kamptner) OKADA AND MCINTYRE, 1977

Genus *Sphaerocalyptra* DEFLANDRE in GRASSÉ, 1952

S. marsilii BORSETTI AND CATI, 1976

Order DISCOASTERALES HAY, 1977

Family DISCOASTERACEAE VEKSHINA, 1959

Genus *Hayaster* BUKRY, 1973

H. perplexus (Bramlette and Riedel) BUKRY, 1973

Family CERATOLITHACEAE NORRIS, 1965

Genus *Ceratolithus* KAMPTNER, 1950

C. cristatus KAMPTNER, 1950

Family BRAARUDOSPHAERACEAE DEFLANDRE, 1947

Genus *Braarudosphaera* DEFLANDRE, 1947

B. bigelowi (Gran and Braarud) DEFLANDRE, 1947

Table 5 (Continued)

Order EIFFELITHALES ROOD, HAY, AND BARNARD, 1971
Family PONTOSPHAERACEAE LEMMERMANN in BRANDT AND APSTEIN, 1908
Genus *Pontosphaera* LOHMANN, 1902
P. messinae BARTOLINI, 1970
P. multipora (Kamptner) ROTH, 1970
Family SCYPHOSPHAERACEAE JAFAR, 1975
Genus *Scyphosphaera* LOHMANN, 1902
S. apsteinii LOHMANN, 1902
Family HELICOSPHAERACEAE Black, 1971, emend. JAFAR AND MARTINI, 1975
Genus *Helicosphaera* KAMPTNER, 1954
H. carteri (Wallich) KAMPTNER, 1954
H. hyalina GAARDER, 1970
H. pavimentum OKADA AND MCINTYRE, 1977
H. wallichii (Lohmann) OKADA AND MCINTYRE, 1977
Family CALCIOSOLENIACEAE KAMPTNER, 1937
Genus *Anoplosolenia* DEFLANDRE in GRASSÉ, 1952
A. brasiliensis (Lohmann) DEFLANDRE in GRASSÉ, 1952
Genus *Scapholithus* DEFLANDRE in DEFLANDRE AND FERT, 1954
S. fossilis DEFLANDRE in DEFLANDRE AND FERT, 1954
Order COCCOLITHALES SCHWARZ, 1932 orth. mut., Rood, Hay, and Barnard, 1971
Family COCCOLITHACEAE POCHE, 1913 orth mut., Kamptner, 1928
Subfamily COCCOLITHOIDEAE KAMPTNER, 1928
Genus *Oolithotus* REINHARDT in COHEN AND REINHARDT, 1968
O. fragilis (Lohmann) OKADA AND MCINTYRE, 1977
Subfamily TERGESTIELLOIDEAE REINHARDT, 1966
Genus *Cyclococcolithus* KAMPTNER, 1954
C. leptopora (Murray and Blackman) KAMPTNER, 1954
Genus *Umbilicosphaera* LOHMANN, 1902
U. calvata STEINMETZ, n. sp.
U. hulburtiana GAARDER, 1970
U. scituloma STEINMETZ, n. sp.
U. sibogae (Weber-van Bosse) GAARDER, 1970

Table 5 (Continued)

Order SYRACOSPHAERALES HAY, 1977
Family SYRACOSPHAERACEAE LEMMERMANN in BRANDT AND APSTEIN, 1908
Genus *Alisphaera* HEIMDAL, 1973
A. spatula STEINMETZ, n. sp.
Genus *Anthosphaera* KAMPTNER, 1936
A. oryza (Schlauder) GAARDER in GAARDER AND HASLE, 1971
Genus *Coronosphaera* GAARDER AND HEIMDAL, 1977
C. binodata (Kamptner) GAARDER AND HEIMDAL, 1977
Genus *Syracosphaera* LOHMANN, 1902
S. lamina LECAL-SCHLAUDER, 1951
S. molischi SCHILLER, 1925
S. pulchra LOHMANN, 1902
Family HALOPAPPACEAE KAMPTNER, 1928
Genus *Deutschlandia* LOHMANN, 1912
D. anthos LOHMANN, 1912
Genus *Florisphaera* OKADA AND HONJO, 1973
F. profunda OKADA AND HONJO var. *profunda* OKADA AND HONJO, 1973
F. profunda OKADA AND HONJO var. *elongata* OKADA AND MCINTYRE, 1979
Genus *Halopappus* LOHMANN, 1912
H. adriaticus SCHILLER, 1914
Genus *Thorosphaera* OSTENFELD, 1910
T. flabellata HALLDAL AND MARKALI, 1955
Family RHABDOSPHAERACEAE LEMMERMANN in BRANDT AND APSTEIN, 1908
Genus *Discosphaera* HAECKEL, 1894
D. tubifera (Murray and Blackman) LOHMANN, 1902
Genus *Rhabdosphaera* HAECKEL, 1894
R. clavigera MURRAY AND BLACKMAN, 1898
R. stylifera LOHMANN, 1902
Genus *Umbellosphaera* PAASCHE in MARKALI AND PAASCHE, 1955
U. irregularis PAASCHE in MARKALI AND PAASCHE, 1955
U. tenuis (Kamptner) PAASCHE in MARKALI AND PAASCHE, 1955

Table 6: Index to taxa illustrated in Plates 1–22 and census of taxa present in each trap, including relative frequency and preservational data. Frequency designations: **R** = rare, **F** = frequent, **C** = common, **A** = abundant, **D** = dominant. See text for further explanation. Preservation designations: **G** = good, **M** = moderate, **P** = poor.

Species	Plate Nos.	Figure Nos.	Station: and Depth (m)													
			E: (389)	E: (988)	E: (3,755)	E: (5,068)	P_1: (378)	P_1: (978)	P_1: (2,778)	P_1: (4,280)	P_1: (5,582)	PB_1: (667)	PB_1: (1,268)	PB_1: (2,265)	PB_1: (2,869)	PB_1: (3,769)	PB_1: (3,791)
Alisphaera spatula n. sp.	15	6–8	FG														
Anoplosolenia brasiliensis	13	3		RG	FG	RG	FG										RG
Anthosphaera oryza	16	1–8	CG	CG	FG	RG	FG					RG					
Braarudosphaera bigelowi	10	1–2							RG								
Calcidiscus leptopora	14	3–6	FG	FG	FM	FM			FG	FG	FM	FG	FM	FG	FG	FG	FM
Unidentified sp.	22	5–6														RG	
Calyptrosphaera catillifera	6	1–3	RG	FG	RM	RG											
Calyptrosphaera oblonga	6	4–5	RG	RG													
Calyptrosphaera pirus	6	6–8	FG	FG	FG												
	7	1–2															
Ceratolithus cristatus	9	5–8					FG		FG	RG	RG						
Corisphaera gracilis	7	3	RG														
Coronosphaera binodata	17	1–3	RG		RG				FG						FG		
Crenalithus sessilis	1	1–4	FG	FG	FG		FG	FG	FG	FG	FG	FG		FG		FG	
Deutschlandia anthos	18	6–8							FG			FG					
Discoaster brouweri	9	1				RG											
Discoaster quinqueramus	9	2				RG											
Discosphaera tubifera	19	8	CG	FG	FG				FM	FM		FM					
Emiliania huxleyi	1	5–8	AG	AM	AM	AM	FG	AM	AM	AG	AM	AG	AM	AM	AM	AM	AM
	2	1–2															
Florisphaera profunda	19	1–4	FG		FG	FG	FG		FG	AG	CM						
	2	3–8															
Gephyrocapsa oceanica	3	1–8	FG	FM	FG	AM	FM	CG	CG	CG	FM	AG	AM	AM	AM	AM	AM
	4	1, 3															
Halopappus adriaticus	19	5–7	FG	RG	FG	FG				RM		FM	FG	FG	RP		FG
Hayaster perplexus	9	3–4	RG		FG			RG	RG	FM				RG			
Helicosphaera carteri	12	1–4	RG	FM	FM				FG	RG		FG	FG			FG	RG
Helicosphaera hyalina	12	5, 7	RG	FG			RG		FG	RG		RG			RM	RM	
Helicosphaera pavimentum	12	6, 8	FG	RG	RG	RG			RM			RM				RG	
Helicosphaera wallachii	13	1–2	RG	RG	FM								RG				
Helladosphaera aurisinae	7	4	RG														
Helladosphaera cornifera	7	5	RG		RG												
Helladosphaera dalmatica	7	6	RG	RG	RG							RM					
Helladosphaera fastigata	7	7–8											FG				
	8	1															

Table 6 (Continued)

Species	Plate Nos.	Figure Nos.	Station: and Depth (m)													
			E: (389)	E: (988)	E: (3,755)	E: (5,068)	P_1: (378)	P_1: (978)	P_1: (2,778)	P_1: (4,280)	P_1: (5,582)	PB_1: (667)	PB_1: (1,268)	PB_1: (2,265)	PB_1: (2,869)	PB_1: (3,769)	PB_1: (3,791)
Homozygosphaera ponticulifera	8	2			RG	RG											
Homozygosphaera quadriperforata	—	—	RG														
Homozygosphaera schilleri	8	3–6	RG	FG	RG				RG								
Oolithotus fragilis	14	1–2	RG	FG	RG				FG	FG	RG						
Pontosphaera messinae	10	3–6	RG		RG												
Pontosphaera multipora	10	7–8	RG	RG		RG			RG								
	11	1–5															
Rhabdosphaera clavigera	20	1–2		FG	FG		RG		RG	FG	FM						
Rhabdosphaera stylifera	20	3–4	FG	FG	FG				FG	FG							
Scapholithus fossilis	13	5–8	FG	FG	FM	RM			FG	FG	RG	FG			RG		
Scyphosphaera apsteinii	11	6–8		RG	RG				RG								
Sphaerocalpytra marsilii	8	7–8		FG													
Syracosphaera lamina	17	4–6	FG	FG	FG	FM			FG	FG		FG					
Syracosphaera molischi	17	7–8					RG		RG	FM							
Syracosphaera pirus	18	1–2			FG				RG								
Syracosphaera pulchra	18	3–5	FG	CM	FG	FG		FM	FG	FG	FG			RP	RP	FM	
Thoracosphaera heimii	4	2, 4	RG								RM						
Thoracosphaera tuberosa	4	5–8						RG	RG								RG
Thorosphaera flabellata	—	—		RG	RG												
Umbellosphaera irregularis	20	5–8	AG	AG	AG	CM	FM	AM	CM	CG	CM	CG	FM	RG	FM		
	21	1–4															
Umbellosphaera tenuis	21	5–8	FG	CG	CG		FM	RP	CG	FG	CM	RM		RM			
	22	1–2															
Umbilicosphaera calvata n. sp.	5	1–4			FG				FG			CG	FG	FG	FM		FG
Umbilicosphaera hulburtiana	—	—			FG				RG	RG							
Umbilicosphaera scituloma n. sp.	5	5, 6	FM									CG					
Umbilicosphaera sibogae	14	7, 8	FG	FG	FG	CM	FG	CM	DM	DG	DG	CG	CM	CM	FG	CG	FM
	15	1–5															
Unidentified sp. 1	22	3, 4	RG														
Unidentified sp. 2	22	7	RG														
Unidentified sp. 3	22	8	RG														
Total Number of Species			39	30	35	18	13	9	31	22	14	19	10	12	10	9	9

Table 7: Comparison of fluxes at the three sediment-trap sites.

Site	Average Mass Flux[a] (mg/m²/day)	Average Biogenic Fraction[a] (%)	Average Biogenic Flux[a] (mg/m²/day)	Average Biogenic Carbonate Flux[a] (mg/m²/day)	Average Coccosphere Flux (# spheres/m²/day)	Average Coccolith Flux ((×10⁶)/m²/day)
E	53.0	80.3	42.5	28.5	4728	316.3
P_1	12.8	97.2	12.4	7.6	24	334.9
PB_1	143.4	72.0	103.3	42.9	8030	909.6

[a]Calculated from data in Honjo et al., 1982.

Discussion

Total Calcareous Nannoplankton Flux

The flux of biogenic material (i.e., carbonate, silica, and organic matter) in the water column is a reflection of the biological productivity of the surface water. The differences in fluxes at the three sediment trap sites indicate the variation in surface productivity. This is apparent in the average total biogenic mass fluxes and the average total carbonate fluxes, as well as in the coccosphere and coccolith fluxes. Data from Honjo et al. (1982a) were used to calculate these values; see Table 7. The lowest fluxes (i.e., average biogenic flux, average biogenic carbonate flux, average coccosphere flux, and average coccolith flux) were recorded at Station P_1 in the low productivity region of the central Pacific. Intermediate flux values occur at Station E in the equatorial Atlantic. The highest values occur in the Panama Basin, Station PB_1, in a region of coastal upwelling. There, flux values are approximately double or more for each of the parameters measured. Modification of the coccolith-carbonate flux by carbonate dissolution is indicated by the apparent decrease of flux with depth. The only deviation from this trend is seen in the average coccolith flux value for Station P_1. This will be explained in the section below.

Station P_1, Central Pacific

The coccosphere and coccolith fluxes at Station P_1 are unusual for several reasons. First the average coccosphere flux is 24 coccospheres/m^2/day, almost 200 times lower than the flux at Station E (Table 7). Were it in proportion to the average biogenic carbonate flux seen at the other two sites, an average flux of about 1,300 coccospheres/m^2/day would be expected. Second, the free-coccolith flux increases with depth (Table 3 and Figure 3). This results in an anomolously high average coccolith flux for the site. It is also remarkable, since the profile of coccolith flux decreases with depth at the other two sites, which is normal considering the increased dissolution of calcium carbonate with depth.

In explaining this unusual profile, I initially suspected an artifact from the laboratory procedure. I repeated the coccolith enumerations using the hemocytometer, but this time counted only those coccoliths that could be identified as such without equivocation. (The reasoning for this second count was that some of the small circles and ovals seen through the microscope, and perhaps counted, may have been dead ciliates or fragments of diatoms or radiolaria, thus inflating the counts). The recount did not indicate this to be a problem.

The "fractional" profile (shown in Figures 3 and 4 by the long-dashed line in the Station P_1 profile) thus represents the contribution of ceratoliths, helicospheres, rhabdoliths, and scyphospheres only (i.e., calcareous nannoplankton with unique shapes). This fractional profile is also seen to increase with depth before decreasing at the lowermost trap, thus paralleling the original (total count) coccolith flux. The answer to the reason for the unusual trend was provided by SEM examination of the samples. The "bulge" in the profile is due mainly to the predominance of one species in the assemblages, *Umbilicosphaera sibogae*. What the profile likely represents is the record of a nannoplankton bloom which occurred on the surface just before the sediment-trap array was deployed in September 1978.

The coccospheres and coccoliths produced in the bloom were apparently already packaged in fecal pellets or other oceanic aggregates and had descended below the second trap depth (978 m) when the trap array was deployed. Hence, the intermediate traps (2,778 m and 4,280 m) and lowest trap (5,582 m) collected material already "in transit" to the seafloor.

Evidence of the blooms of *U. sibogae* have also been observed by Honjo et al. (1982b) and Honjo (1982) in the Panama Basin. Using rotating collector cups on sediment traps to provide a means to determine the seasonality of fluxes and flux constituents, they noted that 93% of the June/July 1980 flux was accounted for by *U. sibogae*. At Station P_1, the bloom was not constrained only to this one species of coccolithophore, since the "fractional" members of the assemblage are also seen to increase with depth. Why this is not reflected in the coccosphere flux profile is not readily evident; however, *U. sibogae* was seldom observed with the SEM in whole coccospheres at any of the stations or depths. This suggests that the coccosphere of *U. sibogae* easily disaggregates and may not survive the passage through a zooplankton gut except as individual coccoliths.

In the late summer and early fall 1969, an oceanographic expedition aboard the R/V HAKUHO MARU collected along a north-south transect along the 155°W meridian of longitude. The coccolithophore community was studied in the surface-water and subsurface-water column down to 200 m (Okada and Honjo, 1973; Honjo and Okada, 1974). Station P_1 (15°21′N, 151°28′W) is close enough to permit comparison of coccolith assemblages between 10° and 25°N within the North Equatorial Current. Okada and Honjo (1973) reported that *Umbellosphaera irregularis* was the dominant species in the surface waters, usually comprising more than 50% of the assemblage. The next most abundant species was *Emiliania huxleyi* (less than 20%), followed, in approximate decreasing abundance, by *Discosphaera tubifera, Umbellosphaera tenuis, Umbilicosphaera sibogae, Umbilicosphaera hulburtiana, Rhabdosphaera clavigera*, and *Syracosphaera* spp. The dominant species was replaced in the lower photic waters (125–200 m) by two deep-water species, *Florisphaera profunda* and *Thorosphaera flabellata* (together commonly accounting for more than 70% of the assemblage).

In the present study, species in assemblages were evaluated in terms of relative frequency (see Table 6), so direct comparison with the results of Okada and Honjo (1973) and Honjo and Okada (1974) is not possible. However, several points are noteworthy. First, with the exception of one taxon, all species mentioned above occur regularly and frequently at Station P_1. The exception is *Thorosphaera flabellata*; it was not recorded at Station P_1. Second, *Umbellosphaera irregularis* was usually common to abundant in Station P_1 traps,

but it was not dominant in any assemblage. Finally, *Umbilicosphaera sibogae* never accounted for more than 10% of any assemblage within waters of the North Equatorial Current along the 155°W transect in the study by Okada and Honjo (1973) and Honjo and Okada (1974), yet it was dominant at depth in Station P_1 traps. The last two points are, again, probably best explained by the seasonal, fall blooming of *Umbilicosphaera sibogae* in the North Equatorial Current.

While the evidence for a bloom at Station P_1 is not altogether overwhelming, it does, at least, support the limited evidence at hand. Until more seasonal and time-related studies can be run, it is best to remember a comment by Sheldon (1984, p. 1345) to help us accommodate the hypotheses advanced to explain such strange phenomena: "... The oligotrophic central regions of the ocean have often been compared to deserts, but they resemble deserts in only one characteristic—low biomass. In their other features, notably, high growth rates and rapid recycling, they perhaps more closely resemble tropical forests."

Station E, Equatorial Atlantic

The coccosphere and coccolith flux profiles at this station are not unusual, except that the coccolith flux increases sharply in the lowermost trap (5,068 m). An increase with depth in clay and rock forming minerals also was noted by Honjo (1980). All other flux profiles show a tendency of materials to decrease with depth, an indication of progressive dissolution with depth. Collectively, these observations suggest that the sharp increase in the coccolith, clay, and rock forming mineral fluxes are due to two possibilities. They could result from the resuspension of *in situ* sediment. The bottom sediment is firm silty clay (Honjo, 1980). The lowermost trap is 724 m above the sea-floor. Alternatively, the sediments could result from the horizontal advective transport of very fine particles from the Amazon Cone. The mineralogy of the clays in the region of the Amazon Cone and in the lowermost trap appears to be similar (Milliman et al., 1975; Emelyanov and Trimonis, 1977; Honjo, 1980). Deep advective transport of lithogenic particles has been demonstrated in the Panama Basin (Honjo et al, 1982c; 1982d). Smectite caught there in sediment traps originated from the continental slope northeast of the station and was laterally transported at mid-water depths to the station.

The presence of the calcareous nannofossils *Discoaster brouweri* TAN SIN HOK (extinct since the end of the Pliocene) and *Discoaster quinqueramus* GARTNER (extinct since the late Miocene) in the Station E trap demonstrates the fact that particles at least about 7 μm in diameter are being resuspended or transported from elsewhere.

Station PB_1, Panama Basin

The high productivity of the upwelling water in the Panama Basin is demonstrated in the coccosphere and coccolith fluxes. The average coccosphere flux for the water column at Station PB_1 is almost twice that the the equatorial Atlantic, Station E (8,030 vs. 4,728 coccospheres/m^2/day). The average coccolith flux at Station PB_1 is almost three times that for Station E (909.65×10^6 vs. 316.32×10^6 coccoliths/m^2/day). The average coccolith flux measured in <63 μm portion is 7.28 mg/m^2/day or about 17.2% of the biogenic carbonate flux. The coccosphere flux decreases irregularly with depth (Table 2 and Figure 2). The shallowest trap shows a flux of about 23,400 coccospheres/m^2/day. The next deepest

(1,268 m) has about half that, the next two traps (2,804 m and 2,916 m) about one-fourth of that. The lowermost trap shows an increased flux for an unknown reason.

The flux of coccoliths through the water column shows an unusual profile. The flux of coccolith carbonate at the topmost four traps is almost the same, averaging 9.04 mg/m^2/day (s.d. = .43; range: 8.49–9.44 mg/m^2/day). There is a rapid decrease to the lowermost two traps to an average flux of 3.75 mg/m^2/day (Figure 3). The change in flux between the upper traps and the lower traps represents a decrease of 58.6%. These results correlate well with the findings of Thunell et al. (1981), who conducted an *in situ* study of calcite dissolution in the Panama Basin using foraminifera. Their results also indicated that the rate of dissolution in the water column increased at 2,869 m, but particularly below that depth. This coincides with the depth at which the calcium carbonate content of surface sediments began to decrease rapidly (the sedimentary lysocline). They concluded from their study that neither the sedimentary lysocline nor the hydrographic lysocline could be directly related to a transition from saturation to undersaturation.

The Fate of Coccoliths Suspended at Depth

Fecal pellets produced by zooplankton serve as a means of vertical transport of coccoliths and coccospheres from the euphotic zone to the deep-sea floor (Honjo, 1976). This was first suggested by Lohmann (1902). Since then coccoliths have been reported in the gut contents of various zooplankton (Murray and Hjort, 1912; Esterly, 1966; Mullin, 1966), as well as in zooplankton fecal pellets (Marshall and Orr, 1956, 1962; Bernard, 1963; Roth et al., 1975; Honjo and Roman, 1978). Fecal pellets also serve to protect coccoliths in their descent through undersaturated waters. This role has been directly demonstrated by scanning electron microscopy (Schrader, 1971; Honjo, 1975; Roth et al., 1975; Honjo and Roman, 1978).

Coccoliths and coccospheres apparently pass through the alimentary canal of copepods with no dissolution effect. While Marshall and Orr (1955) stated that the gut of copepods is acidic, Honjo and Roman (1978) found no evidence to support this. Aragonite crystals mixed with food were fed to copepods. These crystals readily dissolved in solution with slightly lowered pH (<6), but showed no evidence of dissolution or etching in the fecal pellets. Honjo and Roman concluded that the pH of the copepod gut was close to that of seawater, and that coccoliths, including delicate forms such as *Umbilicosphaera irregularis*, would not show any dissolution in natural fecal pellets. Honjo and Roman (1978) suggested that fecal pellets are thus protective rather than destructive to skeletal particles of less than 10 μm. The present study indicates that the lower limit of "protection" certainly extends to the sub-micron range. *Calyptrosphaera catillifera* and *Helladosphaera fastigata*, both composed of calcite crystallites less than 0.1 μm in diameter, were found intact and showed no evidence of dissolution.

The sinking rates of fecal pellets have been variously reported. Wiebe et al. (1976) collected pellets in sediment traps and measured their sinking rates in the laboratory. Rates ranged from 50 to 225 m/day, with a mean of 160 m/day. Honjo and Roman (1978) measured the sinking rates of fecal pellets from copepods fed *Emiliania huxleyi* in the laboratory. The sinking rates for fecal pellets from *Acartia tonsa* were approximately 120 m/day (range 80 to 150 m/day) and for the larger pellets from *Calanus finmarchicus*, 180 to 220 m/day.

Pellets produced in the laboratory were less dense than fecal pellets of similar size from sediment traps. Pilskaln (1982) calculated the sinking rate of green fecal pellets and found that 75% descended 237–750 m/day (mean: 343 m/day). Residence time in the deep ocean is a few weeks to months. The lateral displacement of a pellet through a 4-km deep water column, assuming unidirectional advection of 3 cm/sec., could be between 26 and 39 km. The resulting sediment thanotocoenosis would reflect variability in oceanic biocoenosis of this scale (Bishop et al., 1977).

Intact fecal pellets account for only 10% to 20% of the coccolith flux (Honjo et al., 1982a). Moreover, fecal pellets account for only a small fraction of the total biogenic carbon flux (carbonate flux plus organic flux) to deep water. The bulk of carbonate and organic matter is believed to be transported in particles variously known as macroscopic amorphous aggregates, large amorphous aggregates, or 'marine snow' (Bishop et al., 1977; Silver et al., 1978; Alldredge, 1979; Honjo et al., 1982a). While the origin of these aggregates is not fully understood, they are believed to come from the disintegration of fragile fecal pellets or other particulate organic matter (zooplankton fragments, free algal cells, pigmented granules, and waxy particles) (Honjo et al., 1982a). Laboratory experiments indicate that the sinking rate of amorphous aggregates (ranging from 10 to 100 m/day) is equivalent to that of middle-sized fecal pellets (Bishop et al., 1977; Shanks and Trent, 1980; Alldredge and Cox, 1982). Fecal pellets are believed to be particularly efficient in transporting surface-induced fine particles, while settling amorphous aggregates are thought to play the dominant role in transport to the deeper layers (Honjo, 1984).

Okada and Honjo (1973) observed up to 100 suspended coccoliths per liter in the deep equatorial Pacific. The abundant suspended coccoliths distributed at depth in the ocean are presumed to have been spilled from fecal pellets (Honjo, 1975). Coprophagy (Frankenberg and Smith, 1967; Paffenhöfer and Strickland, 1970), bacterial degradation (Johannes and Satomi, 1966), and other modes of destruction (Smayda, 1969) of the protective organic pellicle surrounding the fecal pellet are believed largely responsible for the breakage of pellets at depth. Microbial activity, however, is very slow in the deep sea (Jannasch and Wirsen, 1973). Fresh coccoliths and coccospheres are thus continually replenished at all depths by rapidly descending fecal pellets or aggregates. Once spilled or released from a fecal pellet, coccoliths undergo a thousandfold decrease in their rate of descent (Honjo, 1976). Moreover, they are fully exposed to the undersaturated deep water and proceed to undergo immediate dissolution (Honjo, 1975, 1976). Hence, only very recently spilled coccoliths are collected by sediment traps, which explains the presence of undissolved coccoliths in undersaturated water.

In the present study, except in the shallowest trap from each of the sediment trap sites, coccoliths were found in all stages of preservation at all depths. Not only were well-preserved, as well as nearly-dissolved, forms found in even the deepest traps, but the ratio of well-preserved to poorly-preserved forms did not change with depth. In the shallowest traps, only well-preserved forms were found; any dissolution was minimal. The diversity of the assemblage changed with depth, in general, decreasing with depth. At Stations E and PB_1 the number of species in the lowermost traps contained half the number found in the shallowest. This evidence of selective dissolution with depth was most apparent among the holococcoliths (e.g., *Calyptrosphaera, Corisphaera, Helladosphaera*, and *Homozygosphaera*); rarely were specimens observed below about 3,800 m.

These general trends were also noted by Honjo (1975) in his analysis of suspended coccoliths retrieved in filtered water samples from various depths in the Pacific Ocean. However, he did not observe any strongly dissolved coccoliths. The microarchitecture of coccoliths is such that even a slight amount of dissolution will greatly weaken the entire structure. Honjo (1975) suggested that the weakened forms disintegrated and were lost during filtration. The presence of well-preserved, or pristine, forms at depth, particularly in undersaturated waters, indicates that fecal pellets and aggregates do provide means of protection and rapid transport to these depths. It also indicates that the free-coccoliths were released from the fecal pellets or aggregates immediately above the trap mouths, that the fecal pellet pellicles broke or were biodegraded within the traps, or that the pellets merely broke during the mechanical handling of the samples. Any exposure of free-coccoliths to the undersaturated deep waters would likely result in immediate dissolution, so it is reasonable to assume that the pristine forms are derived from fecal pellets and aggregates broken in laboratory handling of the samples. This is supported by the observations of Honjo and Roman (1978), that the "green" fecal pellets are loosely formed and easily broken. Similarly, Pilskaln (1982) noted that large fecal pellets, such as produced by salps and euphausids and contributing a large proportion to the flux, also have a soft consistency thus assuring their breakdown in the sediment trap, or certainly in the laboratory.

Conclusions

1. Coccospheres and coccoliths can be effectively enumerated in sediment trap samples utilizing settling chamber-inverted microscope techniques and hemocytometer counting chamber techniques.

2. Coccosphere fluxes at the three sampling sites range from zero at depth at Station P_1 up to 23,400 coccospheres/m^2/day in the high productivity region of the Panama Basin. In general, coccosphere flux decreases with depth in the ocean.

3. Coccolith fluxes range from trace levels (Station P_1, 378 m) up to over 2000 $\times$ 10^6 coccoliths/m^2/day in the Panama Basin. Coccolith flux profiles differ at each of the three sample sites. In general, the flux tends to decrease with depth in the ocean, except in the central Pacific where the increased flux at depth is due to a suspected coccolithophore bloom (particularly *Umbilicosphaera sibogae*) which occurred shortly before the sediment trap array was deployed in September 1978. A marked increase in the flux at the lowermost trap in the equatorial Atlantic is attributed to either resuspension of bottom sediment or advective transport of fine material into the sediment trap.

4. The average coccolith carbonate fluxes for the entire columns for Stations E, P_1, and PB_1, are respectively, 2.53, 2.68, and 7.28 mg/m^2/day. These fluxes represent minimum values, since coccospheres and coccoliths in the <63 μm-sized fraction were studied. Coccospheres and coccolith contained in fecal pellets and other particles were not considered.

5. The relative contribution of free-coccolith carbonate in <63 μm-sized fraction to the biogenic carbonate flux is lowest at Station E (averaging 9.1% for the entire column),

moderate at Station PB_1 (16.4%), and highest at P_1 (26.6%). The high value at Station P_1 is almost entirely attributable to the coccolithophore bloom.

6. SEM examination of all the sediment trap samples revealed 56 species of calcareous nannoplankton belonging to 33 genera. The most diverse assemblage was found at Station E (50 species), the least diverse at Station PB_1 (26 species), and Station P_1 with an intermediate level (35 species).

7. Preservation of the taxa ranged from good (pristine) to poor in all the traps except the shallowest at each site where all specimens were preserved in good condition. Well-preserved specimens in traps at greater depths were rapidly transported there, even through undersaturated waters, in fecal pellets or amorphous aggregates. The breakdown of fecal pellets or aggregates proceeds within or just above the traps, allowing coccoliths to be partially, if not wholly, dissolved. This explains why fragile taxa, such as holococcoliths, are found preserved in only the shallower traps in an array, and why there is a general decrease in the diversity of an assemblage with depth.

8. An atlas of calcareous nannoplankton recovered in the sediment traps is presented. Three new species are described and illustrated: *Alisphaera spatula* n. sp., *Umbilicosphaera calvata* n. sp., and *Umbilicosphaera scituloma* n. sp.

Systematics of New Species

Kingdom PLANTAE
Division HAPTOPHYTA
Class COCCOLITHOPHYCEAE ROTHMALER, 1951
Order COCCOLITHALES SCHWARZ, 1932 orth.
mut. ROOD, HAY, AND BARNARD, 1971
Family COCCOLITHACEAE POCHE, 1913 orth.
mut. KAMPTNER, 1928
Subfamily TERGESTIELLOIDEAE REINHARDT, 1966
Genus *Umbilicosphaera* LOHMANN, 1902

Umbilicosphaera calvata STEINMETZ new species
Plate 5, figures 1–4

Cricosphaera sp. I CONNLEY, 1979, p. 28; pl. 5, fig. 14; pl. 6, fig. 11.

DERIVATION OF NAME: From Latin, *calvata*, bald or made bare.

DESCRIPTIO COCCOLITHORUM: *Coccolithi simplices ovati, magna centralia foramina habentes. Bina scuta fistula brevissima coniunguntur. Scuta distalia sunt paullo maiora interque elementa eorum subimbricata suturae rectae intersunt. Sunt in scutis distalibus c. 32 elementa latitudinibus diversis. Scuta proximalia a proximali parte observata aliquantulum convexa videntur. Suturae elementorum minus apparent omnesque se leviter in dexteram partem ab interiore peripheria in exteriora inclinant.*

DESCRIPTION OF COCCOLITHS: Simple elliptical coccoliths with large central openings. The two shields are connected by a very short tube. The distal shields are slightly larger and have straight sutures between slightly imbricate elements. There are about 32 elements of differing widths in the distal shields. The proximal shields are slightly convex when viewed proximally. The element sutures are less distinct and all inclined slightly to the right, from the inner periphery outward.

DIMENSIONS:

distal shield length:	4.2–4.6 μm,	width:	3.6–3.9 μm;
proximal shield length:	3.75–4.0 μm,	width:	3.1–3.25 μm;
central opening length:	2.5–2.75 μm,	width:	2.0–2.1 μm.

HOLOTYPE: Plate 5, figure 2. Negative 17-X-24.

HOLOTYPE DIMENSIONS:

distal shield length:	4.6 μm,	width:	3.9 μm;
proximal shield length:	4.0 μm,	width:	3.25 μm;
central opening length:	2.75 μm,	width:	2.1 μm.

TYPE LOCALITY: Panama Basin, Pacific Ocean (5°21′N, 81°53′W), PARFLUX Station PB_1.

BIOGEOGRAPHY: *Umbilicosphaera calvata* n. sp. occurs in frequent numbers at all three PARFLUX sites investigated in this study: equatorial Atlantic (Station E), central Pacific (Station P_1), and Panama Basin (Station PB_1). It also occurs in the Coral Sea (Conley, 1979).

Umbilicosphaera scituloma STEINMETZ new species
Plate 5, figures 5–6

Cricosphaera sp. II CONLEY, 1979, p. 28; pl. 5, fig. 17; pl. 6, fig. 10.

DERIVATION OF NAME: From Latin, *scitula*, handsome, pretty, elegant; plus *loma*, fringe, hem, border.

DESCRIPTIO COCCOLITHORUM: *Coccolithi simplices ovati, magna centralia foramina habentes. Bina scuta brevissima fistula coniunguntur. Scuta distalia paullo maiora sunt interque c. 35 elementa suturae rectae intersunt. Haec elementa sunt leviter imbricata et latitudine fere paria. Breves spinae atque truncatae a media regione distali super vel omnia vel paene omnia elementa prominent. Scuta proximalia a proximali parte observata aliquantulum convexa videntur. Suturae elementorum in scutis proximalibus minus apparent.*

DESCRIPTION OF COCCOLITHS: Simple elliptical coccoliths with large central openings. The two shields are connected by a very short tube. The distal shields are slightly larger and have straight sutures between about 35 elements. The elements are slightly imbricate and of approximately equal width. Short, blocky spines project from the distal central area over all, or almost all, of the elements. The proximal shields are slightly convex when viewed proximally. The element sutures of the proximal shield are less distinct.

HOLOTYPE: Plate 5, figure 5. Negative 17-X-20.

HOLOTYPE DIMENSIONS:

distal shield length:	5.2 μm,	width:	4.4 μm;
central opening length:	3.3 μm,	width:	2.5 μm;
length of spine:	about 0.1 μm.		

TYPE LOCALITY: Panama Basin, Pacific Ocean (5°21′N, 81°53′W), PARFLUX Station PB_1.

BIOGEOGRAPHY: *Umbilicosphaera scituloma* n. sp. occurs in frequent numbers at Station E in the equatorial Atlantic, and in common numbers at Station PB_1 in the Panama Basin. It also occurs in the Coral Sea (Conley, 1979).

Order SYRACOSPHAERALES HAY, 1977
Family SYRACOSPHAERACEAE LEMMERMANN, in BRANDT AND APSTEIN, 1908
Genus *Alisphaera* HEIMDAL, 1973

Alisphaera spatula STEINMETZ new species
Plate 15, figures 6–8

DERIVATION OF NAME: From Latin, diminutive of *spatha*, broad flat instrument or blade.

DESCRIPTIO COCCOLITHI: *Coccolithus ovatus cum peripheria impari. Orae distalis una pars, quae axi coccolithi longiori parallelos observatur, latitudine alteram multo superat. Elementum aliquod latum, in medio situm, ensiformum, ab ora paullo tollitur et a distali parte protruditur. Margo eiusdem extremus processum quendam continet, obtusum, in medio situm, qui ultra marginem coccolithi paullo extenditur. Peripheria interior orae distalis angustae, ad partem ensiformam adversa, in pinna crenata angusta consistit, quae a distali parte protruditur. Octo novemve dentes, inter se intervallis paribus distantes, in pinna apparent. Coccolithi partes proximalis et distalis brevi fistulae adiunguntur. Ora proximalis ovata multo angustior est quam pars ulla orae distalis. Elementa inter se aptata, rectis angulis formata, quae a columna superficiei proximalis centrali ad medium centrum extenduntur, rimam enormiter lineatam (ad litterae flexuosae "W" figuram) praebent. Longitudo de 1.5 ad 1.8 μm, latitudo de 0.9 ad 1.1 μm variat. Latitudo autem quasi gladii (e regione axis longioris) c. 0.5 m videtur.*

DESCRIPTION OF COCCOLITH: Elliptical coccolith with asymmetrical periphery. One side of the distal rim parallel to the longitudinal axis of the coccolith is much wider than the other. A broad centrally-located, blade-shaped element is slightly elevated from the rim and protrudes distally. Its outer edge contains a centrally-located, blunt projection which extends slightly beyond the edge of the coccolith. The inner periphery of the narrow distal rim, opposite the side with the blade, consists of a narrow crenate fin which protrudes distally. Eight or nine regularly-spaced teeth are evident on the fin. Proximal and distal parts of the coccolith are attached to a short tube. The elliptical proximal rim is much narrower than any part of the distal rim. Interlocking rectangular elements extending centerward from the central column on the proximal surface create an irregularly-outlined (zig-zig) longitudinal slit. Length ranges from 1.5 to 1.8 μm, width from 0.9 to 1.1 μm. Width of blade (parallel to long axis) is about 0.5 μm.

REMARKS: The coccolith of *Alisphaera spatula* STEINMETZ n. sp. differs from that of *Alisphaera ordinata* (Kamptner) HEIMDAL, 1973, and *Alisphaera unicornis* OKADA AND MCINTYRE, 1977, by having a blade-shaped element on its distal rim, with a centrally-located, short, distally-pointing projection. The pointed projection of *A. unicornis* is longer, extends farther beyond the coccolith rim, and originates from the wide margin, not from a distinctly separate rectangular blade as in *A. spatula* n. sp.

HOLOTYPE: Plate 15, figure 6. Negative 12-L-2.

TYPE LOCALITY: Equatorial Atlantic Ocean (13°30′N, 54°00′W), PARFLUX Station E.

BIOGEOGRAPHY: Observed frequently at Station E, trap at 389 m depth, in the equatorial Atlantic Ocean.

Acknowledgments

I thank Dr. Susumu Honjo (Woods Hole Oceanographic Institution) for stimulating my interest in the study of Recent calcareous nannoplankton. His encouragement, constructive advice, and critical reviews of the manuscript are gratefully acknowledged. Dr. Hisatake Okada provided me with valuable suggestions on the taxonomy of coccoliths which were incorporated into this paper. Drs. Kozo Takahashi and Robert Thunell provided constructive suggestions in this study. Dr. Gabriel Vargo graciously allowed me use of his phytoplankton laboratory. Dr. Victor Castellani provided Latin translations for the new species description. Mr. Anthony Greco aided in much of the SEM and darkroom work. Mrs. Gladys Swigert assisted in the darkroom.

This research was supported by funding provided by the Oceanography Section of the National Science Foundation under Grant OCE 79-13233 and the Division of Sponsored Research of the University of South Florida. The samples used in this research were collected during 1976 to 1979 PARFLUX experiments and 1979 Sediment Trap Intercomparison Experiment (Station PB_1) which were supported by NSF grants; OCE 7682063, OCE 7727004 and OCE 7925429.

References

Alldredge, A.L. (1979). The chemical composition of macroscopic aggregates in two neritic seas. *Limnol. Oceanogr.*, **24**:855–866.

Alldredge, A.L. and J.L. Cox (1982). Primary production and age of marine snow in surface waters off Southern California. *Amer. Geophys. Union Trans.*, **63**(3):80 (abstract).

Bartolini, C. (1970). Coccoliths from sediments of the western Mediterranean. *Micropaleontology*, **16**(2): 129–154.

Berger, W.H., C.G. Adelseck and L.A. Mayer (1976). Distribution of carbonate in surface sediments of the Pacific Ocean. *Jour. Geophys. Res.*, **81**(5):2617–2627.

Bernard, F. (1963). Vifesse de chute en mer des amas palmeloides de *Cyclococcolithus*. Ses Consequences pour le cycle vital des mers chaudes. *Pelagos, Bull. Inst. Oceanogr., Alger*, **1**:1–34.

Bishop, J.K.B., J.M. Edmond, D.R. Ketten, M.P. Bacon and W.G. Silker (1977). The chemistry, geology, and vertical flux of particulate matter from the upper 400 m of the equatorial Atlantic Ocean. *Deep-Sea Res.*, **24**(6):511–548.

Black, M. (1971). The systematics of coccoliths in relation to the palaeontological record. **In:** B.M. Funnell and W.R. Riedel (eds.), *The Micropalaeontology of Oceans*, Cambridge Univ. Press, Cambridge, pp. 611–624.

Borsetti, A.M. and F. Cati (1976). Il nannoplancton calcareo vivente nel Tirreno centro-meridionale Parte II. *Giorn. Geol.*, ser. 2a, **40**: 209–240.

Boudreaux, J.E. and W.W. Hay (1969). Calcareous nannoplankton and biostratigraphy of the late Pliocene-Pleistocene-Recent sediments of the Submarex cores. *Rev. Esp. Micropaleont.*, **1**: 249–292.

Bukry, D. (1973). Phytoplankton stratigraphy, Deep Sea Drilling Project Let 20, Western Pacific Ocean. **In:** B.C. Heezen, I.D. MacGregor et al., *Initial Reports of the Deep Sea Drilling Project*, Vol. 20, U.S. Government Printing Office, Washington, D.C., pp. 307–317.

Cohen, C.L.D. and P. Reinhardt (1968). Coccolithophorids from the Pleistocene Caribbean deep-sea core CP-28. *N. Jb. Geol. Palãont. Abh.*, **131**(3): 289–304.

Conley, S.M. (1979). Recent coccolithophores from the Great Barrier Reef Coral Sea Region. *Micropaleontology*, **25**(1):20–43.

Cromwell, T. and E.B. Bennett (1959). Surface drift charts for the eastern tropical Pacific Ocean. *Inter-Amer. Trop. Tuna Comm., Bull.*, **3**(5):215–238.

Deflandre, G. (1947). *Braarudosphaera* nov. gen., type d'une famille nouvelle de Coccolithophoridés actuels à éléments composites. *C.R. Seances Acad. Sci. Paris*, **225**: 439–441.

Deflandre, G. (1952). Classe des Coccolithophoridés. **In:** P.P. Grassé, *Traité de Zoologie*, Masson, Paris, **1**: 439–470.

Deflandre, G. (1954). Premiers apports de la paléontologie à nos connaissances sur l'évolution des Coccolithophoridés. *Rapp. & Commun. VIII Congr. Int. Bot. Paris*, **17**: 119–120.

Deflandre, G. and C. Fert (1954). Observations sur les Coccolithophoridés actuels et fossiles en microscopie ordinaire et électronique. *Ann. Paléont.*, **40**: 115–176.

Emelyanov, E.M. and E.S. Trimonis (1977). Cenozoic terrigenous sediments in the western South Atlantic. **In:** P.R. Supko, K. Perch-Nielsen et al., *Initial Reports of the Deep Sea Drilling Project*, Vol. 39, U.S. Government Printing Office, Washington, D.C., pp. 453–475.

Esterly, C.O. (1966). The feeding habits and food of pelagic copepods and the question of nutrition by organic substances in solution in the water. *Univ. Calif. Publ. 2001*, **9**:253–340.

Forsbergh, E.D. (1969). On the climatology, oceanography and fisheries of the Panama Bight. *Inter-Amer. Trop. Tuna Comm. Bull.*, **14**:49–385.

Frankenberg, D. and K.L. Smith (1967). Coprophagy in marine animals. *Limnol. Oceanogr.*, **12**:443–450.

Gaarder, K.R. (1962). Electron microscope studies on holococcolithophorids. *Nytt Mag. Botan.*, **10**: 35–51.

Gaarder, K.R. (1970). Three new taxa of Coccolithineae. *Nytt. Mag. Botan.*, **17**: 113–126.

Gaarder, K.R. and G.R. Hasle (1971). Coccolithophorids of the Gulf of Mexico. *Bull. Marine Sci.*, **21**(3): 519–544.

Gaarder, K.R. and B.R. Heimdal (1977). A revision of the genus *Syracosphaera* Lohmann (Coccolithineae). *"Meteor" Forsch.-Ergebnisse*, **D/24**: 54–71.

Gartner, S. (1972). Late Pleistocene calcareous nannofossils in the Caribbean and their interoceanic correlation. *Palaeogeogr., Palaeoclimatol., Palaeoecol.*, **12**:169–191.

Grassé, P.P. (1952). *Traité de Zoologie*, Masson, Paris.

Haeckel, E. (1894). *Systematische Phylogenie der Protisten und Pflanzen*, Reimer, Berlin, 400 pp.

Halldall, P. and J. Markali (1955). Electron microscope studies on coccolithophorids from the Norwegian Sea, the Gulf Stream and the Mediterranean. *Avh. Norske Vid.-Akad. Oslo, Mat.-Naturv Kl.*, **1955**(1): 30 pp.

Haq, B.U. (1978). Calcareous nannoplankton. **In:** B.U. Haq and A. Boersma (eds.), *Introduction to Marine Micropaleontology*, Elsevier, New York, pp. 79–107.

Hay, W.W. (1977). Calcareous nannofossils. **In:** A.T.S. Ramsay (ed.), *Oceanic Micropalaeontology*, Academic Press, London, pp. 1055–1200.

Hay, W.W. and H.P. Mohler (1967). Calcareous nannoplankton from early Tertiary rocks at Pont Labau, France, and Paleocene-Eocene correlations. *Jour. Paleont.*, **41**: 1505–1541.

Heath, G.R., T.C. Moore, Jr. and G.L. Roberts (1974). Mineralogy of the surface sediments from the Panama Basin, eastern equatorial Pacific. *Jour. Geology*, **82**(2):145–160.

Heimdal, B.R. (1973). Two new taxa of Recent coccolithophorids. *"Meteor" Forsch. - Ergebnisse*, **13**(13):70–75.

Honjo, S. (1975). Dissolution of suspended coccoliths in the deep-sea water column and sedimentation of coccolith ooze. **In:** W.B. Sliter, A.W.H. Bé and W.H. Berger (eds.), *Dissolution of Deep-Sea Carbonates, Cushman Found. Foraminiferal Res., Spec. Publ., No. 13*, pp. 115–128.

Honjo, S. (1976). Coccoliths: production, transportation and sedimentation. *Marine Micropaleontology*, **1**(1):65–79.

Honjo, S. (1978). Sedimentation of materials in the Sargasso Sea at a 5,367 m deep station. *Jour. Marine Res.*, **36**(3):469–492.

Honjo, S. (1980). Material fluxes and modes of sedimentation in the mesopelagic and bathypelagic zones. *Jour. Marine Res.*, **38**(1):53–97.

Honjo, S. (1982). Seasonality and interaction of biogenic and lithogenic particulate flux at the Panama Basin. *Science*, **218**(4575):883–884.

Honjo, S. (1984). Transport mechanism of pelagic particles in time and space. *Amer. Geophys. Union Trans.*, **65**(16):225 (abstract).

Honjo, S. and H. Okada (1974). Community structure of coccolithophores in the photic layer of the mid-Pacific. *Micropaleontology*, **20**(2):209–230.

Honjo, S. and M.R. Roman (1978). Marine copepod fecal pellets: production, preservation, and sedimentation. *Jour. Marine Res.*, **36**:45–57.

Honjo, S., J.F. Connell and P.L. Sachs (1980). Deep-ocean sediment trap; design and function of PARFLUX Mark II. *Deep-Sea Res.*, **27**:745–753.

Honjo, S., S.J. Manganini and J.J. Cole (1982a). Sedimentation of biogenic matter in the deep ocean. *Deep-Sea Res.*, **29**(5A):609–625.

Honjo, S., S.J. Manganini and K.W. Doherty (1982b). Seasonality and interaction of biogenic and lithogenic particulate flux by planktonic mediation. *Amer. Geophys. Union Trans.*, **63**(3):80 (abstract).

Honjo, S., S.J. Manganini and L.J. Poppe (1982c). Sedimentation of lithogenic particles in the deep ocean. *Marine Geology*, **50**:199–220.

Honjo, S., D.W. Spencer and J.W. Farrington (1982d). Deep advective transport of lithogenic particles in Panama Basin. *Science*, **216**(4545):516–518.

Jafar, S.A. (1975). Some comments on the calcareous nannoplankton genus *Scyphosphaera* and the neotypes of *Scyphosphaera* species from Rotti, Indonesia. *Senckenberg. Leth.*, **56**: 365–379.

Jafar, S.A. and E. Martini (1975). On the validity of the calcareous nannoplankton genus *Helicosphaera. Senckenberg. Leth.*, **56**(4/5): 381–397.

Jannasch, H.W. and C.O. Wirsen (1973). Deep-sea microorganisms: *in situ* response to nutrient enrichment. *Science*, **180**:641–643.

Johannes, R.E. and M. Satomi (1966). Composition and nutritive value of fecal pellets of a marine crustacean. *Limnol. Oceanogr.*, **11**:191–197.

Kamptner, E. (1927). Beitrag zur Kenntnis adriatischer Coccolithophoriden. *Arch. Protistenkd.*, **58**: 173–184.

Kamptner, E. (1928). Über das System und die Phylogenie der Kalkflagellaten. *Arch. Protistenkd.*, **64**: 19–43.

Kamptner, E. (1936). Über die Coccolithineen der Südwestküste von Istrien. *Anz. Akad. Wiss. Wien, Math.-Naturw. Kl.*, **73**: 243–247.

Kamptner, E. (1937). Neue und bemerkenswerte Coccolithineen aus dem Mittelmeer. *Arch. Protistenkd.*, **89**; 279–316.

Kamptner, E. (1941). Die Coccolithineen der Südwestküste von Istrien. *Ann Naturh. Mus. Wien.*, **51**: 54–149.

Kamptner, E. (1943). Zur Revision der Coccolithineen-Spezies *Pontosphaera huxleyi* Lohm. *Anz. Akad. Wiss. Wien, Math.-Naturw. Kl.*, **80**: 43–49.

Kamptner, E. (1950). Über den submikroskopischen Aufbau der Coccolithen. *Anz. Österr. Akad. Wiss., Math.-Naturw. Kl.*, **87**: 152–158.

Kamptner, E. (1954). Untersuchungen über den Feinbau der Coccolithen. *Arch. Protistenkd.*, **100**: 1–90.

Kamptner, E. (1963). Coccolithineen-Skelettreste aus Tiefseeablagerungen des Pazifischen Ozeans. *Ann. Naturh. Mus. Wien*, **66**: 139–204.

Knauer, G.A., J.H. Martin and K.W. Bruland (1979). Fluxes of particulate carbon, nitrogen, and phosphorous in the upper water column of the Northeast Pacific. *Deep-Sea Res.*, **26**(1A):97–108.

Koblentz-Mischke, 0.J., V.V. Volkovinsky and J.G. Kavanova (1970). Plankton primary production of the world ocean. **In:** W.S. Wooster (ed.), *Scientific Exploration of the South Pacific*, National Academy of Sciences, Washington, D.C., pp. 183–193.

Kowsmann, R.0. (1973). Coarse components in surface sediments of the Panama Basin. *Jour. Geology*, **81**(4):473–494.

Lecal-Schlauder, J. (1951). Recherches morphologiques et biologiques sur les Coccolithophoridés nord-Africains. *Ann. Inst. Océanogr., Monaco*, ser. 2, **26**:255–352.

Lemmermann, E. (1908). Flagellatae, Chlorophyceae, Coccosphaerales und Silicoflagellatae. **In:** K. Brandt and C. Apstein (eds.), *Nordisches Plankton*, Lipsius & Tischer, Kiel and Leipzig, pp. 1–40.

Lohmann, H. (1902). Die Coccolithophoridae, eine Monographie der Coccolithen bildenden Flagellaten, zugleich ein Beitrag zur Kenntnis des Mittelmeerauftriebs. *Arch. Protistenkd.*, 1:89–165.

Lohmann, H. (1912). Untersuchungen über das Pflanzen- und Tierleben der Hochsee. *Veroff. Inst. Meereskd. Univ. Berlin, N.F., Georg.-Naturw. Reihe*, **1**: 1–92.

Love, C.M. (1970). Biological and nutrient chemistry data from principal participating ships, first and second monitor cruise, August–September 1967. *U.S. Dept. Commerce, Washington, D.C., EASTROPAC Atlas, vol. 4.*

Love, C.M. (1971). Biological and nutrient chemistry data from principal participating ships, first survey cruise, February–March 1967. *U.S. Dept. Commerce, Washington, D.C., EASTROPAC Atlas, vol. 2.*

Lund, J.W.G., C. Kipling and E.D. LeCren (1958). The inverted microscope method of estimating algal numbers and the statistical basis of estimations by counting. *Hydrobiologia*, **11**:143–170.

Markali, J. and E. Paasche (1955). On two species of *Umbellosphaera*, a new marine coccolithophorid genus. *Nytt. Mag. Botan.*, 4: 95–100.

Marshall, S.M. and A.P. Orr (1955). On the biology of *Calanus finmarchicus* VIII. Food uptake, assimulation and execution in adult and state V *Calanus*. *Jour. Mar. Biol. Assn. U.K.*, **34**:495–529.

Marshall, S.M. and A.P. Orr (1956). On the biology of *Calanus finmarchicus*. IX. Feeding and digestion in the young stages. *Jour. Mar. Biol. Assn. U.K.*, **35**:587–603.

Marshall, S.M. and A.P. Orr (1962). Food and feeding in copepods. *Rapp. Cons. Explor. Mer*, **152**:92–98.

Milliman, J.D., C.P. Summerhayes amd H.T. Barretto (1975). Oceanography and suspended matter off the Amazon river February–March. *Jour. Sediment. Petrol.*, **45**(1):189–206.

Moore, T.C., Jr., G.R. Heath and R.O. Kowsmann (1973). Biogenic sediments of the Panama Basin. *Jour. Geology*, **81**(4):458–472.

Mullin, M.M. (1966). Selective feeding by calanoid copepods from the Indian Ocean. **In:** H. Barnes (ed.), *Some Contemporary Studies in Marine Science*, George Allen and Unwin, London, pp. 313–334.

Murray, G. and V.H. Blackman (1898). On the nature of the coccospheres and rhabdospheres. *Philos. Trans. R. Soc. London*, **190B**: 427–441.

Murray, J. and J. Hjort (1912). *The Depths of the Ocean. A General Account of the Modern Science of Oceanography Based Largely on the Scientific Researches of the Norwegian Steamer MICHAEL SARS in the North Atlantic.* Macmillan, London, 821 pp.

Norris, R.E. (1965). Living cells of *Ceratolithus cristatus* (Coccolithophorineae). *Arch. Protistenkd.*, **108**: 19–24.

Okada, H. and S. Honjo (1973). The distribution of oceanic coccolithophorids in the Pacific. *Deep-Sea Res.*, **20**:355–374.

Okada, H. and A. McIntyre (1977). Modern coccolithophores of the Pacific and North Atlantic Oceans. *Micropaleontology*, **23**(1):1–55.

Ostenfeld, C.H. (1910). *Thorosphaera*, eine neue Gattung der Coccolithophoriden. *Ber. Deutsch. Bot. Ges.*, **28**: 397–400.

Paffenhöfer, G.-A. and J.D.H. Strickland (1970). A note on the feeding of *Calanus helgolandicus* on detritus. *Marine Biol.*, **5**:97–99.

Pascher, A. (1910). Chrysomonaden aus dem hirschberger Grossteiche. *Int. Rev. Hydrobiol. u. Hydrogr.*, Monogr. u. Abh. **1**, 66 pp.

Pilskaln, C. (1982). Fecal pellets in PARFLUX sediment traps. *Amer. Geophys. Union Trans.*, **63**(3):54 (abstract).

Poche, R. (1913). Das System der Protozoa. *Arch Protistenkd.*, **30**: 125–321.

Reinhardt, P. (1966). Fossile Vertreter coronoider und styloider Coccolithen (Familie Coccolithaceae Poche 1913). *Monatsber. Deutsch. Akad. Wiss. Berlin*, **8**: 513–524.

Rood, P., W. Hay and T. Barnard (1971). Electron microscope studies of Oxford Clay coccoliths. *Eclogae geol. Helv.*, **64**(2): 245–272.

Roth, P.H. (1970). Oligocene calcareous nannoplankton biostratigraphy. *Eclogae geol. Helv.*, **63**(3): 799–881.

Roth, P.H. (1973). Calcareous nannofossils – Leg 17, Deep Sea Drilling Project. **In:** E.L. Winterer, J.E. Ewing et al., *Initial Reports of the Deep Sea Drilling Project*, Vol. 17, U.S. Government Printing Office, Washington, D.C., pp. 695–795.

Roth, P.H., M.M. Mullin and W.H. Berger (1975). Coccolith sedimentation by fecal pellets: Laboratory experiment and field observations. *Geol. Soc. Amer. Bull.*, **86**(8):1079–1084.

Rothmaler, W. (1951). Die Abteilungen und Klassen der Pflanzen. *Repert. Sp. Nov.*, **54**: 256–266.

Rowe, G.T. and W.D. Gardner (1979). Sedimentation rates in the slope water of the northeast Atlantic Ocean measured directly with sediment traps. *Jour. Marine Res.*, **37**(3):581–600.

Samtleben, C. and R. Bickert (1990). Coccoliths in sediment traps from the Norwegian Sea. *Marine Micropaleontology*, **16**(1/2): 39–64.

Schiller, J. (1914). Bericht über Ergebnisse der Nannoplanktonuntersuchungen anlässlich der Kreuzungen S.M.S. *Najade* in der Adria. *Int. Rev. Hydrobiol. u. Hydrogr.*, Biol. Suppl. 6, Heft 4, Art. 5, 15 pp.

Schiller, J. (1925). Die planktonischen Vegetationen des adriatischen Meeres. *Arch. Protistenkd.*, **51**: 1–130.

Schiller, J. (1930). Coccolithineae. **In:** *Dr. L. Rabenhorst's Kryptogamen-Flora von Deutschland, Österreich und der Schweiz*, Akad. Verlagsges., Leipzig, **10**(2): 89–267.

Schrader, H.J. (1971). Fecal pellets: role in sedimentation of pelagic diatoms. *Science*, **174**(4004):55–57.

Schwarz, E. (1932). Beitrage zur Entwicklungsgeschichte der Protophyten. IX, Der Formwechsel von *Ochrosphaera neapolitana*. *Arch. Protistenkd.*, **77**: 434–462.

Shanks, A.L. and J.D. Trent (1980). Marine snow: sinking rates and potential role in vertical flux. *Deep-Sea Res.*, **27**(2A):137–143.

Sheldon, R.W. (1984). Phytoplankton growth rates in the tropical ocean. *Limnol. Oceanogr.*, **29**(6):1342–1346.

Silver, M.W., M.M. Gowing and A.L. Alldredge (1982). Differences between fecal pellet and marine snow transport systems in the deep-sea. *Amer. Geophys. Union Trans.*, **63**(3):80 (abstract).

Silver, M.W., A.L. Shanks and J.D. Trent (1978). Marine snow: microplankton habitat and source of small-scale patchiness in pelagic populations. *Science*, **201**(4353):371–373.

Smayda, T.J. (1966). A quantitative analysis of the phytoplankton of the Gulf of Panama. III. General ecological conditions and the phytoplankton dynamics at 8°45'N, 79°23'W from November 1954 to May 1987. *Inter-Amer. Trop. Tuna Comm., Bull.*, **11**(5):355–612.

Smayda, T.J. (1969). Some measurements of the sinking rate of fecal pellets. *Limnol. Oceanogr.*, 14:621–625.

Soutar, A., S.A. Kling, A. Crill, E. Duffrin and K.W. Bruland (1977). Monitoring the marine environment through sedimentation. *Nature*, **266**(5598):136–139.

Spencer, D.W., P.G. Brewer, A.P. Fleer, S. Honjo, S. Krishnaswami and Y. Nozaki (1978). Chemical fluxes from a sediment trap experiment in the deep Sargasso Sea. *Jour. Marine Res.*, **36**(3):493–523.

Steinmetz, J.C. (1979). Calcareous nannofossils from the North Atlantic Ocean, Leg 49, Deep Sea Drilling Project. **In:** B.P. Luyendyk, J.R. Cann et al., *Initial Reports of the Deep Sea Drilling Project*, vol. 49, U.S. Government Printing Office, Washington, D.C., pp. 519–531.

Stevenson, M. (1970). Circulation in the Panama Bight. *Jour. Geophys. Res.*, **75**:659–672.

Tappan, H. (1980). *The Paleobiology of Plant Protists*. W.H. Freeman and Co., San Francisco, 1028 pp.

Tchernia, P. (1980). *Descriptive Regional Oceanography*. Pergamon Press, Oxford, 253 pp.

Thunell, R.C. and S. Honjo (1981). Planktonic foraminiferal flux to the deep ocean: sediment trap results from the tropical Atlantic and the central Pacific. *Mar. Geology*, **40**(314):237–253.

Thunell, R.C., R.S. Keir and S. Honjo (1981). Calcite dissolution: an *in situ* study in the Panama Basin. *Science*, **212**(4495):659–661.

Utermöhl, H. (1958). Zur Vervollkommung der quantitativen Phytoplankton-Methodik. *Int. Assoc. Theor. Appl. Limnol., Comm.*, **9**:1–38.

van Andel, Tj.H. (1973). Texture and dispersal of sediments in the Panama Basin. *Jour. Geology*, **81**(4):434–457.

van Andel, Tj.H., G.R. Heath and T.C. Moore (1975). Cenozoic history and paleoceanography of the central equatorial Pacific Ocean. *Geol. Soc. Amer. Mem. 143*, pp. 1–134.

Vekshina, V.N. (1959). Coccolithophoridae of the Maastrichtian deposits of the west Siberian lowland. *Trudy Sib. nauchno-issled. Inst. Geol. Geofiz. mineral Syrya (SNIIGGIMS)*, **2**: 56–81.

Wiebe, P., S.H. Boyd and C. Winget (1976). Particulate matter sinking to the deep sea floor at 2000 m in the Tongue of the Ocean, Bahamas, with a description of a new sedimentation trap. *Jour. Marine Res.*, **34**(3):341–354.

Wooster, W.S. (1959). Oceanographic observations in the Panama Bight, "Askoy" Expedition, 1941. *Bull. Amer. Mus. Nat. Hist.*, **118**(3): 9–151.

Wooster, W.S. and T. Cromwell (1959). An oceanographic description of the eastern tropical Pacific. *Scripps Inst. Oceanography Bull.*, **7**:169–282.

Wyrtki, K. (1967). Circulation and water masses in the eastern Pacific Ocean. *Internat. Jour. Oceanology and Limnology*, **1**(2):117–147.

Yamashiro, C. (1975). Differentiating dissolution and transport effects in foraminiferal sediments from the Panama Basin. **In:** W.V. Sliter, A.W.H. Bé and W.H. Berger (eds.), *Dissolution of Deep-Sea Carbonates,Cushman Found. Foraminiferal Res., Spec. Publ. No. 13*, pp. 151–159.

Plates

PLATE 1

Scale bar = 1 μm unless otherwise specified

1–4 *Crenalithus sessilis* (Lohmann) Okada and McIntyre

1 collapsed coccosphere, Station P_1: 2,770 m, scale bar = 10 μm.

2 detail of figure 1.

3 coccosphere, Station E: 389 m.

4 proximal view, Station E: 389 m.

5–8 *Emiliania huxleyi* (Lohmann) Hay and Mohler

5 coccospheres, Station E: 389 m.

6 distal view, Station E: 389 m.

7 detail of left coccosphere in figure 5, scale bar = 0.5 μm.

8 partially dissolved coccolith, Station P_1: 2,770 m.

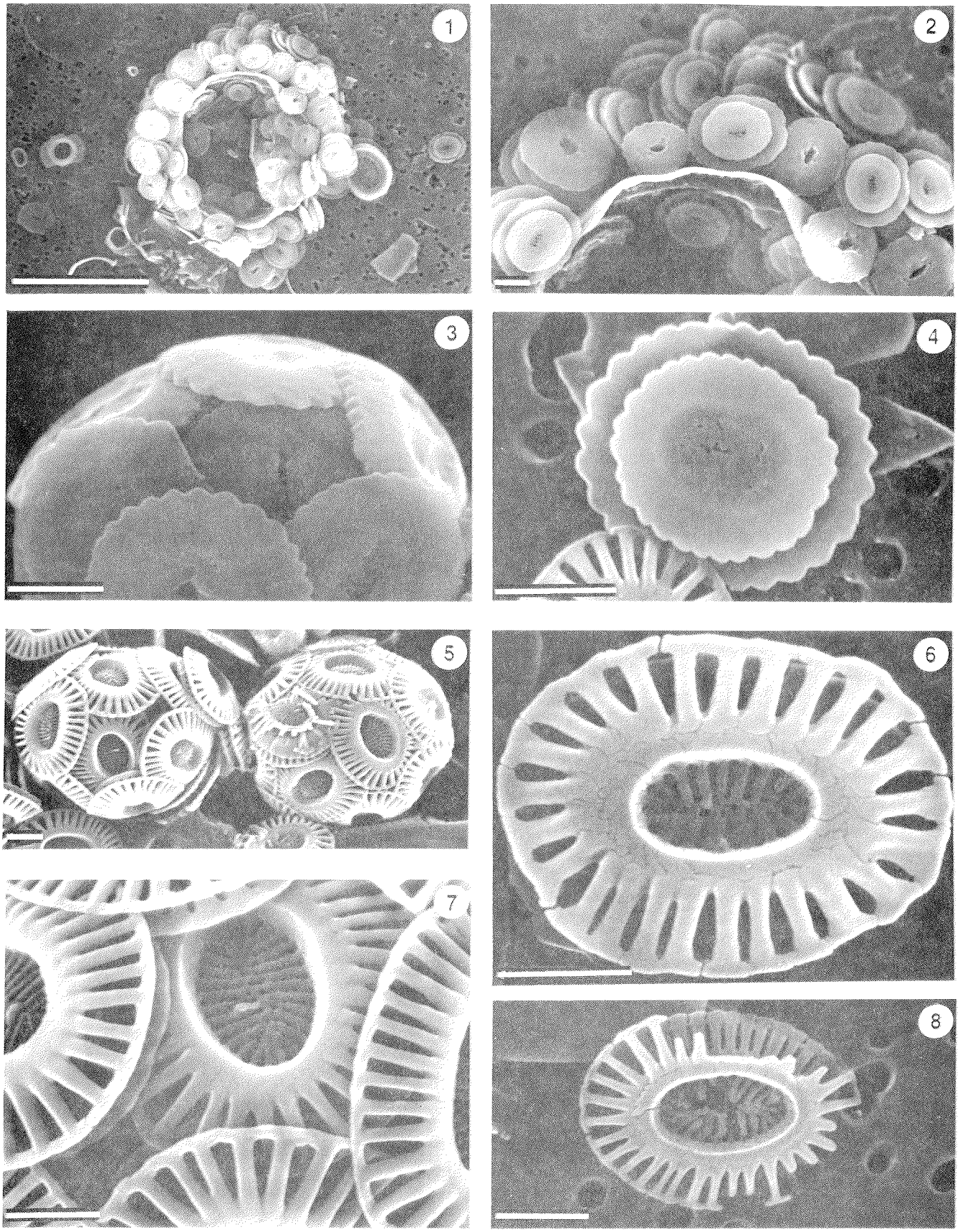
1
2
3
4
5
6
7
8

PLATE 2

Scale bar = 1 μm unless otherwise specified

1–2 *Emiliania huxleyi* (Lohmann) Hay and Mohler

1 proximal view, Station E: 389 m.

2 proximal view highly magnified, Station E: 389 m; scale bar = 0.1 μm.

3–8 *Gephyrocapsa oceanica* Kamptner

3 coccosphere, Station PB_1: 667 m.

4 detail of figure 3.

5–8 various bridge configurations in distal views.

5 Station P_1: 2,770 m.

6 Station E: 389 m.

7 Station PB_1: 667 m.

8 Station P_1: 2,770 m.

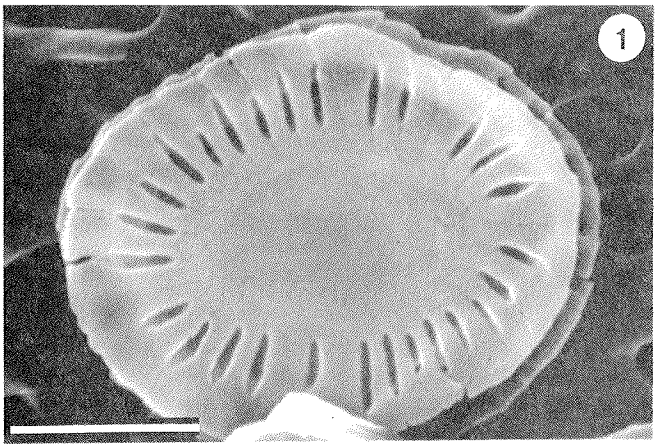
1

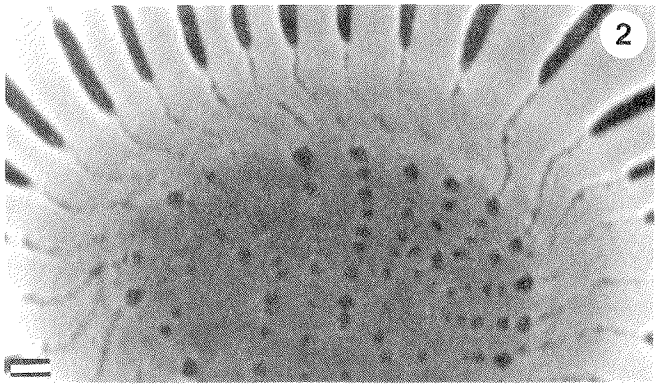
2

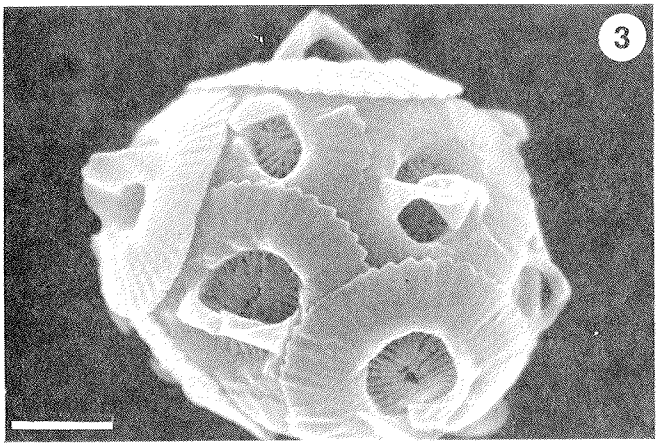
3

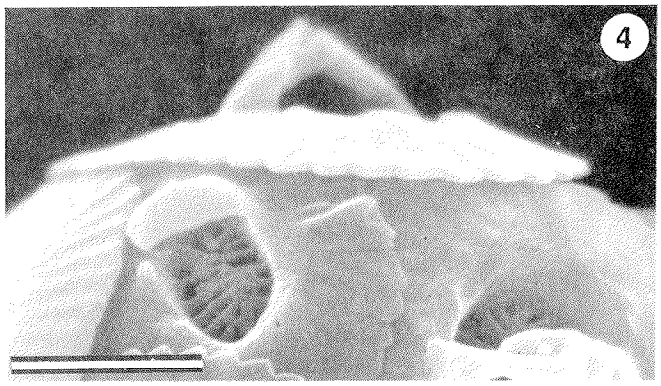
4

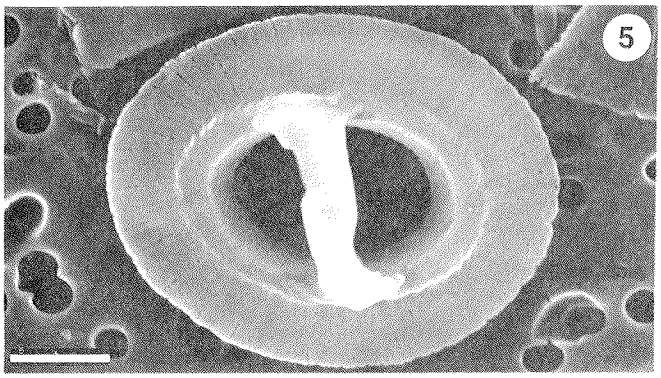
5

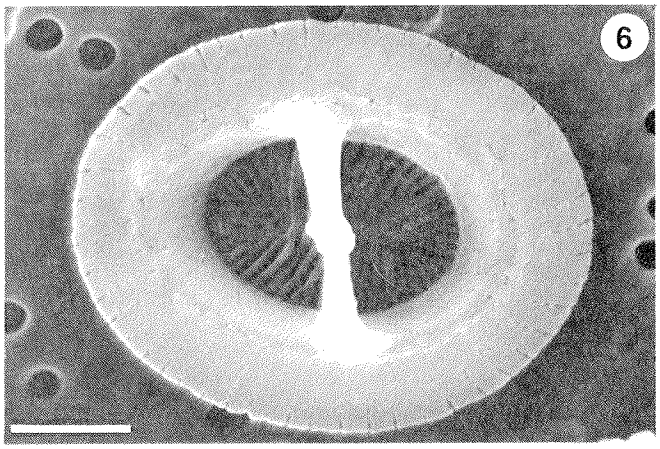
6

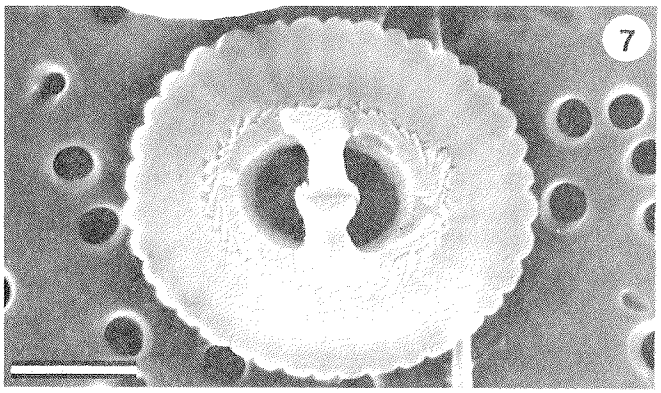
7

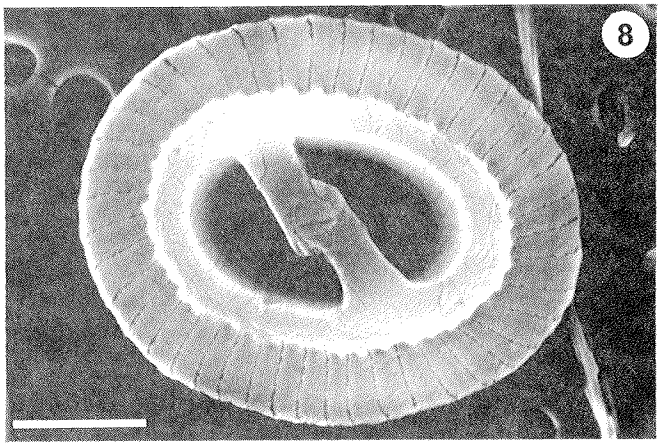
8

PLATE 3

Scale bar = 1 μm unless otherwise specified

1–8 *Gephyrocapsa oceanica* Kamptner
Various bridge configurations in distal views.

1 Station PB_1: 667 m.

2 Station E: 389 m.

3 Station P_1: 2,770 m.

4 Station E: 389 m.

5 Station E: 389 m, scale bar = 0.5 μm.

6 Station PB_1: 667 m, scale bar = 0.5 μm.

7 Station PB_1: 667 m, scale bar = 0.5 μm.

8 Station E: 389 m, scale bar = 0.5 μm.

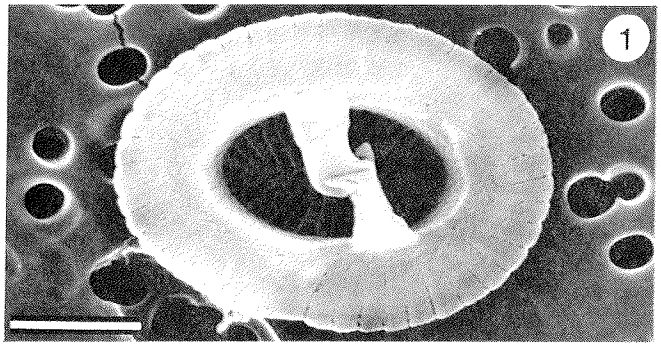
1

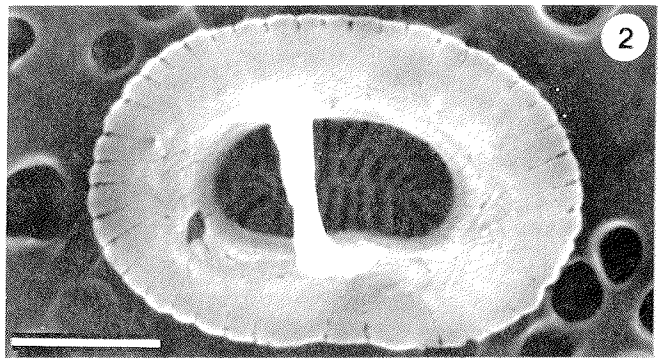
2

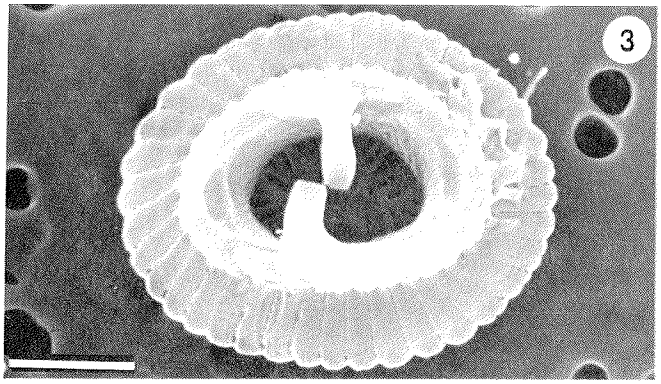
3

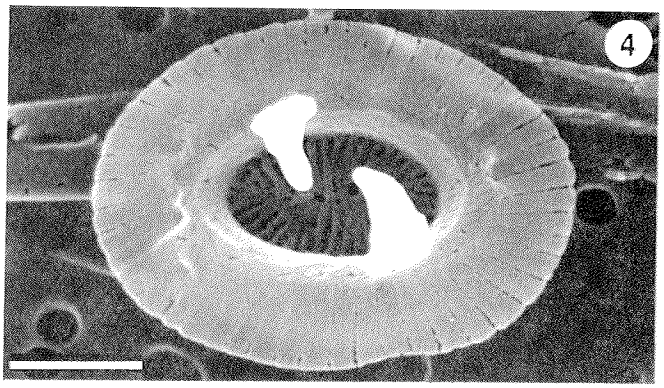
4

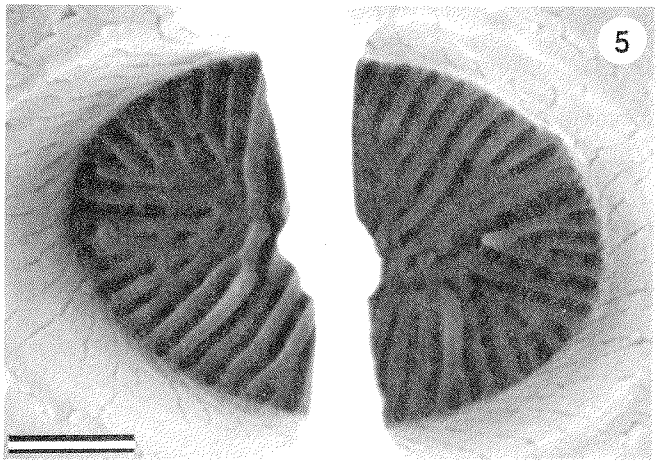
5

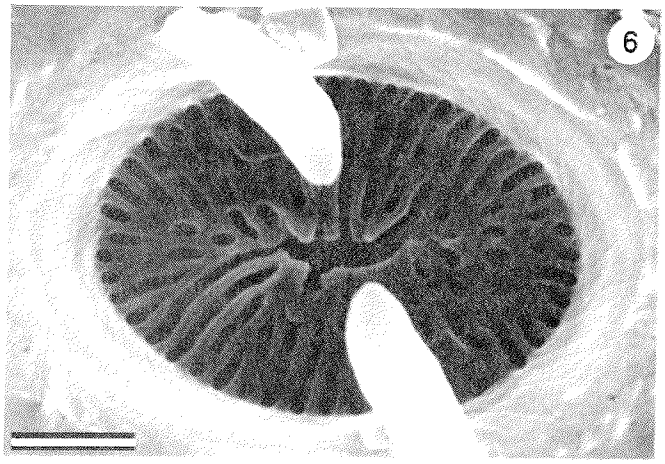
6

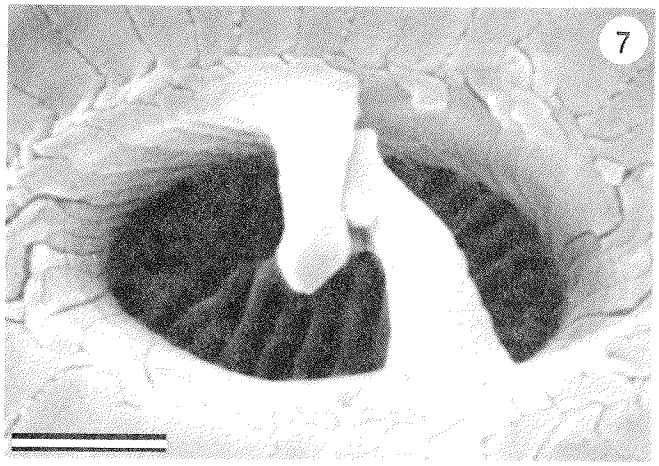
7

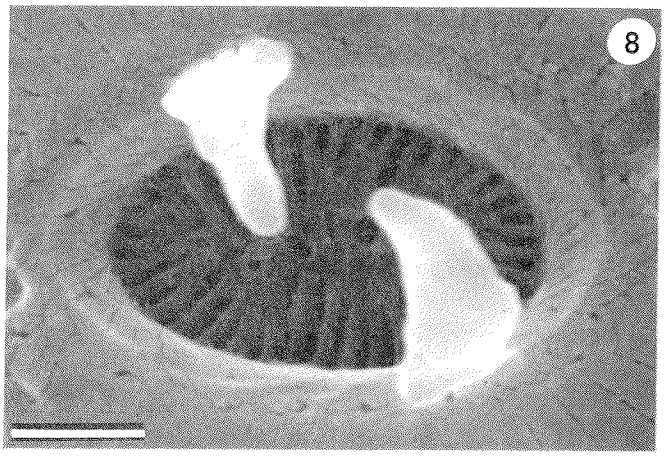
8

PLATE 4

Scale bar = 1 μm unless otherwise specified

1, 3 *Gephyrocapsa oceanica* Kamptner

1 partially recrystallized specimen (?), Station PB_1: 667 m.

3 partially dissolved specimen, Station PB_1: 1,268 m.

2–4 *Thoracosphaera heimii* (Lohmann) Kamptner

2 spherical cell, Station E: 389 m, scale bar = 5 μm.

4 detail of opening and surface structure in figure 2.

5–8 *Thoracosphaera tuberosa* Kamptner

5, 6 spherical cells, Station P_1: 978 m, scale bars = 5 μm.

7, 8 detail of surface structures of figures 5 and 6, respectively.

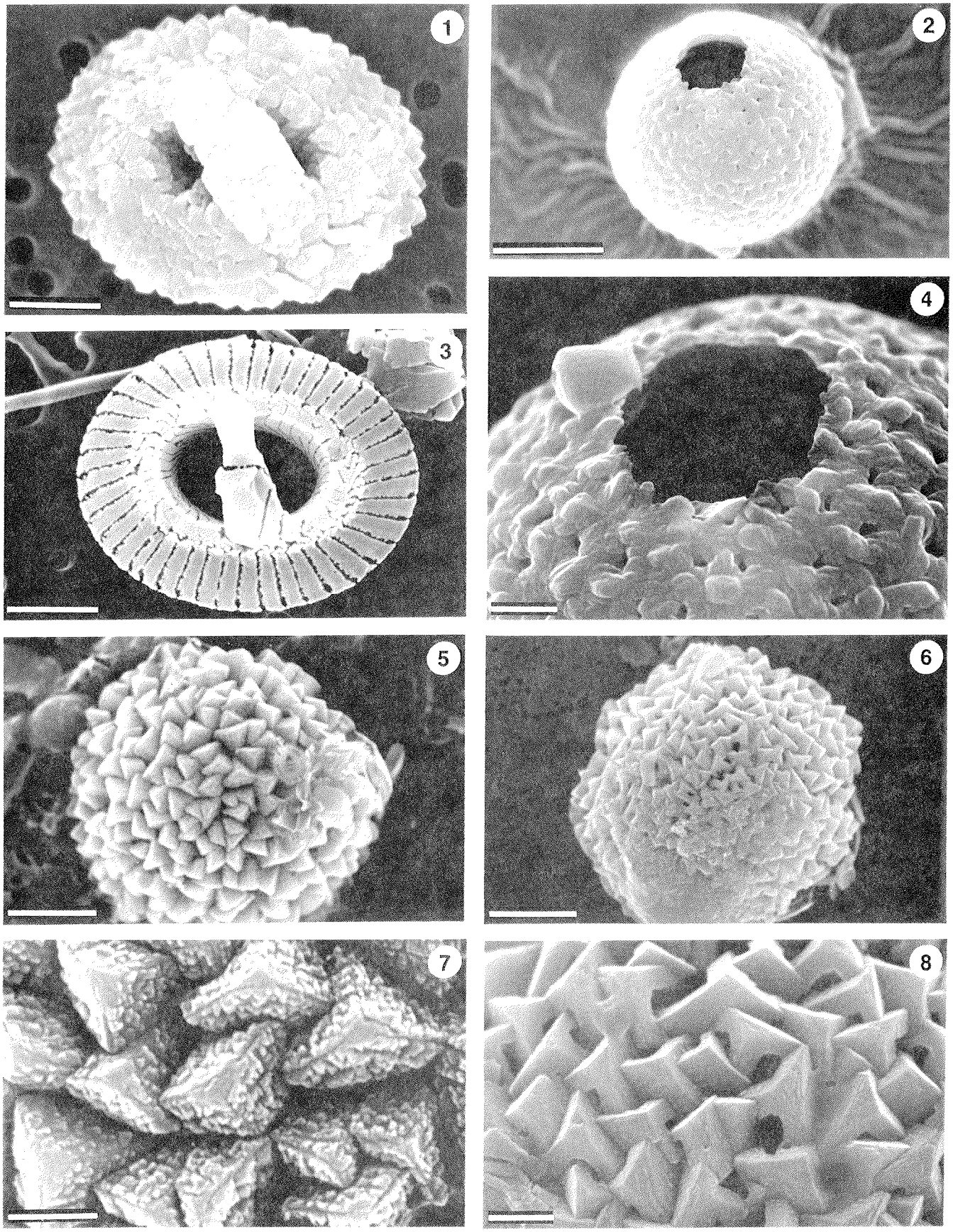
1
2
3
4
5
6
7
8

PLATE 5

Scale bar = 1 μm unless otherwise specified

1–4 *Umbilicosphaera calvata* Steinmetz n. sp.

1 collapsed coccosphere, scale bar = 5 μm, Station PB_1: 667 m.

2 holotype, proximal view, Station PB_1: 667 m.

3–4 proximal views, Station PB_1: 667 m.

5–6 *Umbilicosphaera scituloma* Steinmetz n. sp.

5 holotype, distal view, Station PB_1: 667 m.

6 highly magnified view of distal rim in figure 5, scale bar = 0.5 μm.

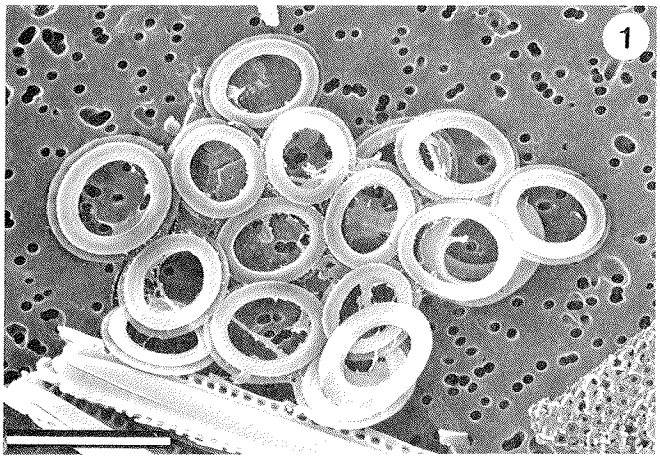
1

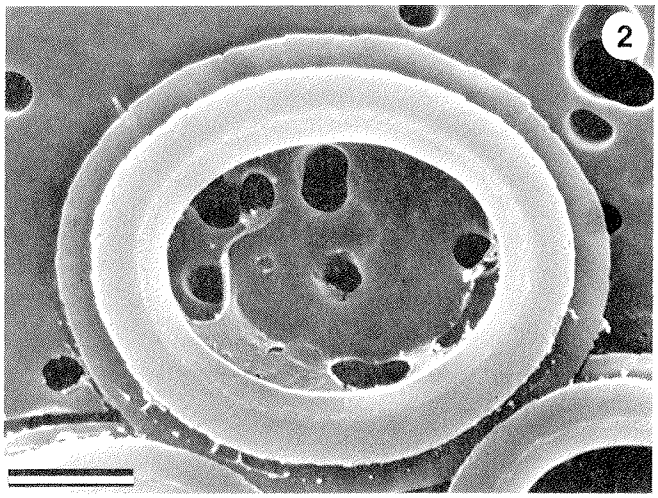
2

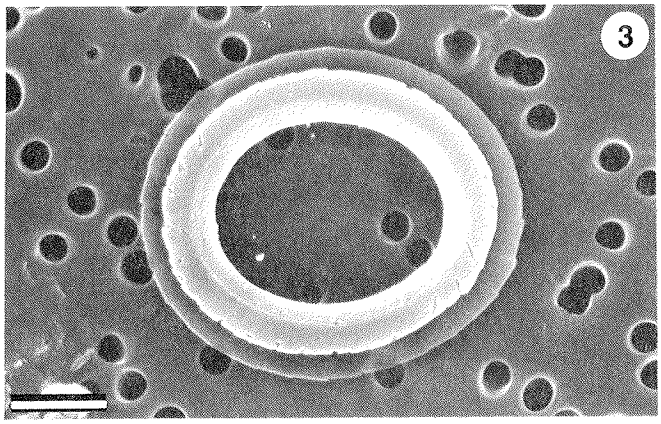
3

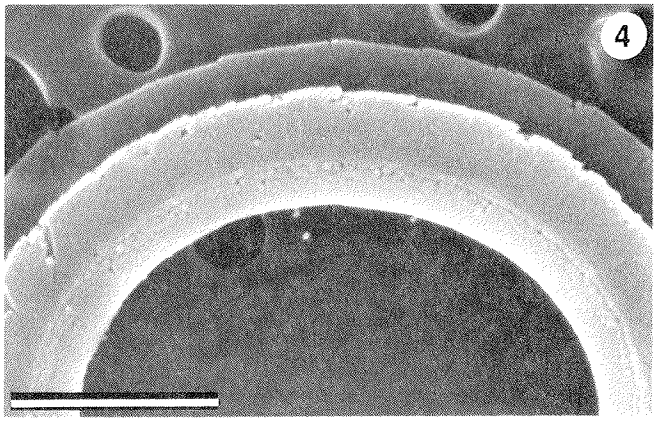
4

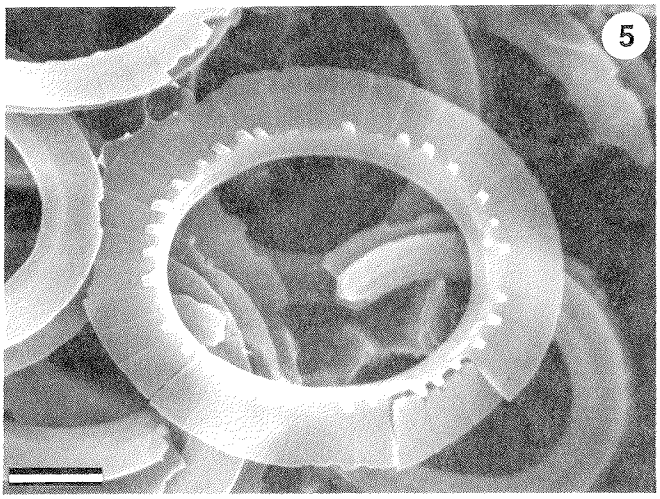
5

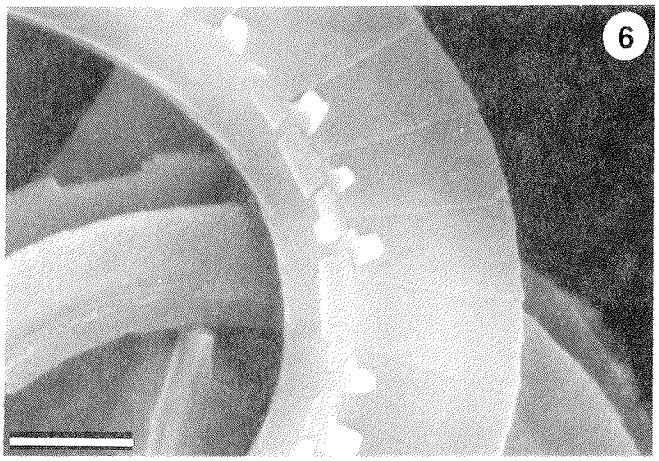
6

PLATE 6

Scale bar = 1 μm unless otherwise specified

1–3 *Calyptrosphaera catillifera* (Kamptner) Gaarder

1 collapsed coccosphere, Station E: 389 m.

2, 3 distal views of holococcoliths, Station E: 389 m, scale bars = 0.5 μm.

4, 5 *Calyptrosphaera oblonga* Lohmann

4 distal view of holococcolith, Station E: 389 m.

5 highly magnified detail of figure 4, scale bar = 0.1 μm.

6–8 *Calyptrosphaera pirus* Kamptner

6 proximal (left) and distal views of holococcolith.

7 distal view.

8 side view, Station E: 389 m.

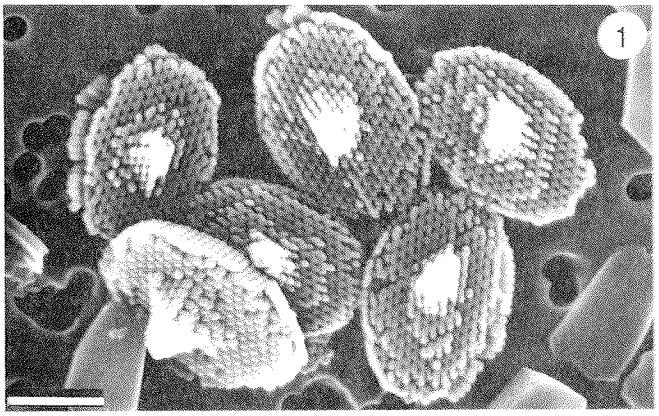
1

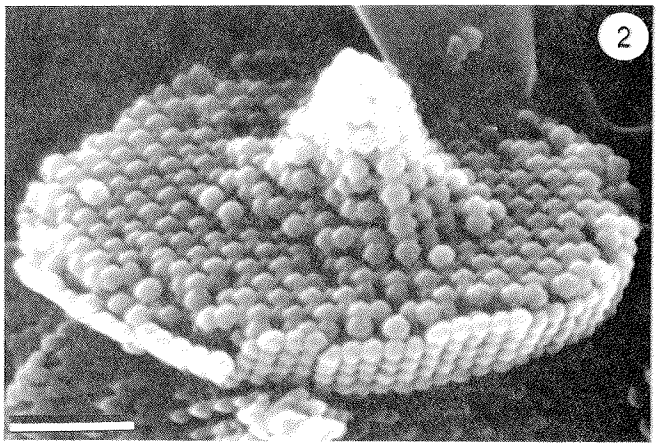
2

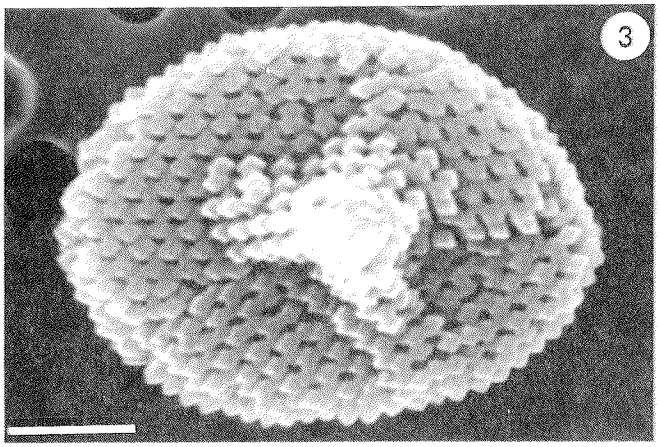
3

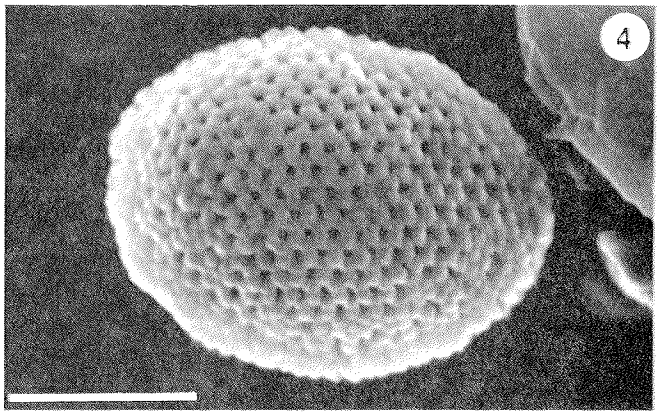
4

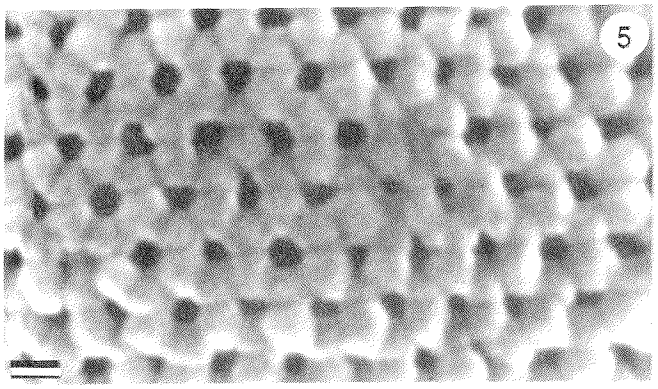
5

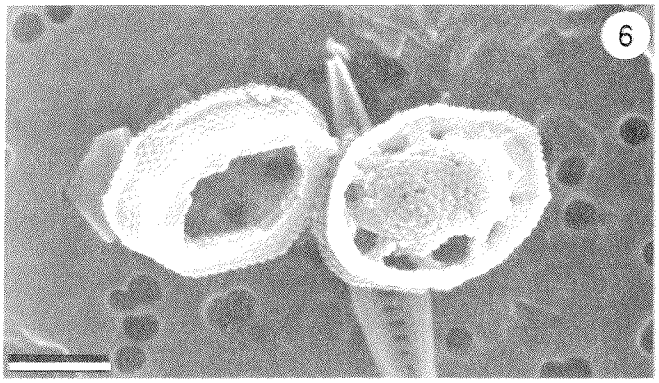
6

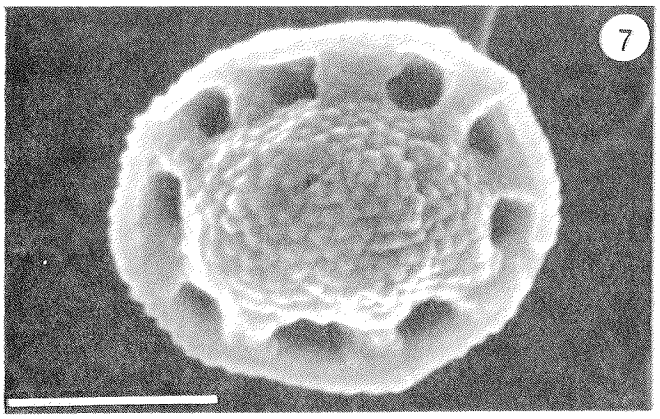
7

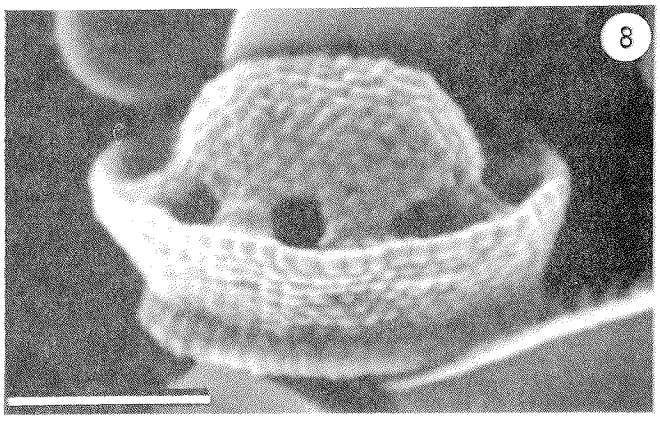
8

PLATE 7

Scale bar = 1 μm unless otherwise specified

1, 2 *Calyptrosphaera pirus* Kamptner

1 side view, Station E: 988 m.

2 proximal view, Station E: 389 m, scale bar = 0.5 μm.

3 *Corisphaera gracilis* Kamptner
Distal view, Station E: 389 m, scale bar = 0.5 μm.

4 *Helladosphaera aurisinae* Kamptner
Distal view, Station E: 389 m, scale bar = 0.5 μm.

5 *Helladosphaera cornifera* (Schiller) Kamptner
Distal view, Station E: 389 m, scale bar = 0.5 μm.

6 *Helladosphaera dalmatica* (Kamptner) Okada and McIntyre
Distal view, Station E: 389 m.

7, 8 *Helladosphaera fastigata* Okada and McIntyre

7 collapsed coccosphere, Station PB_1: 1,268 m.

8 distal view of holococcolith from figure 7, scale bar = 0.5 μm.

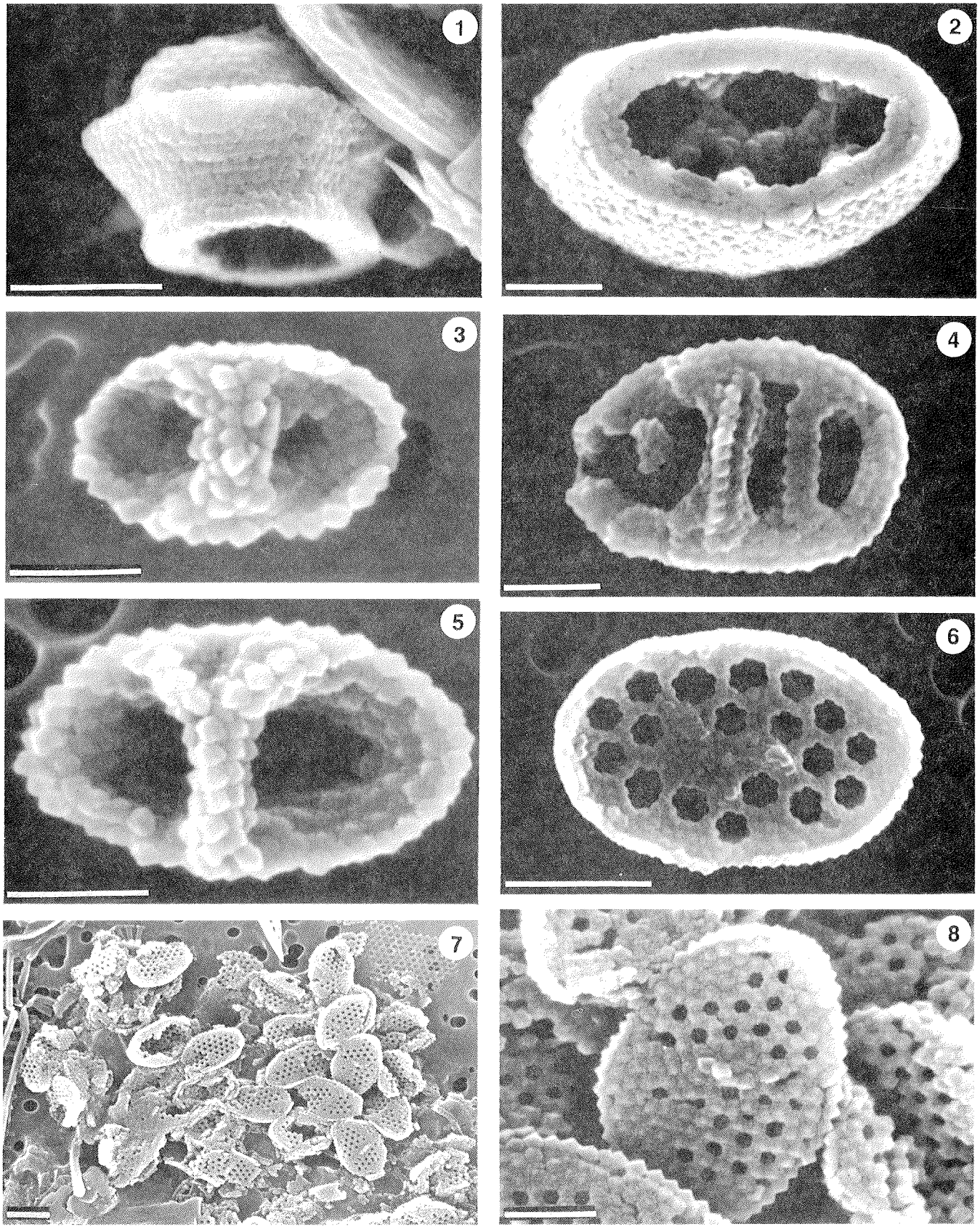
1
2
3
4
5
6
7
8

PLATE 8

Scale bar = 1 μm unless otherwise specified

1 *Helladosphaera fastigata* Okada and McIntyre
Distal view, Station PB_1: 1,268 m, scale bar = 0.5 μm.

2 *Homozygosphaera ponticulifera* (Kamptner) Kamptner
Distal view, Station E: 3,755 m.

3–6 *Homozygosphaera schilleri* (Kamptner) Okada and McIntyre.

3 distal view, Station P_1: 2,770 m.

4 highly magnified detail of figure 3, scale bar = 0.5 μm.

5 highly magnified detail of central structure, Station E: 389 m, scale bar = 0.5 μm.

6 distal view of aberrant form, Station E: 389 m.

7, 8 *Sphaerocalyptra marsilii* Borsetti and Cati

7 holococcolith, Station E: 389 m, scale bar = 0.5 μm.

8 highly magnified detail of figure 7, scale bar = 0.1 μm.

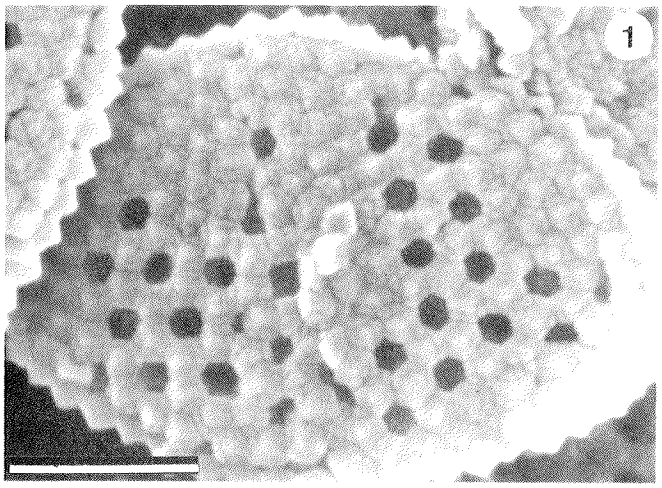
1

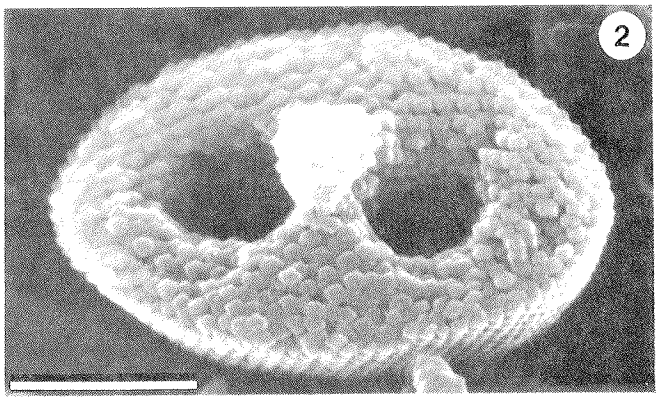
2

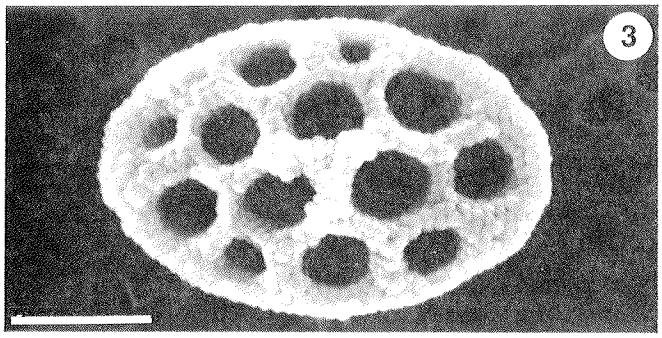
3

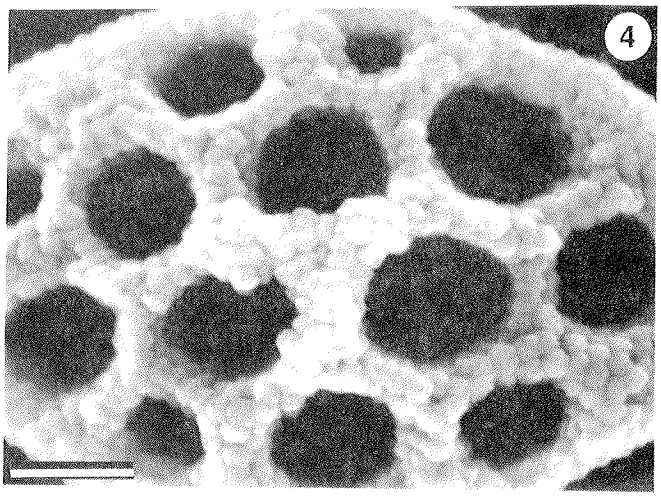
4

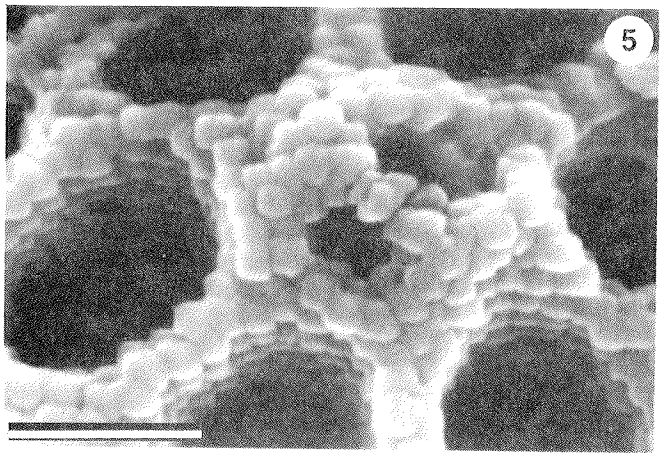
5

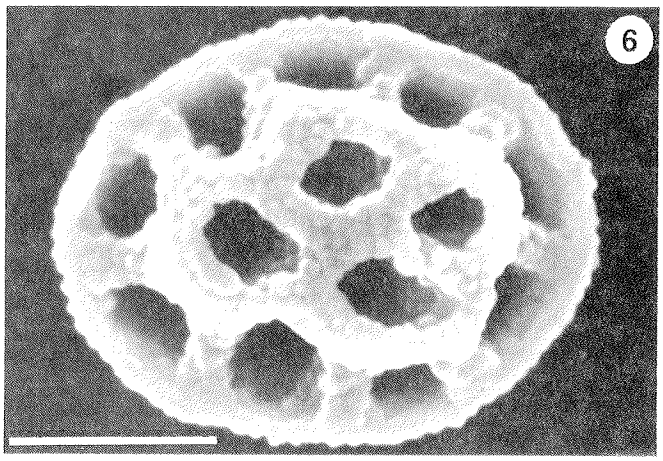
6

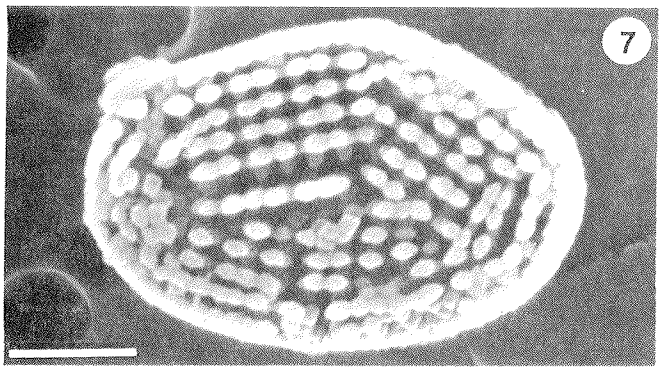
7

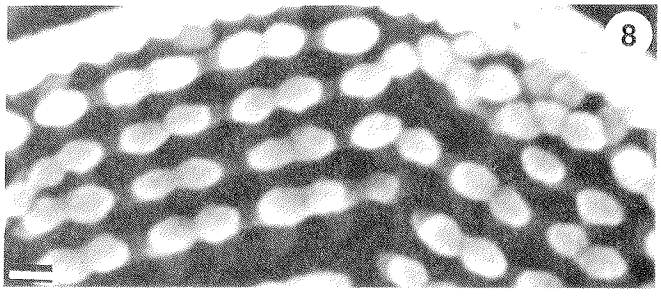
8

PLATE 9

Scale bar = 1 μm unless otherwise specified

1 *Discoaster brouweri* Tan Sin Hok
Proximal view, Station E: 5,068 m.

2 *Discoaster quinqueramus* Gartner
Distal view, Station E: 5,068 m, scale bar = 5 μm.

3, 4 *Hayaster perplexus* (Bramlette and Riedel) Bukry

3 proximal view, Station E: 389 m, scale bar = 5 μm.

4 highly magnified detail of figure 3.

5–8 *Ceratolithus cristatus* Kamptner

5, 6 proximal views, Station P_1: 2,770 m.

7 highly magnified detail of rods on shorter horn of figure 6.

8 highly magnified view of rods on longer horn of figure 6.

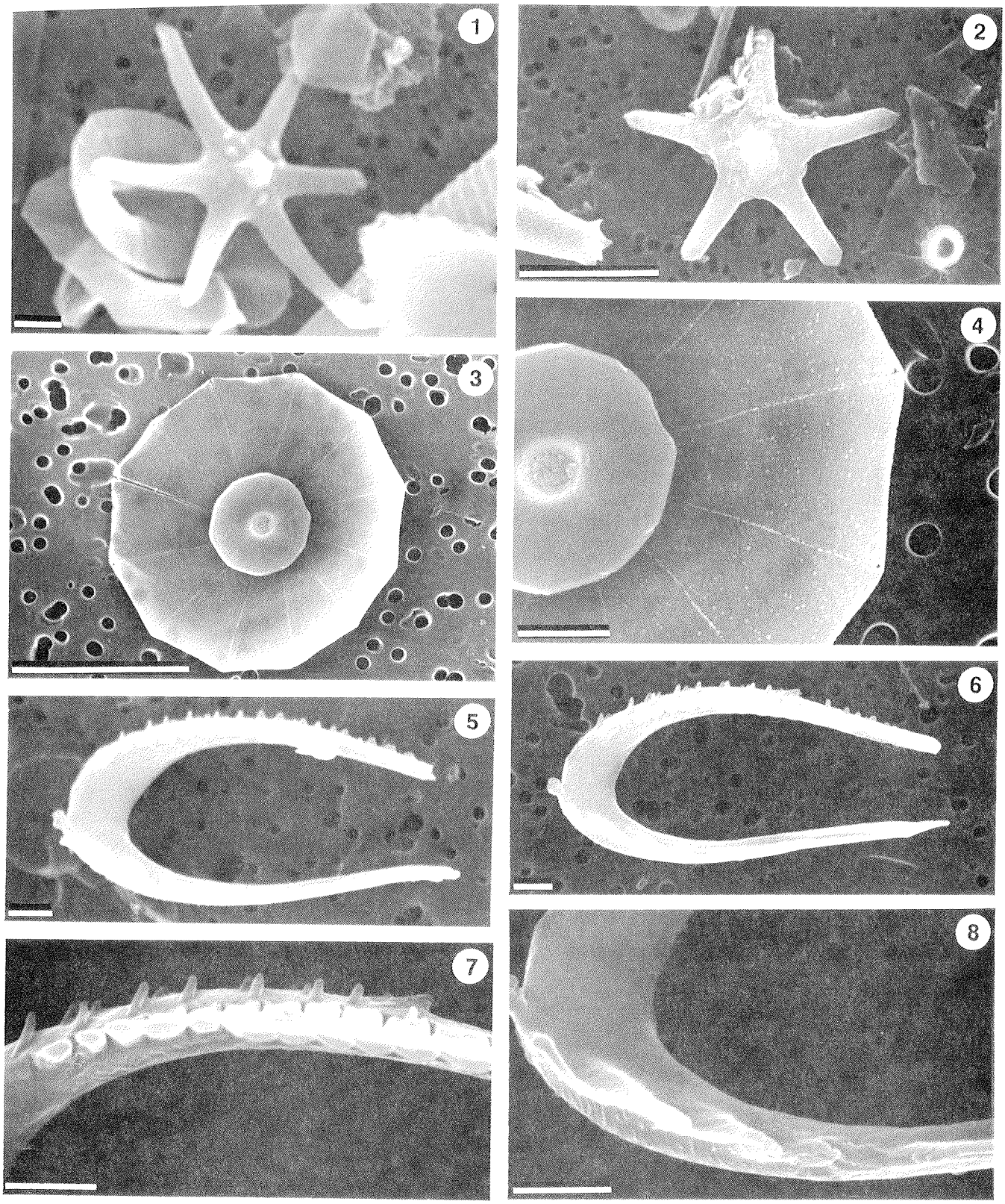
1
2
3
4
5
6
7
8

PLATE 10

Scale bar = 1 μm unless otherwise specified

1, 2 *Braarudosphaera bigelowi* (Gran and Braarud) Deflandre

1 proximal view, Station P_1: 2,770 m, scale bar = 5 μm.

2 highly magnified detail of figure 1.

3–6 *Pontosphaera messinae* Bartolini, emend. Burns

3 proximal view, Station E: 988 m.

4 proximal view, Station E: 389 m.

5, 6 highly magnified detail of figure 4.

7, 8 *Pontosphaera multipora* (Kamptner) Roth

7 distal view, Station P_1: 2,770 m.

8 highly magnified detail of figure 7.

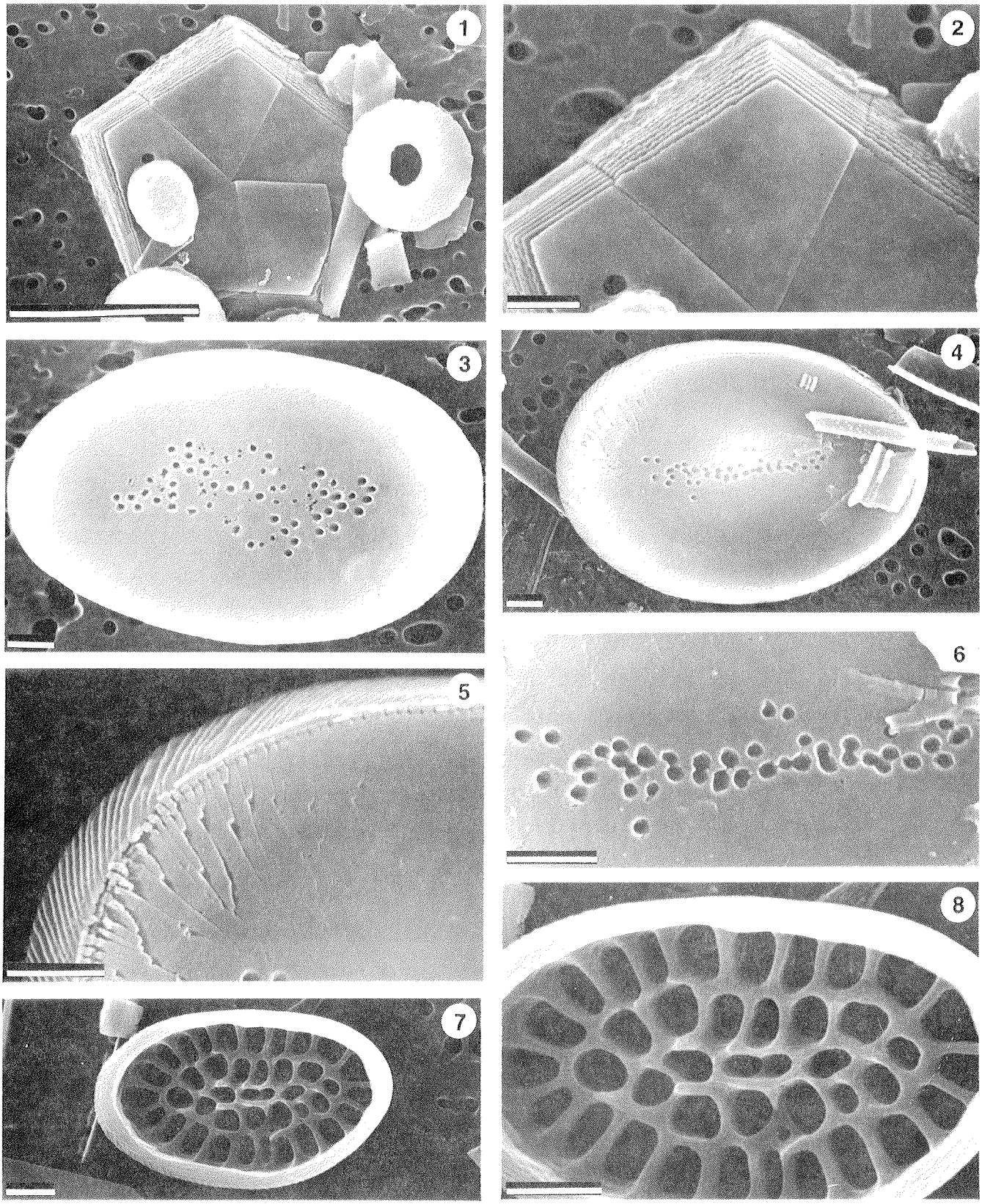
1
2
3
4
5
6
7
8

PLATE 11

Scale bar = 1 μm unless otherwise specified

1–5 *Pontosphaera multipora* (Kamptner) Roth

1 distal view, Station E: 389 m.

2 proximal view, Station P_1: 2,770 m.

3 highly magnified detail of figure 1, scale bar = 0.5 μm.

4 highly magnified detail of figure 2.

5 proximal view, Station E: 988 m.

6–8 *Scyphosphaera apsteinii* Lohmann

6 distal view, Station E: 389 m.

7 side view, Station P_1: 2,770 m, scale bar = 5 μm.

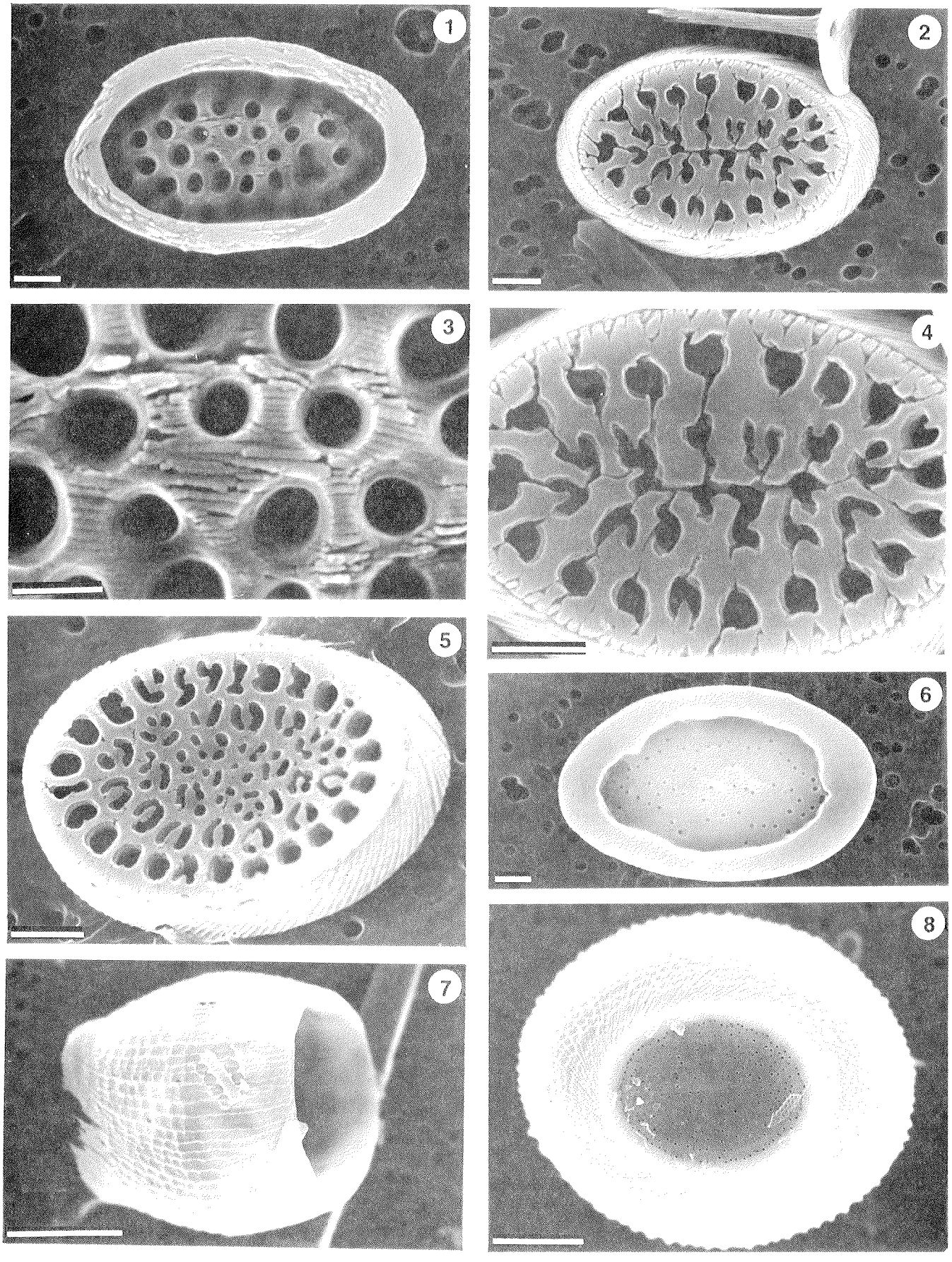
1
2
3
4
5
6
7
8

PLATE 12

Scale bar = 1 μm unless otherwise specified

1–4 *Helicosphaera carteri* (Wallich) Kamptner

1 proximal view, Station E: 389 m.

2 distal view, Station E: 389 m.

3 detail of figure 1.

4 detail of figure 2.

5, 7 *Helicosphaera hyalina* Gaarder

5 proximal view, Station E: 389 m.

7 detail of figure 5.

6, 8 *Helicosphaera pavimentum* Okada and McIntyre

6 distal view, Station E: 988 m.

8 highly magnified detail of figure 6, scale bar = 0.5 μm.

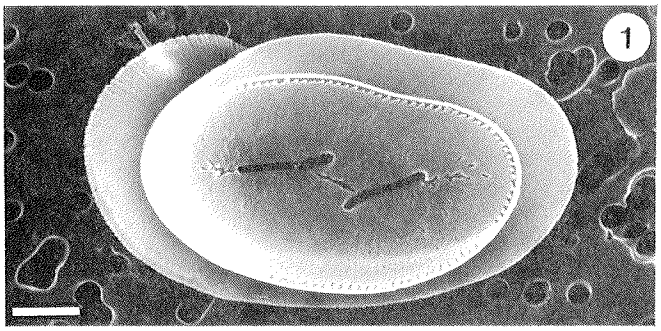
1

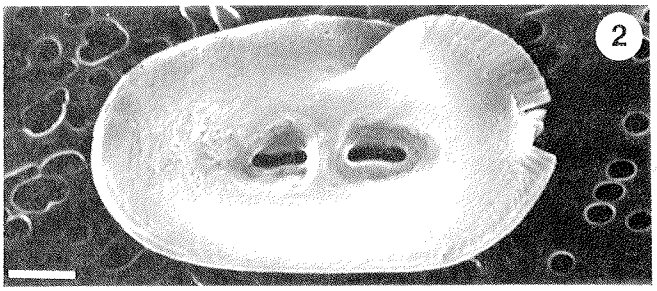
2

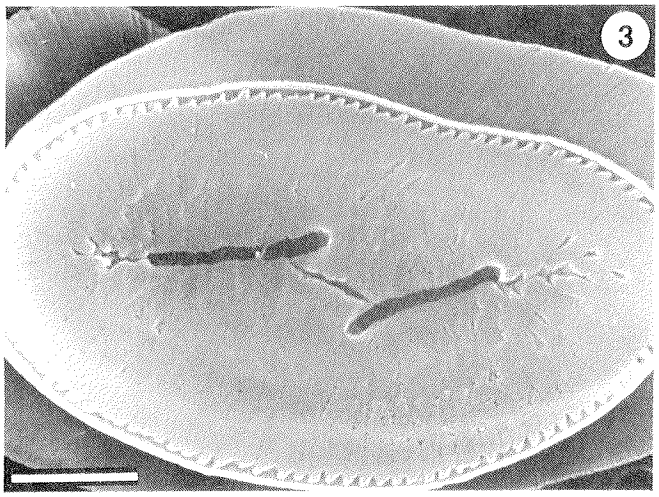
3

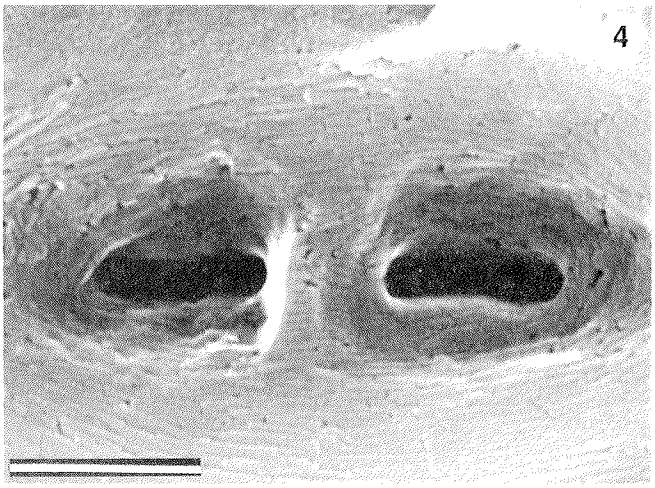
4

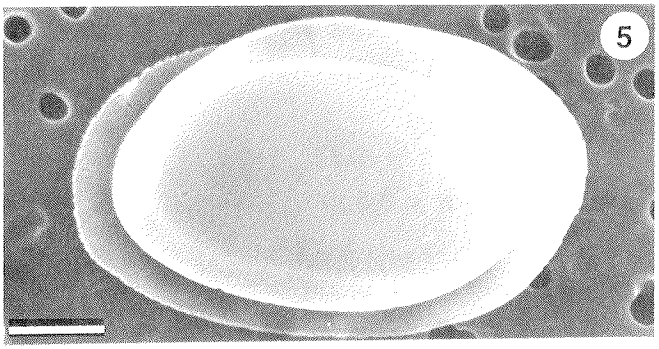
5

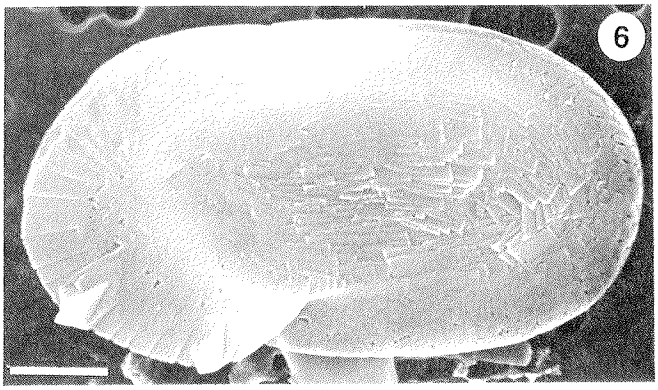
6

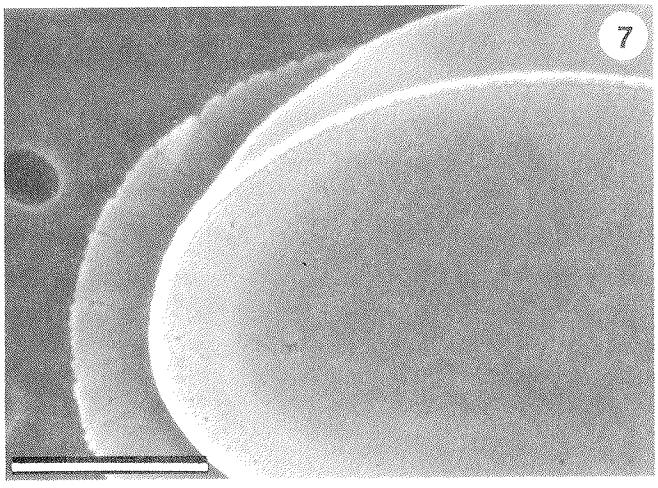
7

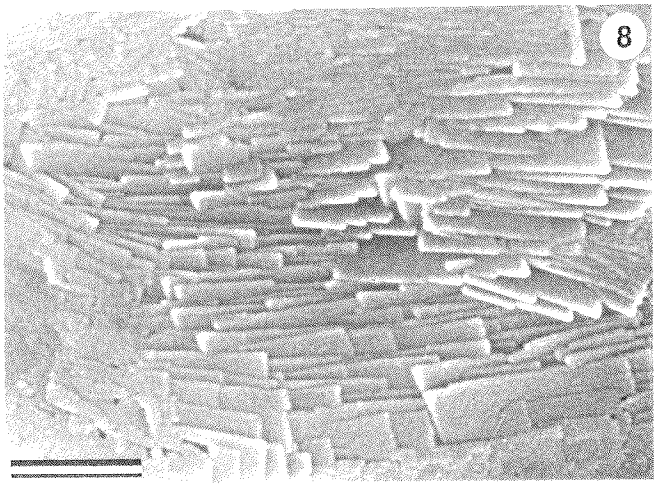
8

PLATE 13

Scale bar = 1 μm unless otherwise specified

1, 2 *Helicosphaera wallichii* (Lohmann) Okada and McIntyre

1 distal view, Station E: 988 m.

2 detail of figure 1.

3 *Anoplosolenia brasiliensis* (Lohmann) Deflandre
Station E: 5,068 m.

4 *Anoplosolenia* sp. Station E: 3,755 m.

5–8 *Scapholithus fossilis* Deflandre

5 Station E: 389 m.

6 highly magnified view of figure 5, scale bar = 0.5 μm.

7 Station E: 3,755 m.

8 partially dissolved specimen, Station P_1: 5,581 m.

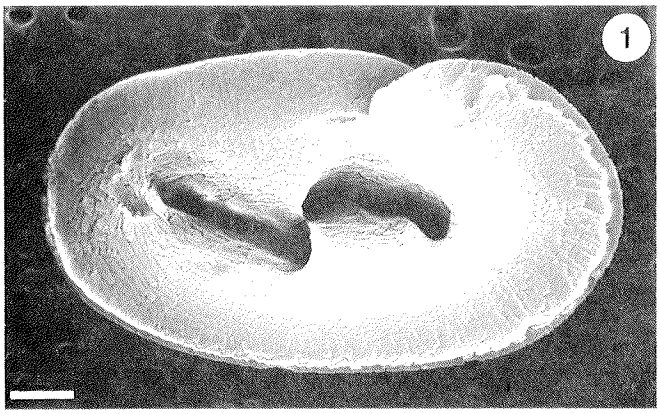
1

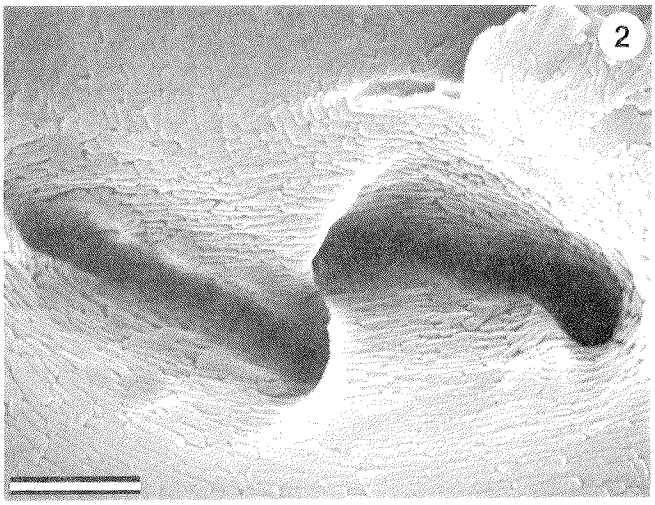
2

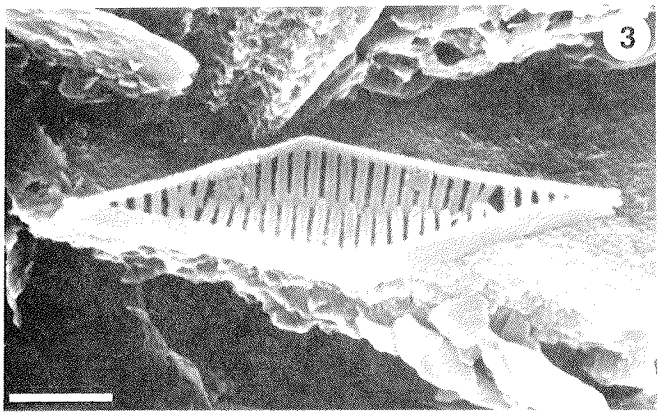
3

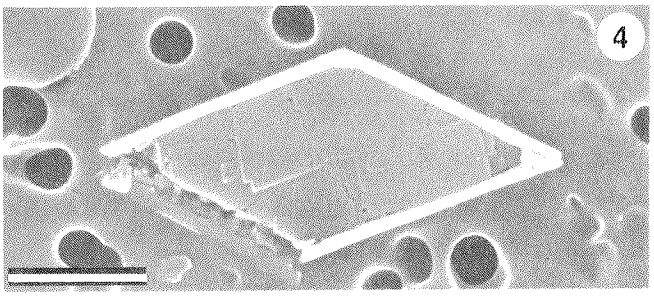
4

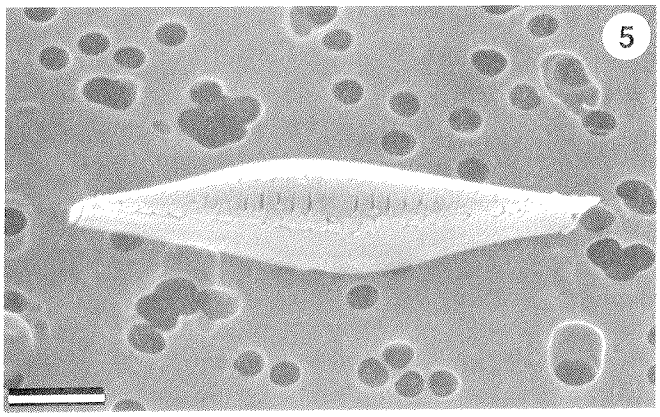
5

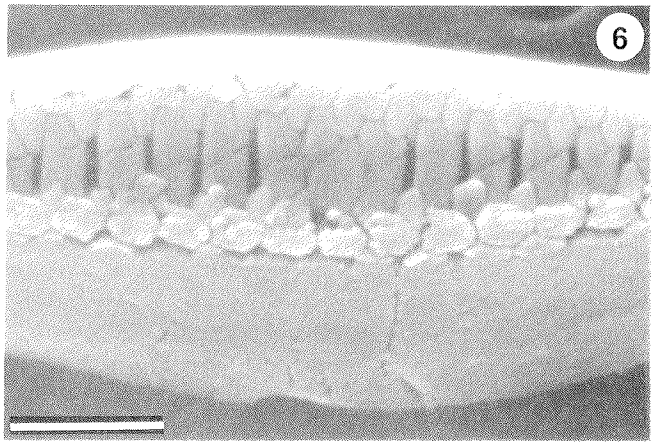
6

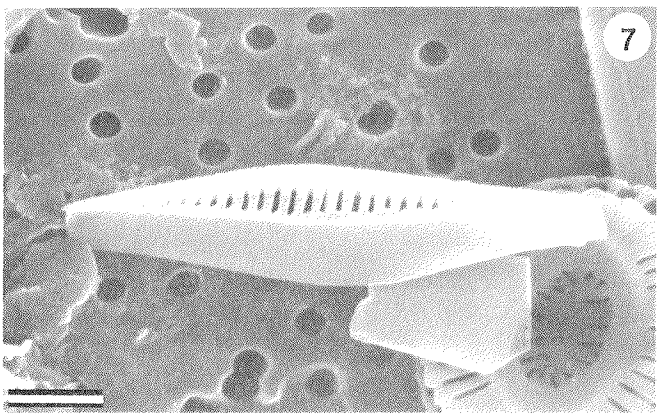
7

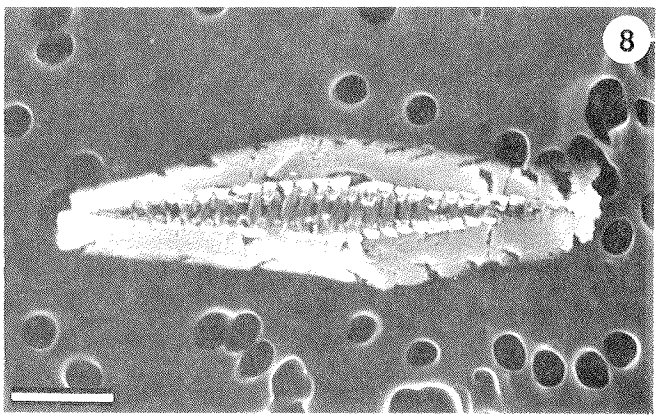
8

PLATE 14

Scale bar = 1 μm unless otherwise specified

1, 2 *Oolithotus fragilis* (Lohmann) Okada and McIntyre

1 proximal view, Station P_1: 2,770 m.

2 highly magnified view of figure 1, scale bar = 0.5 μm.

3–6 *Calcidiscus leptopora* (Murray and Blackman) Loeblich and Tappan

3 distal view, Station E: 389 m.

4 distal view of partially dissolved specimen, Station PB_1: 2,869 m.

5 distal view of partially disarticulated coccosphere, Station E: 389 m, scale bar = 5 μm.

6 highly magnified view of partially dissolved distal shield, Station E: 3,755 m.

7, 8 *Umbilicosphaera sibogae* (Weber-van Bosse) Gaarder

7 proximal view of collapsed coccosphere, Station P_1: 378 m, scale bar = 5 μm.

8 detail of figure 7.

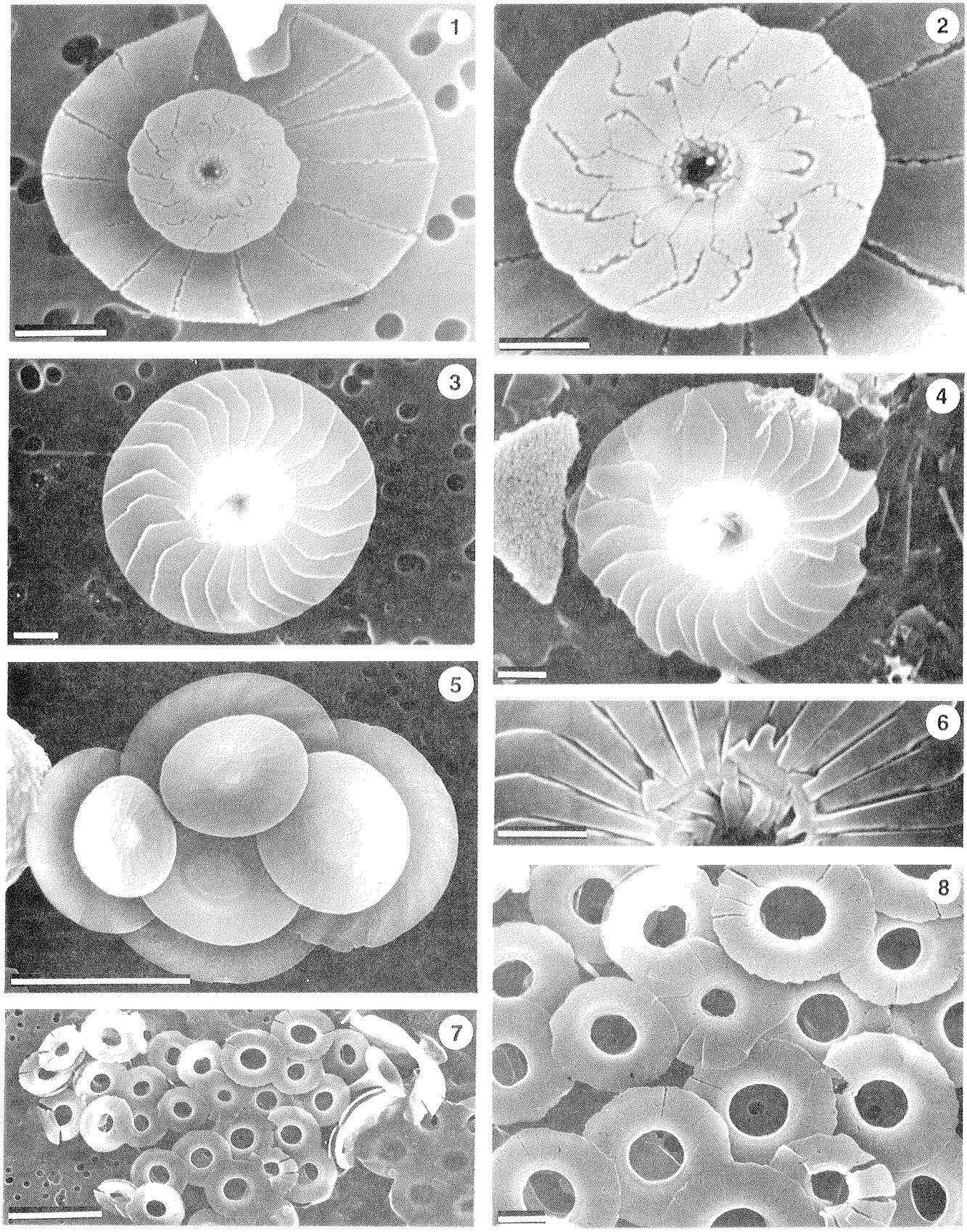
1
2
3
4
5
6
7
8

PLATE 15

Scale bar = 1 μm unless otherwise specified

1–5 *Umbilicosphaera sibogae* (Weber-van Bosse) Gaarder

1, 3 distal views, Station PB_1: 667 m.

2, 4 proximal views, Station E: 389 m, scale bars = 1 μm and 0.5 μm, respectively.

5 distal view of partially dissolved coccolith, Station PB_1: 2,265 m.

6–8 *Alisphaera spatula* Steinmetz n. sp.

6 holotype, collapsed coccosphere, Station E: 389 m.

7 magnified detail of figure 6.

8 highly magnified detail of proximal view of shield in figure 7, scale bar = 0.5 μm.

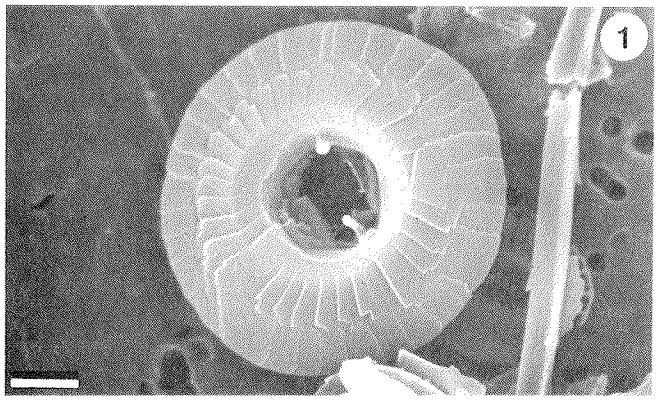
1

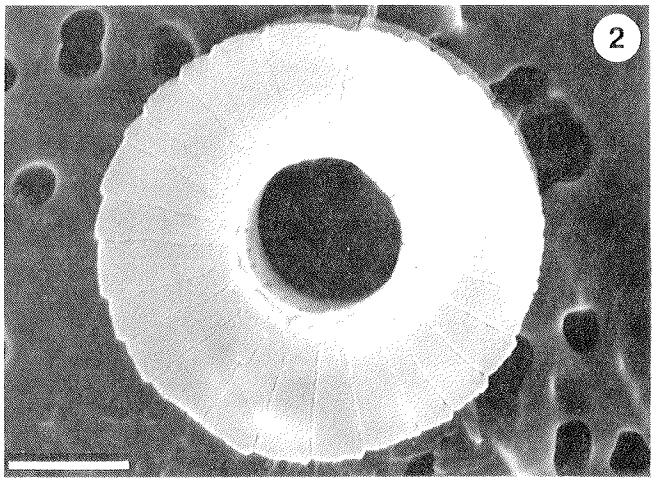
2


3

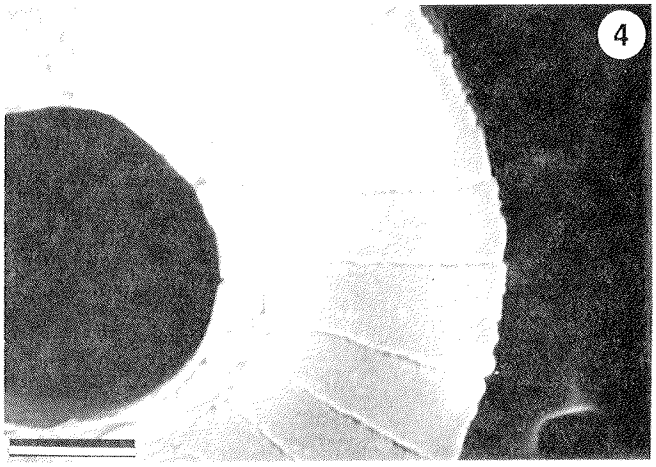
4

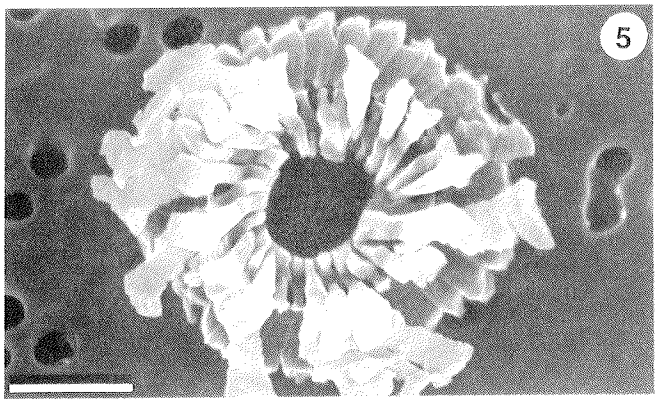
5

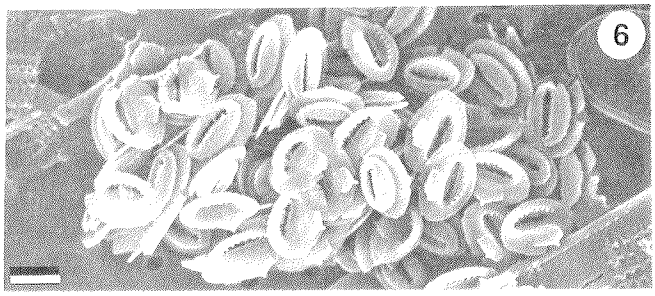
6

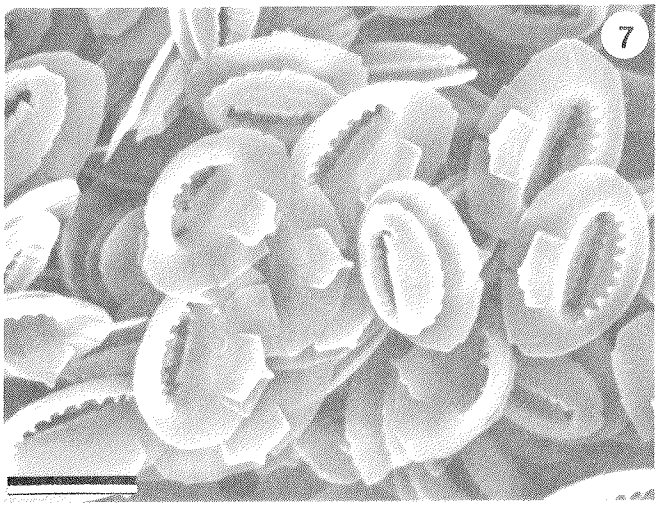
7

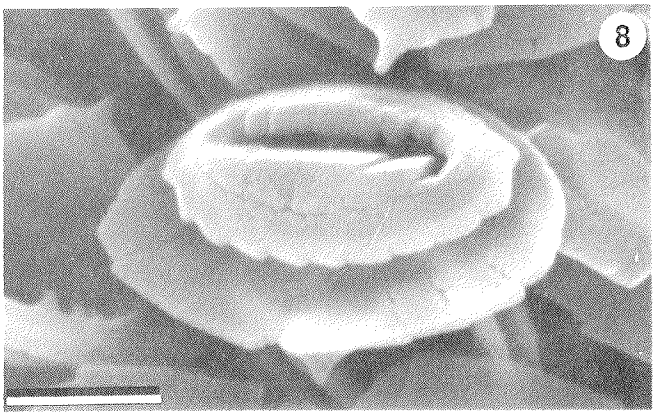
8

PLATE 16

Scale bar = 1 μm unless otherwise specified

1–8 *Anthosphaera oryza* (Schlauder) Gaarder

1 coccosphere, Station E: 389 m.

2 detail of coccosphere surface, Station E: 389 m.

3 highly magnified distal surface, Station E: 389 m, scale bar = 0.5 μm.

4, 5 partially disarticulated coccospheres, Station E: 389 m.

6 proximal surface of partially disarticulated coccosphere, Station P_1: 978 m.

7 side of coccolith, Station E: 389 m.

8 three coccoliths in side view with their proximal surfaces in common contact, Station E: 389 m.

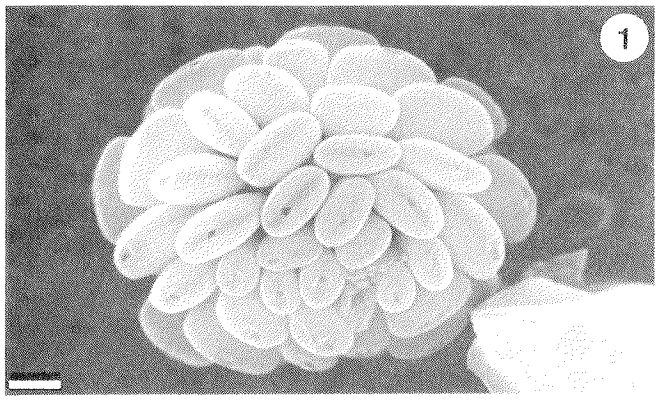
1

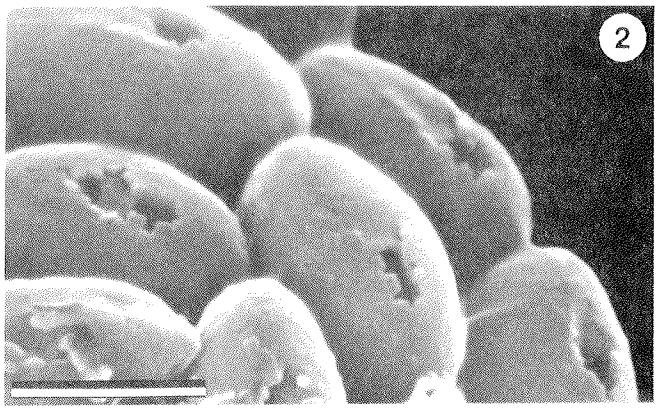
2

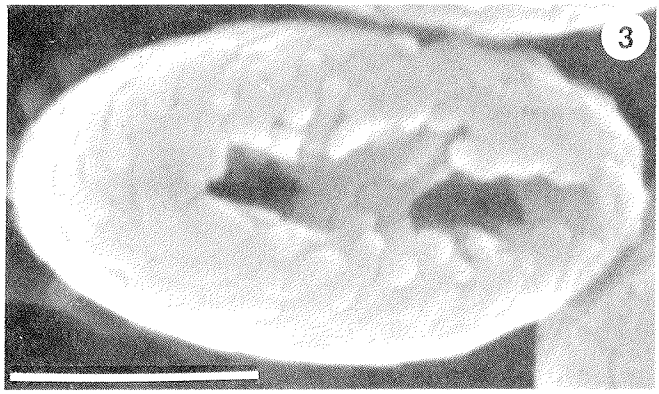
3

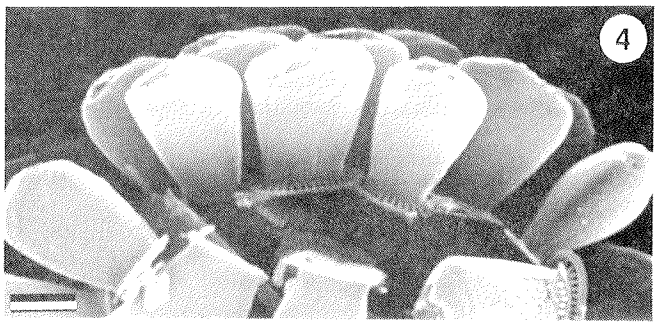
4

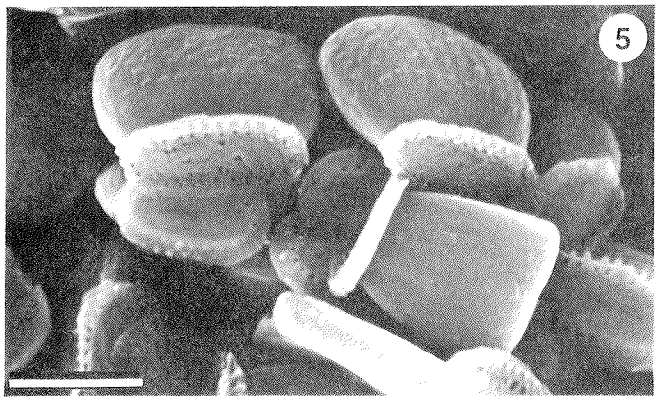
5

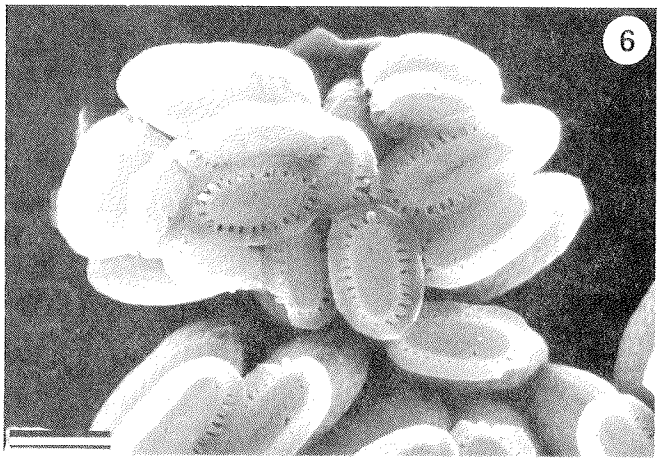
6

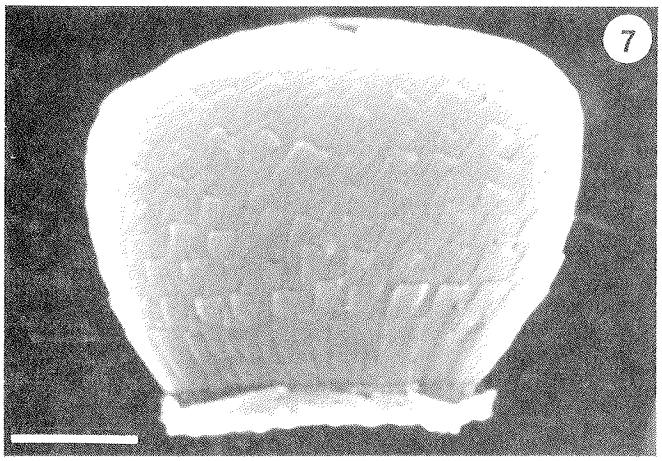
7

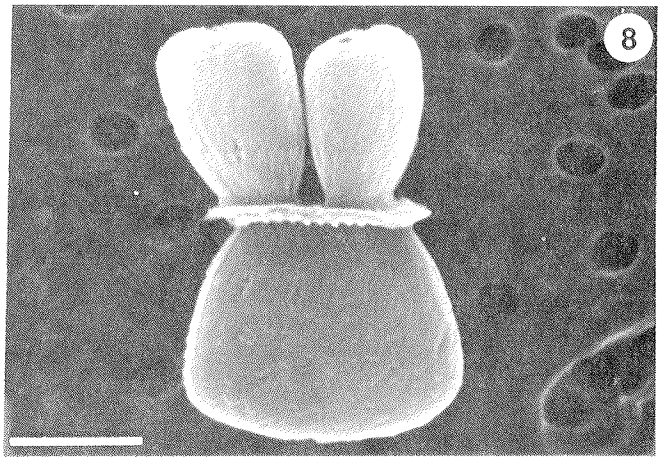
8

PLATE 17

Scale bar = 1 μm unless otherwise specified

1–3 *Coronosphaera binodata* (Kamptner) Gaarder

1 distal view of two coccoliths, Station P_1: 2,770 m.

2 highly magnified view of (left) coccolith in figure 1.

3 proximal view of partially dissolved coccoliths, Station P_1: 2,770 m.

4–6 *Syracosphaera lamina* Lecal-Schlauder

4 proximal view of caneolith, Station PB_1: 667 m.

5 highly magnified view of figure 4, scale bar = 0.5 μm.

6 proximal view of partially disarticulated caneolith, Station PB_1: 2,265 m.

7, 8 *Syracosphaera molischi* Schiller

7 coccosphere, Station P_1: 2,770 m.

8 distal view of partially dissolved coccolith, Station PB_1: 3,791 m.

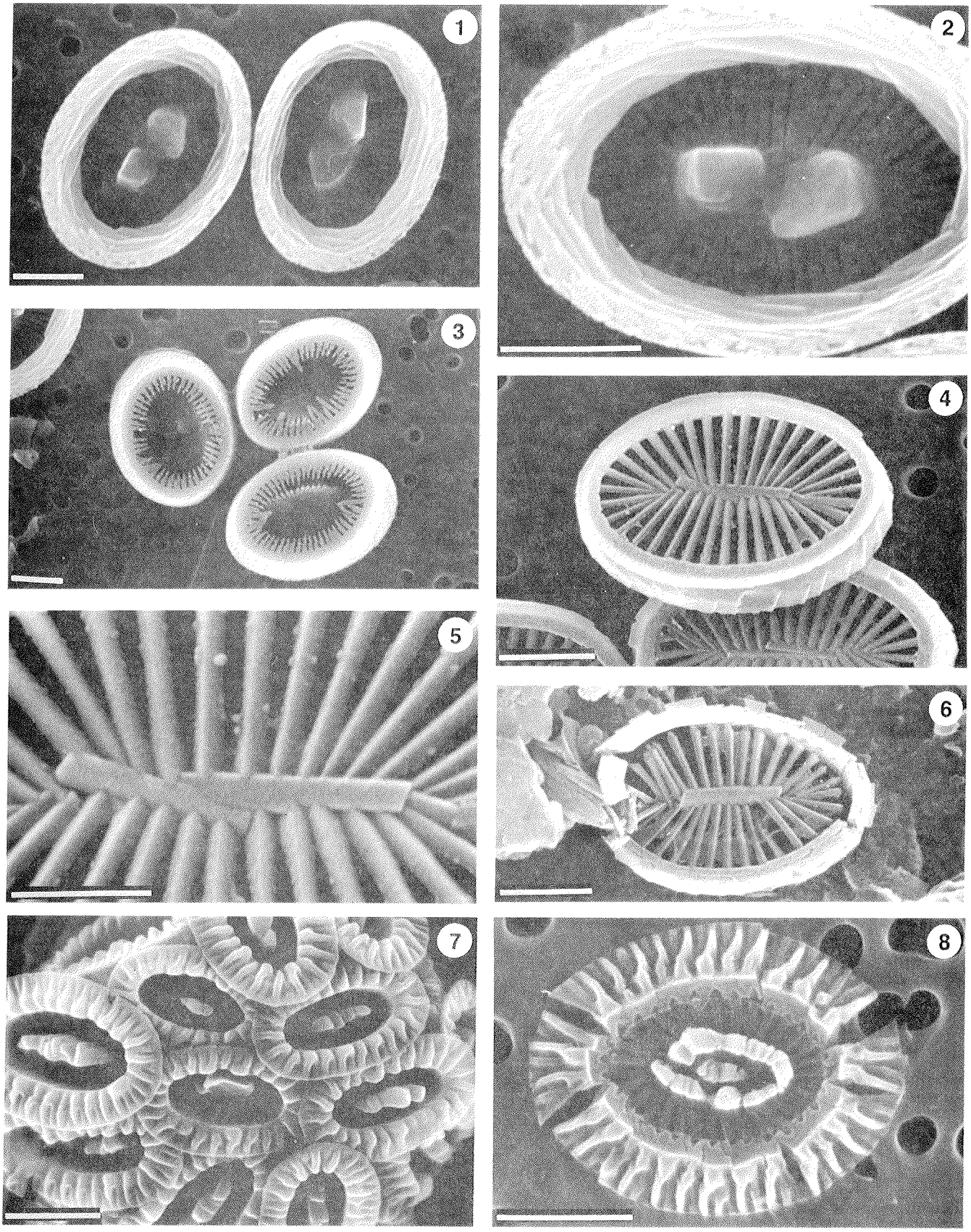
1
2
3
4
5
6
7
8

PLATE 18

Scale bar = 1 μm unless otherwise specified

1, 2 *Syracosphaera pirus* Halldal and Markali

1 distal view, Station P_1: 2,770 m.

2 highly magnified view of figure 1, scale bar = 0.5 μm.

3–5 *Syracosphaera pulchra* Lohmann

3, 4 proximal views, Station E: 389 m.

5 proximal view of partially disarticulated coccolith, Station P_1: 4,280 m.

6–8 *Deutschlandia anthos* Lohmann

6, 7 collapsed coccosphere, Station P_1: 2,770 m.

8 distal view, Station E: 389 m.

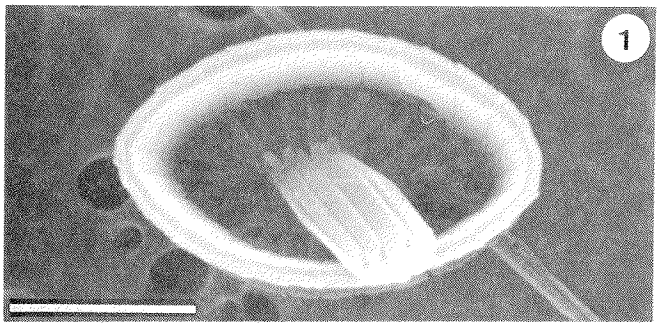
1

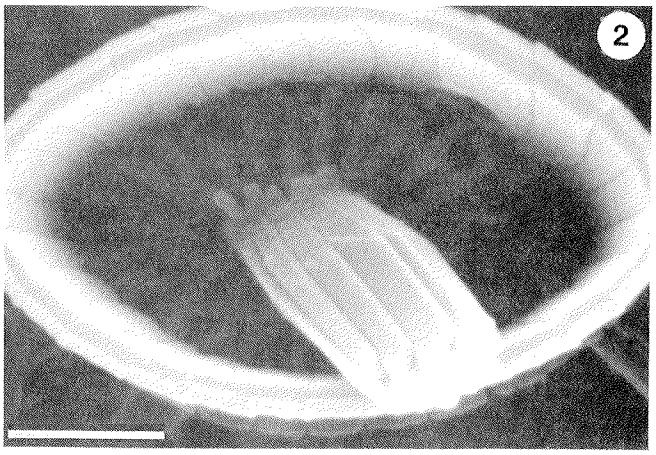
2

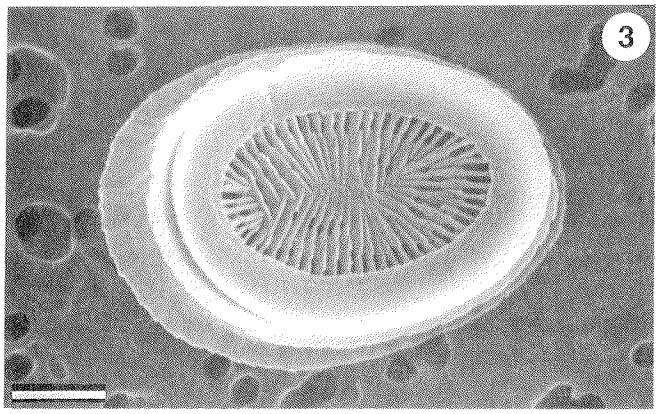
3

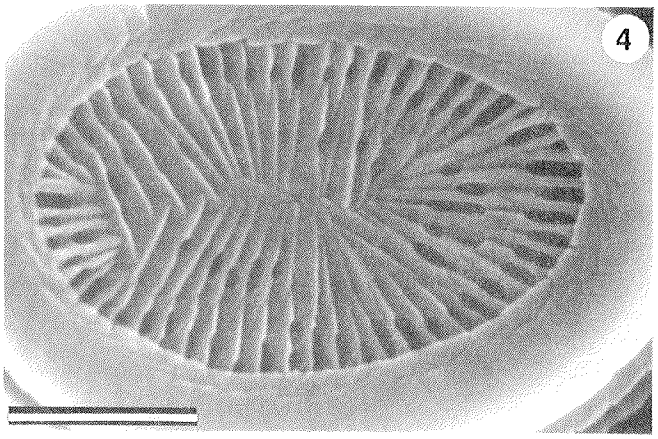
4

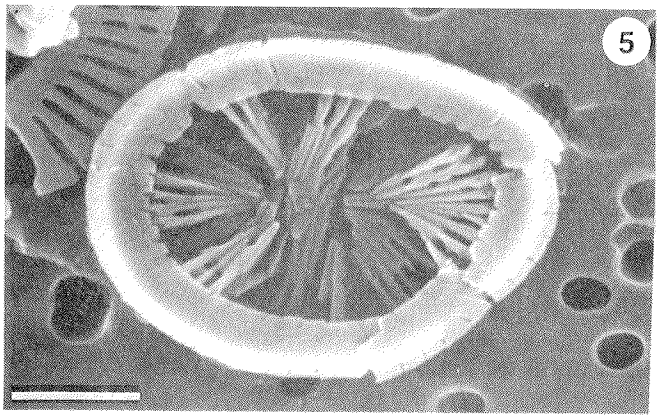
5

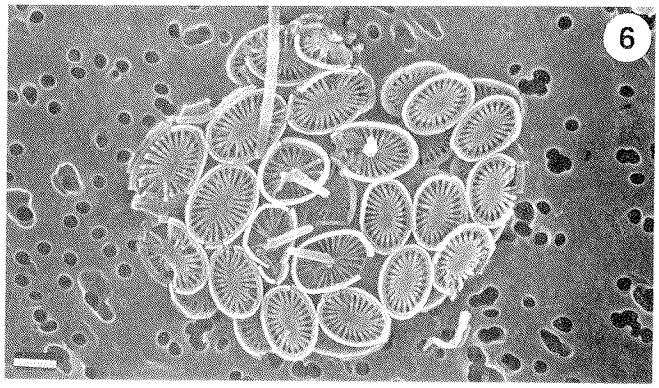
6

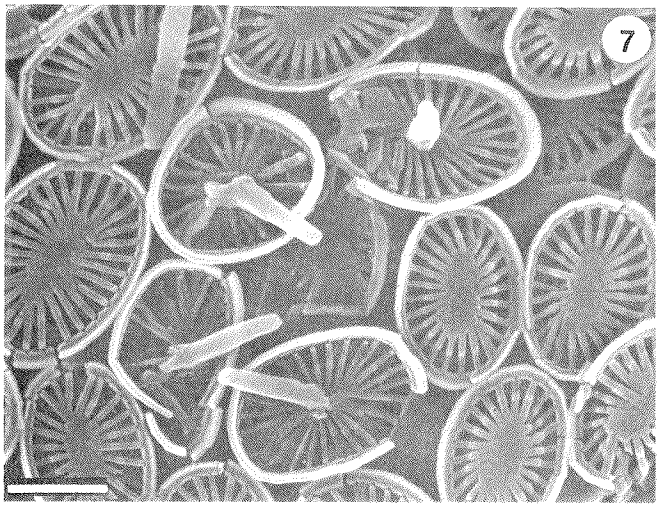
7

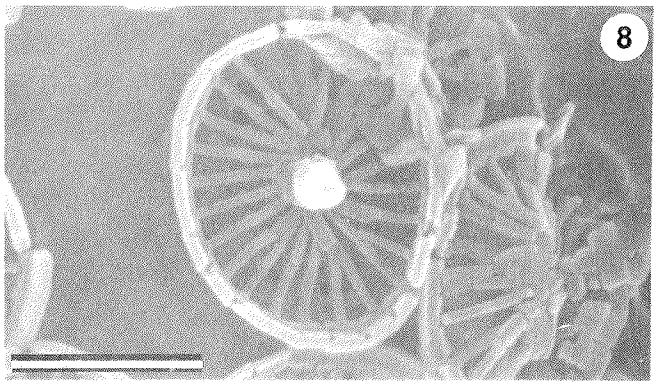
8

PLATE 19

Scale bar = 1 μm unless otherwise specified

1–4 *Florisphaera profunda* Okada and Honjo

1 coccosphere, Station E: 389 m, scale bar = 5 μm.

2 detail of coccosphere interior in figure 1.

3 quadrangular coccoliths from disarticulated coccosphere, Station E: 389 m.

4 highly magnified view of distal ends of quadrangular coccoliths, Station E: 5,068 m, scale bar = 0.5 μm.

5–7 *Halopappus adriaticus* Schiller

5, 6 collapsed coccoliths, Station PB_1: 2,265 m and Station E: 389 m, respectively.

7 distal view of coccolith in figure 6, scale bar = 0.5 μm.

8 *Discosphaera tubifera* (Murray and Blackman) Lohmann
Side view, Station E: 389 m.

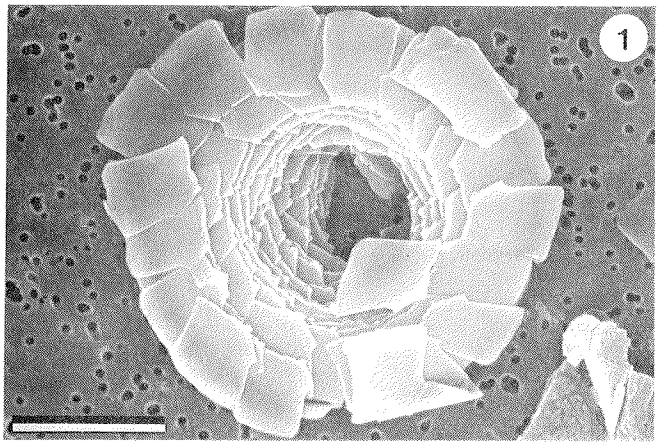
1

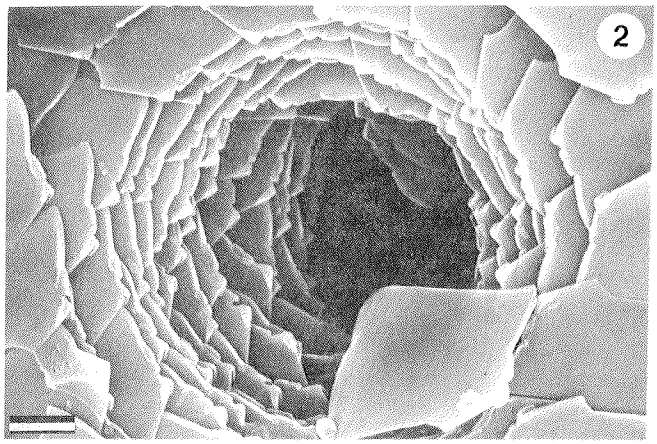
2

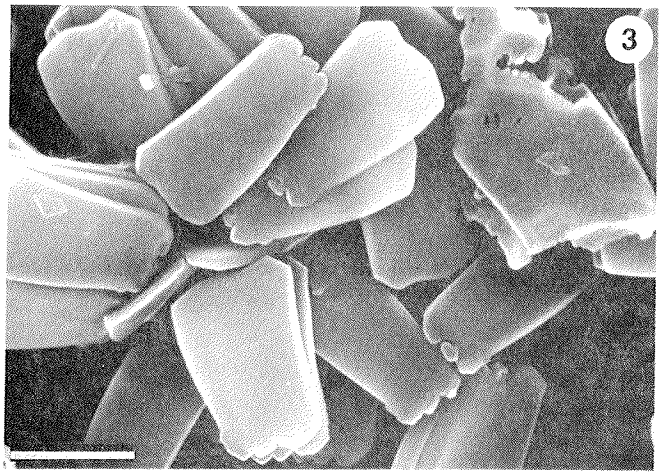
3

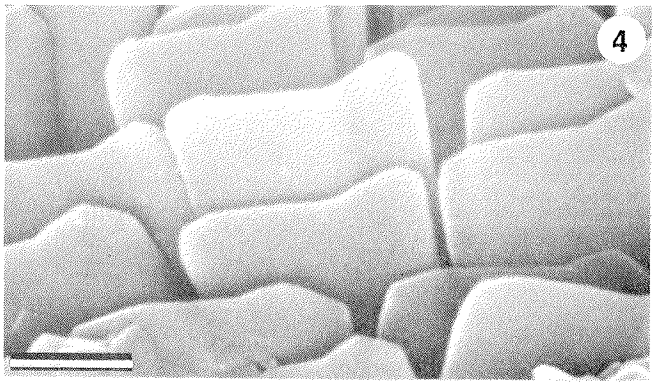
4

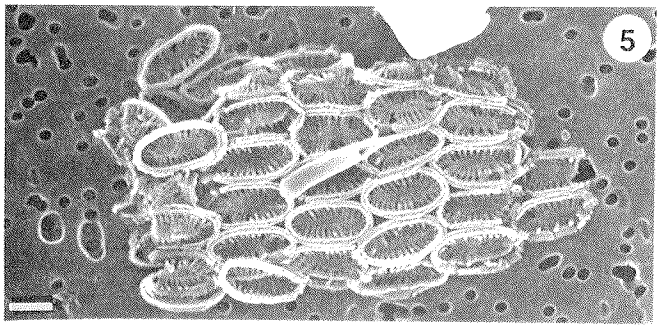
5

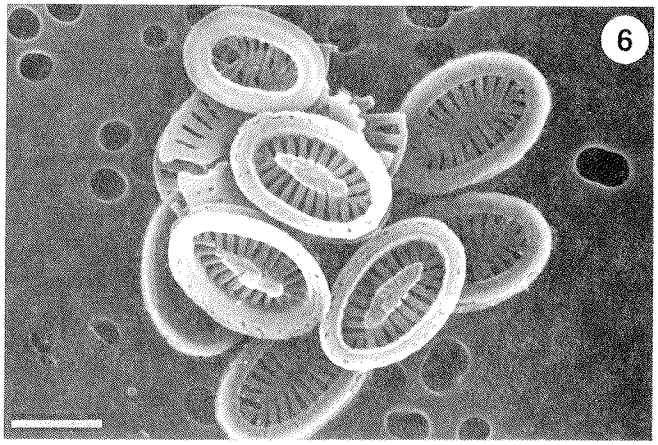
6

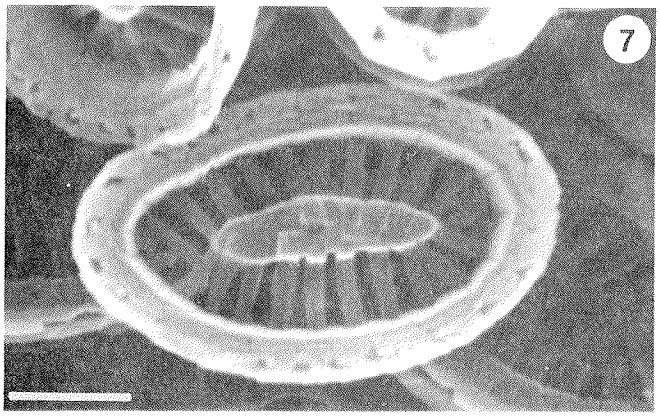
7

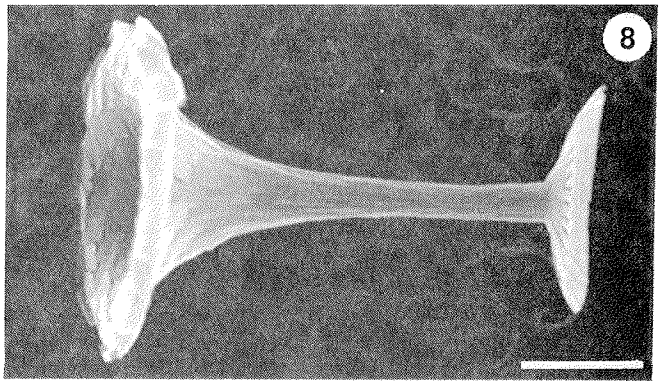
8

PLATE 20

Scale bar = 1 μm unless otherwise specified

1, 2 *Rhabdosphaera clavigera* Murray and Blackman
Side views, Station P_1: 2,770 m.

3, 4 *Rhabdosphaera stylifera* Lohmann
Side views, Station E: 389 m.

5–8 *Umbellosphaera irregularis* Paasche

5, 6 proximal views, Station E: 389 m, scale bars = 5 μm.

7, 8 highly magnified views of figures 5 and 6, respectively.

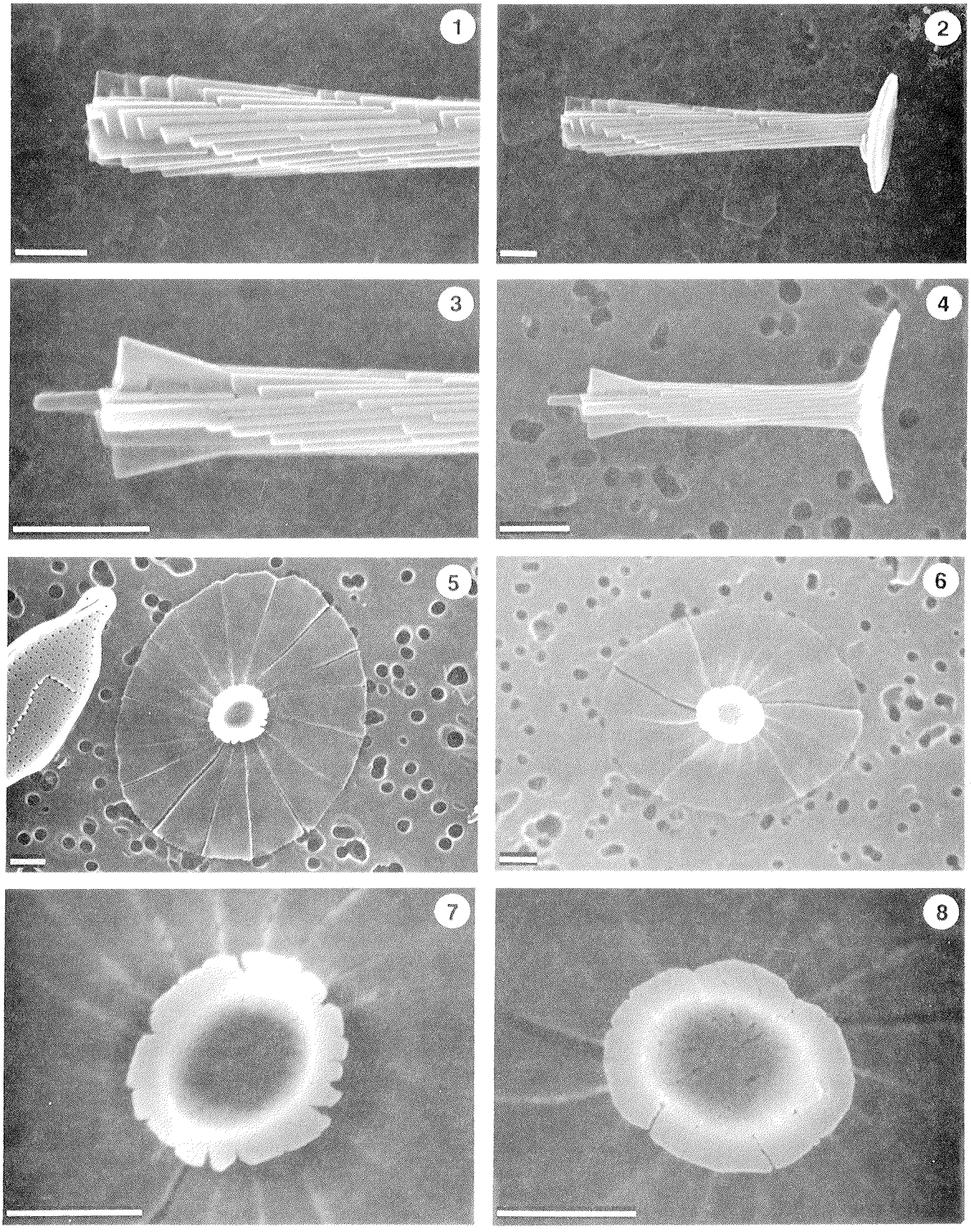
1
2
3
4
5
6
7
8

PLATE 21

Scale bar = 1 μm unless otherwise specified

1–4 *Umbellosphaera irregularis* Paasche

1 partially disarticulated coccolith, Station E: 389 m.

2, 3 proximal views of micrococcoliths, Station E: 389 m.

4 highly magnified view of figure 3, scale bar = 0.5 μm.

5–8 *Umbellosphaera tenuis* (Kamptner) Paasche

5, 6 distal views, Station E: 389 m.

7 highly magnified view of figure 5.

8 highly magnified view of figure 6, scale bar = 0.5 μm.

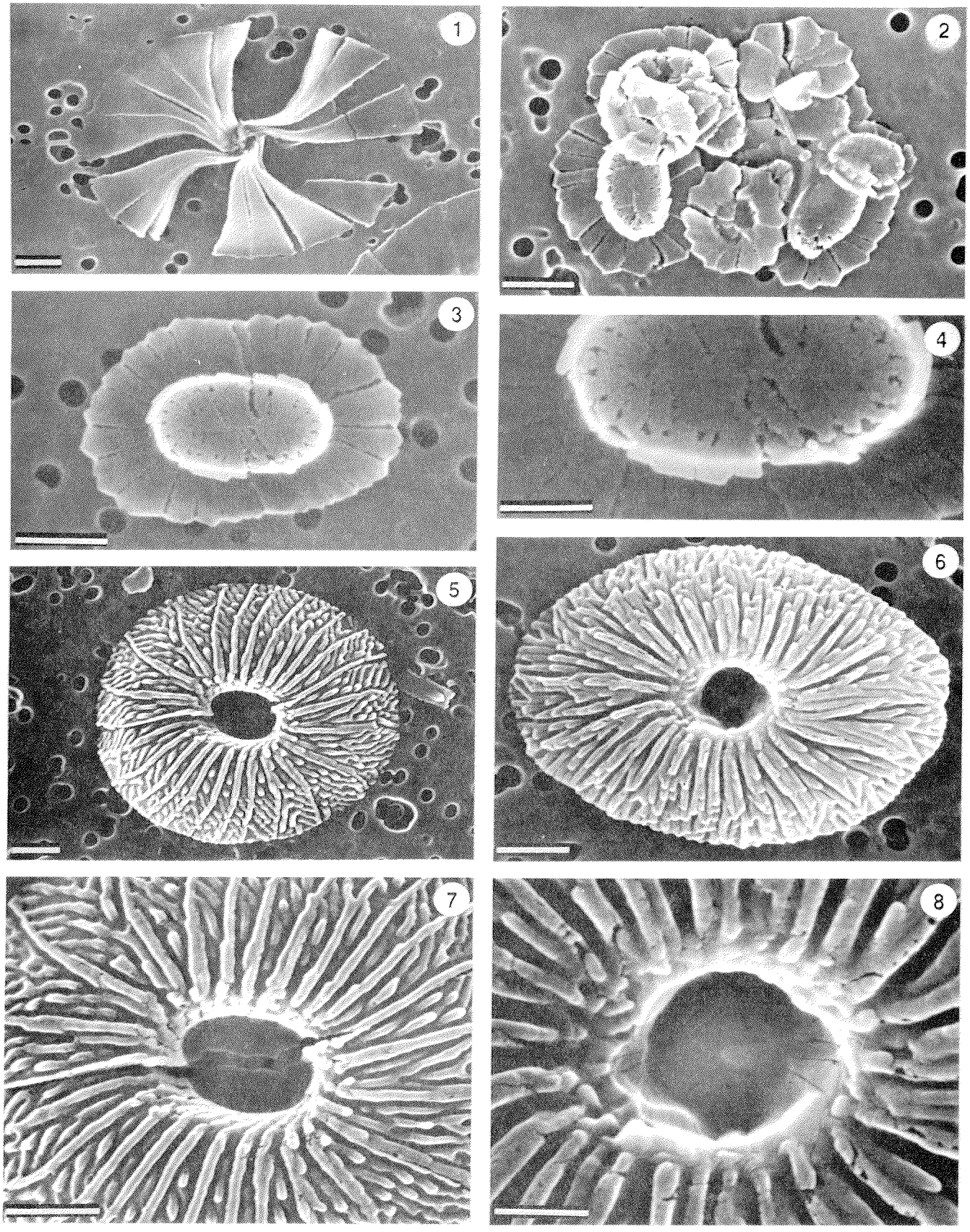
1
2
3
4
5
6
7
8

PLATE 22

Scale bar = 1 μm unless otherwise specified

1, 2 *Umbellosphaera tenuis* (Kamptner) Paasche

1 distal view, Station E: 389 m.

2 highly magnified view of figure 1, scale bar = 0.5 μm.

3, 4 Unidentified sp. 1.

3 side view, Station E: 389 m.

4 highly magnified view of distal (?) end, scale bar = 0.5 μm.

5, 6 *Calcidiscus leptopora* (Murray and Blackman) Loeblich and Tappan

5 proximal view, Station PB_1: 3,769 m.

6 detail of center structure.

7 Unidentified sp. 2 (*Sphaerocalyptra* ? sp.). Distal (?) view, Station E: 389 m, scale bar = 0.5 μm.

8 Unidentified sp. 3. Proximal (?) view, Station E: 389 m.

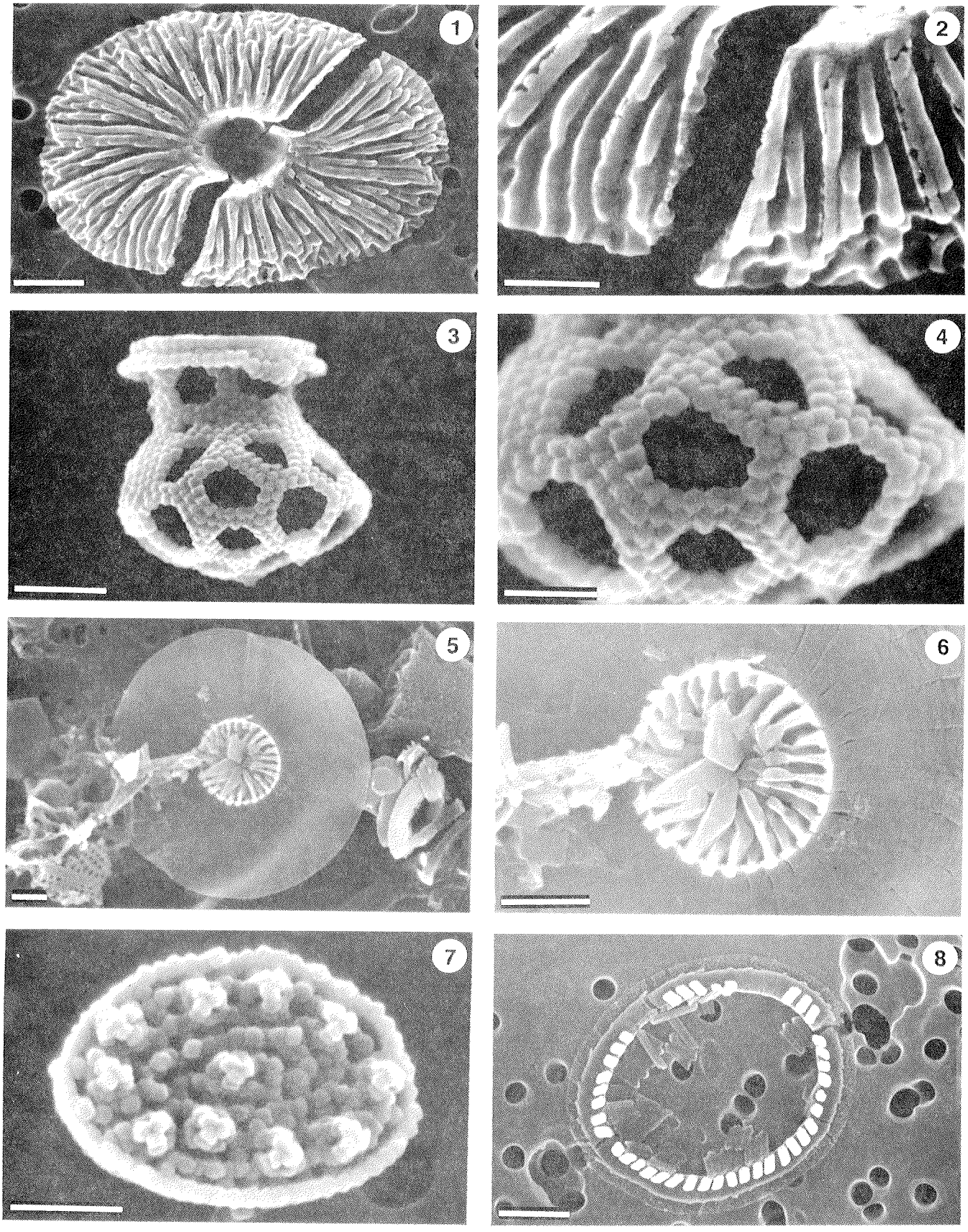
1
2
3
4
5
6
7
8